Section B, Creep, damage processes and transformations

Results of EC-projects: BOS-129-NL and MA1B-0058-NL (1986-1991)
Consist (outer TU-Delft reports and section B-reports) of 4 separated parts:
B.1. Deformation and damage processes in wood,
B.2. Transformations of wood and wood-like polymers
B.3. Theoretical derivation of the WLF- and annealing equations
B.4. A new theory of nucleation,
as discussion of the Section B-reports, which are published in 2 parts: B.1. and separately together: B.2 to B.4.

B.1. Deformation and damage processes in wood

T.A.C.M. van der Put,
TU-Delft, Civil Engineering and Geosciences, Timber Structures and Wood Technology,
Wielengahof 16 NL 2625 LJ Delft, Netherlands Tel: +31 152851980, E-mail: vanderp@xs4all.nl

Discussion and extension of B(1989a)

Delft Wood Science Foundation Publication Series 2015 nr. 2-1 - ISSN 1871-675x

Contents 1

1. Introduction

Strength and material properties of wood, as viscoelastic material, are time and temperature dependent and only can be described by the theory of molecular deformation kinetics. Therefore, time dependent behavior of wood is non-linear and the "viscous" strain rate follows the sinus-hyperbolic law of the initial stress.
The basic concept of this, general applicable, fundamental theory is to regard plastic flow as a matter of molecular bond breaking and bond reformation in a shifted position, what is the same as to state that flow is the result of a chemical reaction like isomerization, thus changing not the composition, but only the bond structure of molecules. Damage occurs when not all broken side bonds reform, providing the sites for a damage process. The theory applies for all materials with a correlation close to one, for all test-results on each specimen, thus test-results on the same structure, (as should apply for large number statistics of molecular behavior). An example of such a precise fit is given in fig. 1 of the stress decrease and density increase at annealing, discussed in Section B.3. Separate creep curves e.g. of each specimen, of your tests, thus will show such precise fit which you should publish in that way.

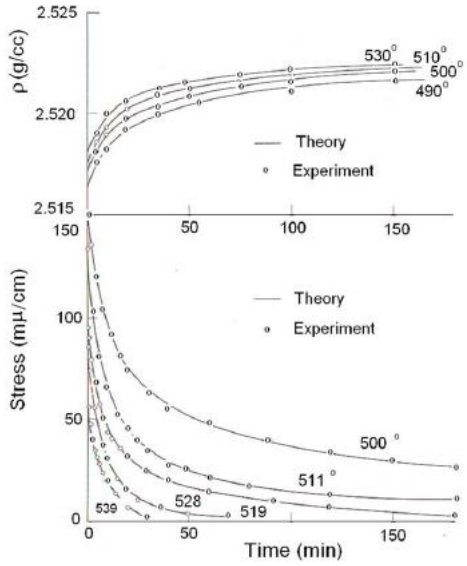

Fig. 1. Annealing, see Section B.3

The applied general theory, developed in B(1989a), is discussed here. This theory is based on the limit analysis equilibrium method and is, as such an exact approach, which is able to predict all aspects of time dependent behavior of materials by the same constitutive equation and may explain the phenomenological laws in this field. Further, possible simplifications could be derived, in order to find the main determining molecular processes.
The mathematical derivation of this general rheological theory is solely based on the reaction equations of the bond-breaking and bond- reformation processes at the deformation sites (i.e. spaces where the molecules may move into) due to the local stresses in the elastic material around these sites. The model doesn't contain other suppositions and only show the consequences of the stated starting point. The form of the parameters in the rate equations, which determine for instance the hardening and the delay time, are according to the general equilibrium requirements of thermodynamics. By expressing the concentration and work terms of the rate equation in the number and dimensions of the flow units, the expressions for the strain rate, fracture, hardening and delay time are directly derived without any assumptions. To obtain simplifications, series expansion of the potential energy curve is applied, leading to the generalized flow theory, thus to a proof of this general flow model, and showing the hypotheses of this generalized theory, to be consequences of the series expansion. This theory thus applies generally, also for structural changes, giving an explanation of the existing phenomenological models and laws of fracture. The theory is further able to explain the different power models (of stress and of time), giving the physical meaning of the exponents and constants. This applies for instance for the explanation of the Forintek model of the strength and the Andrade and Clouser creep-equations.
An explanation of the WLF-equation (Williams-Landel-Ferry is WLF) for glass transition and time-temperature equivalence above glass-rubber transition was derived in B(1998a), but the theory is extended in B(2010). Therefore the WLF-derivation of B(1989a) is not

discussed, but the correction, by extension to an important new vision, given in B(2010) and in final form, in a separate next Section B.3: "Theoretical derivation of the WLF- and annealing equation".
It is shown that a single non-linear process explains the measured, broad, nearly flat mechanical relaxation spectra of glasses and crystalline polymers and an outline of the total relaxation spectrum for wood can be explained by two processes in stead of the assumed infinite number of linear viscoelastic processes (which don't exist). Also the loss-spectrum by forced vibrations and fatigue behavior is explained by only one process. The non-existence of any spectrum follows from the zero-relaxation test (see § 8).
The solutions of the model equations are given for transient processes at different loading histories and it is shown that the model also is able to explain phenomenological laws as for instance the linear dependence of the stiffness on the logarithmic value of the strain rate in a constant strain rate test; the logarithmic law for creep and relaxation and the necessary breakdown of the law for longer times; the shift factor along the log-time axis due to stress and temperature and the influence on this factor of a transition to a second mechanism and the long delay of this second process. As an application of the model, a derivation of the mechano-sorptive effect was given in B(1989a) to explain the behavior at moisture cycling for any cycling history. The derivation throws a new light on the mechanism, being a separated sorption effect due to at the same time relative shrinking and expansion of two adjacent layers. The experimental research of B(1989a) was therefore based on cycling humidity conditions to determine this always present influence on activation energy parameters.

2 Structure and mechanical properties of wood

2.1. Structure of softwoods

Timber can be defined as a low-density, cellular (tubular), polymeric fiber composite [1], [2]. The macro structure is cellular and due to the branches of the tree, there are knots as main disturbances of the structure.
On microscopic level, most cells are aligned in the vertical axis and only 5 to 10% are aligned in the radial planes (rays). These rays are the main disturbances of the alignment of the vertical cells. In softwood two types of cells are available. The greater number are tracheid and have a supporting and conducting role. Most cells of the second type, the parenchyma, are in the rays and are block-like cells having a function for food storage. The tracheid are thin walled in early-wood and are thick walled in latewood). The cells are interconnected by pits (holes in the cell wall) to permit food passage and these holes are the main disturbances of the structure of the cell walls.
Chemical analysis shows four constituents: cellulose, hemicelluloses, lignin and extractives. The cellulose molecule is not folded and there is no evidence of primary bonding laterally between the chains. The laterally bonding between the chains is a complex mixture of fairly strong hydrogen bonds and weak van der Waals forces. The length of the cellulose molecules is about 5000 nm (0.005 mm). The crystalline regions are only 60 nm (length) by 5 nm (width) and 3 nm thickness. Thus the cellulose molecule will pass through several of these regions of high crystallinity with intermediate non-crystalline or low-crystalline zones. The collective unit passing the crystallites is termed micro-fibril, having an infinite length. It is clothed with chains of sugar units (other than glucose) which lie parallel, but are not regularly spaced making the micro-fibril to about 10 nm in breadth. Hemicelluloses and lignin are regarded as cementing materials. Hemicelluloses is a carbohydrate like cellulose, however the degree of crystallization and polymerization (less than

150 units) are low. Lignin is a complex aromatic compound composed of phenyl groups and is non-crystalline; 25% is in the middle lamella (the intercellular layer composed of lignin and pectin) and 75% is within the cell wall.
Thus the cell wall is a fiber composite with slender micro-fibrils as fibers in a cementing matrix of relatively un-oriented (amorphous) short-chained or branched polymers (lignin and hemicelluloses) containing also tiny voids and second order pore spaces.
The cell wall also is a laminated composite because of the layered structure of the wall. To be distinguished are in succession: the middle lamella, a lignin-pectin complex without micro-fibrils; the primary wall with loosely packed random micro-fibrils and the secondary wall with closely packed parallel layers. The outer layer or S_1 layer of this secondary wall is thin (4 to 6 lamellae) with 2 alternating spiral micro-fibrils with a pitch to the longitudinal axis of about 60 degree. The middle layer or S_2 layer is thick (30 to 150 lamellae) with fibrils in a right-hand spiral with a pitch of about 20 degree and the inner layer or S_3 layer is very thin and is similar as S_1 with a pitch of about 80 deg., is however looser and contains lignin in a high proportion (see Fig. 2.1). Because there are 2 cell walls between the adjacent tracheid, a micro-fibril angle deviation from the longitudinal axis in a layer is compensated by the opposite angle in the equivalent layer of the second cell wall causing the orthotropic behavior and the stiffness and strength at an angle to the grain follow the common tensor transformation laws. Thus the behavior of a tracheid alone is far from orthotropic and the results of tests on separated tracheid, as done for the paper industry cannot be used to predict the behavior of wood.

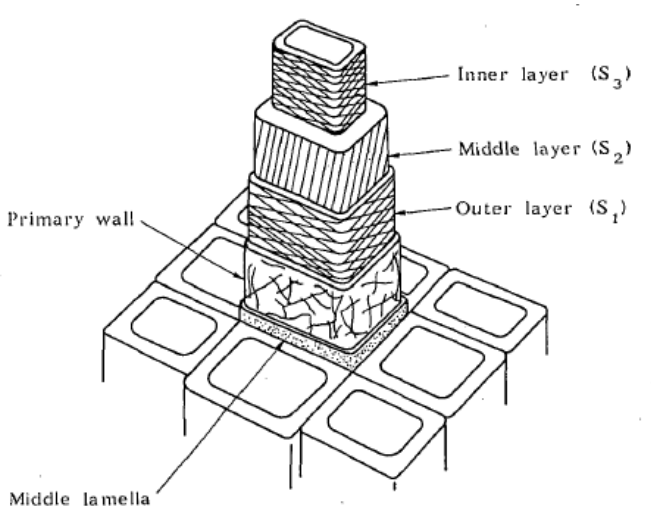

Fig. 2.1. Wall layers with orientation of microfibrils [1]

2.2 Rheology of wood

2.2.1 Discussion of the general applied phenomenological approach [3]

Just like other materials, is time dependent behavior of wood nonlinear and has to be explained by the theory of molecular deformations kinetics, [17], B(1989a). As first expanded, this behavior is regarded to be linear elastic when stress, moisture content, temperature and testing time are sufficiently low, or to be linear viscoelastic at some higher levels of these variables. Phenomenological, the creep compliance therefore is separated into instan-

taneous, delayed elastic, and flow components. The instantaneous or glassy compliance is always regarded to be independent of stress. The delayed elastic and flow compliances are regarded to be approximately independent of stress below certain stress limits depending on time, moisture content (m.c.) and temperature. Mostly this limit is taken between 40 to 50 % level, depending on testing time. These limits are also regarded to be the boundaries below which there is only decelerated creep and above which there is, after decelerated creep, stationary creep and accelerated creep. However, wood is a cross-linked polymer and, stationary creep, thus creep at a constant strain rate, cannot occur. Accelerated creep is due to a structural change process, (the same equation applies e.g. for annealing), what will be discussed later. Nonlinear behavior is not only evident by structural changes. This also follows from the "irrecoverable" flow, which still can be recovered by an increase of m.c. and or temperature. This behavior is explained by the time-stress equivalence following from nonlinear viscoelastic behavior providing a very stiff "dashpot" for the low internal stresses after unloading, making recovery very slow and thus showing a quasi-permanent strain. Repeated stressing may lead to stiffening, shown by a decrease in hysteresis and an increase in elastic modules (by crystallization). However, at sufficient high stress, a structural change process may dominate (at common testing times), which causes an increase of the glassy compliance. Transitions of processes at higher temperatures and m.c., are discussed in Section B.2: “Transformations of wood and wood-like polymers”. Outer the superposition of time and temperature and time and stress, is simple superposition of time and moisture content not valid because of other structural changes (shape and volume) associated with the change of moisture content. As generally known, absorption of water in wood causes swelling up to a m.c. of about 28%. The swelling is roughly proportional to the water uptake. Although water enters only in the amorphous zones, the strength and stiffness are reduced. The tangential shrinkage exceeds the radial shrinkage partly by the restraint of the rays. The swelling and shrinkage in longitudinal direction are very small compared with the other two directions. It is the smallest for steep micro-fibril helixes in the S_2 layer as can be expected in the direction of the crystalline micro-fibrils. Swelling of the secondary wall is much higher than swelling of the middle lamella. Thus the latter restrains the shrinkage of the wood causing high internal stresses. The planes, which are the richest in hydroxyl groups, lie parallel to the micro-fibril surface and part of the non-crystalline material is oriented in parallel with the cellulose and this material is accessible to water. Thus the planes between the lamellae of the cell wall are the places for bond breaking processes due to water movement. In fact the cell wall acts as one layer for dry wood and the S_2 layer is split in hundreds of lamellae in the saturated stage. It is to be expected that the high restraints for swelling and shrinkage will cause "flow" in the gel-like matrix. This flow is directed when a specimen is maintained under stress during a change in moisture content. The moisture movement through wood involves breaking of stressed hydrogen bonds and reformation of these bonds in an unstressed position causing the large creep deformation at desorption when one of two adjacent layers shrinks, while the other swells (with respect to the total stress free expansion movement). This mechanism determines the behavior at cycling moisture content conditions (the mechano-sorptive effect). There is an increase of creep during desorption and recovery during the first, or for tension also possible in the second absorption period, depending on the initial moisture content. At high stresses and small moisture content changes there is no recovery but a reduction of the creep rate during adsorption. The deformation is usually divided in three components: overall shrinkage by moisture change; time-dependent strain by the stress history and the mechano-sorptive effect. The same can be said for temperature changes. There is further an interaction influence of temperature and moisture content if one of these cycles. As stated above these interaction effects are not real interactions but can be explained as conse-

quences of the differential swelling and shrinkage of adjacent layers. This is shown and calculated in B(1989a): "Theoretical explanation of the mechano-sorptive effect in wood" and in § 7.3.2. The sorption influence is, for a single change, linear with the amount of moisture change, independent on m.c., temperature, rate of sorption and previous creep-history, indicating a flow process. The rate of deformation is dependent on the rate of change of moisture content. The moisture gradient is not the cause of the increased deformation (there is no influence of the size of the specimen). As explained by the model, a stepwise increase in moisture under loading gives a maximal deflection at the first moisture increase and the deformation at changing moisture conditions is not much dependent on the loading, at not too low, and not too high, loading levels. There is no decrease in the modulus of elasticity (thus no damage).

2.2.2. Viscoelastic structural behavior in comparison with other polymers

Cellulose molecules are very long and have very short side chains and are able to be packed close together forming crystalline areas. Hemicelluloses have different forms between the linear structure and the very strong branched structure. The linear form with not regular spaced short side chains and many polar hydroxyl groups has, as celluloses, good fiber forming properties and the branched type has good entanglement and filler properties. Lignin is cross-linked in all directions and is able to form strong bonds with the celluloses and has also hydroxyl groups. Cellulose is highly crystalline (~ 70 %) and the crystallinity doesn't change much on straining or drying. Because of the physically side bonds (hydrogen- and van der Waals bonds) it is to be expected that the binding energy will be time- and temperature dependent. However the deformation of a crystallite is energy elastic (representing displacements from equilibrium positions) and time dependent behavior is only noticeable in the amorphous regions. The modulus of elasticity is $1.1\ 10^5$ N/mm^2 in chain direction and about 10^4 N/mm^2 perpendicular to this direction. The amorphous regions of the cellulose are highly oriented and will have many cross-links (hydrogen bonds). Because there is no "coiling" structure, an uncoiling process cannot be expected to occur.
The branched hemicelluloses polymers have the function as filler of the lignin and because the strong bonds with the lignin it increases the cross-linking, acting as copolymer. The linear hemicelluloses acts by hydrogen bonds as flexible bridge between the micro-fibrils, making movements of the fibrils possible and avoiding stress peaks between fibrils on loading. Lignin is a random amorphous cross-linked polymer that is able to form strong bonds with the polysaccharides. Real rubbery behavior (uncoiling) thus is not possible. Thus the polymers in wood, which determine the time dependent behavior, contain densely cross-linked filled amorphous polymers as well as highly crystalline and oriented polymers. Although such polymers don't possess a zone of rubber-like behavior, there is a transition possible to a more flexible state (e.g. by the possible shifts of the micro fibrils with respect to each other).
Crystalline polymers with the amorphous region in the flexible state (above the transition temperature of these regions) normally show a quick stress relaxation loosing 25 to 50 % of the stress in a few minutes. This is followed by a slow process and the remaining stress after 17 decades (the age of the universe) is above 5 to 10 %, as follows from the time-temperature equivalence. Thus this stress reduction of about one order is much less drastic than that for the rubbery transition where the stress reduces 5 to 6 orders. However this quick relaxation mechanism is not measured for wood, even not at high temperatures, suggesting a very high cross-linking. Thus the slow process is dominating in wood (at low stresses) and has the same properties as for other crystalline and cross-linked polymers. This means that creep is recoverable; that increase of stress shortens the retardation time

(crystalline materials) and that the creep rate is more than linear proportional to the stress at higher stresses with the consequence that the creep and recovery functions have different shapes. The temperature dependence of the viscoelastic properties follows the WLF- or the Arrhenius equation. The WLF equation applies to wood components as lignin but not to the copolymer wood. The Arrhenius form applies for cellulose. Because the crystallinity doesn't change much, there are no vertical shifts (due to change of the pseudo equilibrium modulus) of the creep lines along the log- time- axis. The creep was described in the past by the Andrade-equation and is mainly a straight line on a log-time-plot. This mechanism is attributed to the mobility of the short strands in the amorphous regions, probably due to co-operative motions of groups of strands coupled through linkage points. The thermal and mechanical history is very critical for the behavior, as applies for glasses, and also traces of diluents have an influence.
At room temperature the amorphous parts in wood are in the glassy state, and only the so called β – mechanism appears (the α – mechanism represents the glass-leather transition due to mobility of the back-bones of the polymers). The β – or secondary mechanism is due to local readjustment of side groups in glassy amorphous polymers or in the amorphous strands of crystalline polymers. These side groups can be, chemically attached groups, or hydrogen bonds, which act as side group on the polymer chain and even can be only polar water molecules. In this last case the β – mechanism disappears on removal of water. Dielectric measurements support this model because they reflect dipole orientation due to side group motions, showing the same temperature dependence as the visco-elastic behavior. This temperature dependence follows the Arrhenius equation and the activation energy lies between 20 and 30 kcal/mole. For the stress reduction in relaxation by the secondary mechanism is a factor 0.5 used as a rule of thumb for wood. The same as for the α – mechanism, is the behavior nonlinear and the properties only can be explained by the molecular deformation kinetic theory.

2.3. Strength and time dependent behavior

2.3.1. Factors affecting the strength

The influence on the strength of the native origin of wood, determined by the character of the soil, climate, density of the forest, etc. is not important, because the variability within one area is comparable with the variability of the whole population.
The main features of the macro-structure, which determine the strength, are the density, moisture content, width of the growth rings and width of the latewood part of those rings. Disturbances also have influence. The main disturbances of the structure are the knots, deviations of the grain angle, compression wood, resin channels, growth defects and checks. Because timber is selected for structural use, larger disturbances by cracks, resin heaps, growth faults, etc. are excluded and only minor disturbances are allowed having a little influence on the strength. Compression wood will cause twisting and splitting due to differential shrinkage by seasoning and also serious grain angle deviations may cause twisting. Thus by selection, this timber will not be used for structural applications and it appears that, for gross wood, the regression of the strength is nearly totally determined by only the knot area, the density and the moisture content (see e.g. the discussion in [4]).
Knots act similar like holes and the strength dependent on the KAR (knot area ratio) can be fully explained by the stress field around a hole [5].
An increase in moisture content in wood gives a reduction in strength by the weakening of the inter -chain hydrogen bonds of the cellulose components in the amorphous regions.

The moisture effects will be explained later by the chemical reaction kinetics of this water binding. At a moisture content of about 28% there is no further reduction of the strength and also no further increase in swelling of wood.
There is a very general correlation between strength and density also when comparing different wood species. The amount of latewood is highly correlated with the density. This is not so for the total ring width. Thus the density of early-wood varies in every ring. Because of the correlation of the strength with the density, it can be expected that mainly the latewood part determines the strength. This can be true if there is early plastic flow in the early-wood transmitting the stresses to the latewood. This also explains the higher magnitude of the tensile strength of the individual fibers compared with gross wood. In gross wood early crack formation occurs at imperfections between the layers due to stress concentrations. Because there is sufficient overlap of the adjacent fibers, these cracks have to propagate through the clear wood layers for total fracture where the amount of latewood determines the strength.
Measurements in tension of wet early wood and late wood single fibers, indicate a 1.1 to 3 times higher ultimate strength (at about the same ultimate strain) and stiffness of the late wood fibers (from the same species) [6]. In [7] higher differences between early-wood and latewood were measured. Dry late wood was about 6 x stronger than early wood, closer to the theoretical expectation and wet late wood was about 4 x stronger, indicating more influence of plasticity for wet wood. It was also found that the ultimate strain for failure of latewood was higher than for early-wood. Preparation of single fibers test-specimens will always induce cracked surfaces with the possibility of crack propagation, diminishing the strength differences between early and late wood. Probably this explains the differences of the measurements of [6] and [7].
Elastic models of the mechanical behavior of cell wall layers (e.g.[8]) indicate a much worse loading of springwood in comparison with summer-wood. The maximum stress parallel to the micro-fibril is about 4 times higher and the stress perpendicular and the shear stress is about 7 times higher in springwood than in summerwood. This indicates early plastic flow in the cell wall layers of the springwood with considerable stress redistributions between the layer components because else, the relatively high experimental strength of this layer cannot be explained.
The summerwood fiber has an almost ideal stress pattern in accordance with the strengths of the different constituents and can be expected to behave elastic up to high stresses, making probably a description possible by an elastic model of the cell wall strength. Thus, whatever the mode of failure is, the strength is close to the fiber strength. Such elastic model for the tensile strength of the cell wall, [9], indicates that fracture first occurs in the S_1 layer by a shearing mechanism with a very high shear stress at failure, suggesting a strong bonding between lignin, hemi-cellulose and cellulose. This initial fracture of the S_1 layer follows also from the theory of maximum energy of distortion (which is shown in A(2009) to apply also generally for wood). The model further shows opposite signs of the shear stresses in the S_1 and S_2 layers, indicating also high stresses in the interface between the S_1 and S_2 layers. Microscopic studies have confirmed this interlayer fracture by the pulling out of the S_2 and S_3 layers out of the enclosing sheet of the S_1 .
As second type of failure, helical break along the direction of the S_2 micro-fibrils was observed leading to the ultimate rupture of this layer.

2.3.2 Mode of fracture

Failure of wood is dependent on the type of stress. The cleavage behavior of wood was studied by fracture mechanics tests on notched samples (e.g.[10]). The strain-energy release rate depends on temperature and moisture content and there is a dominating stability of crack extension. The slow and stable crack propagation was mainly within the cell wall of the tracheid, either between the primary and S_1 walls, or between the middle lamella and the primary wall and was moving through the middle lamella to the adjacent cells. Thus the cell lumina were not in general exposed. Besides stable crack extension, rapid fracture was possible mainly initiated at a discontinuity in orientation of the tracheid such as the points were the ray cells cross the line of tracheid. At higher temperatures and moisture contents, wood is less brittle because there is more viscous dissipation and unstable cracks are more infrequent and short in length.
Tension tests along the grain on gross wood show mostly failure within the fiber walls rather than between fibers (p.e. along the S_2 microfibrils). The overlap of the adjacent cells where the force is transmitted by shear in the middle lamella is thus in general sufficient long. As mentioned before, failure is possible between the S_1 and S_2 layers.
Tensile failure perpendicular to the grain follows, as in cleavage tests, the radial plane as preferred plane. Both transwall failure, which goes through the cells and the lumen, and intrawall failure, which occurs normally within the zone of the primary wall and S_1, are possible. An increase in temperature (0 to 150 ^{0}C) resulted in a high reduction of the tensile strength perpendicular to the grain and a reduction of trans-wall failures, indicating a reduction in bond strength between adjacent cells.
In compression parallel to the fiber direction, lines of buckling appear which make an angle on the tangential face of the specimen of about 60 degree to the axial direction, which lie in the radial direction. This is a consequence of shear failure between adjacent cells and the angle of 60 deg. in stead of 45 deg. is due to anisotropy. The failure takes place within the cell wall and only occasionally does separation occur along the middle lamella mostly in the regions adjacent to the rays. The existence of microscopic cracks is visible as loosening of the bonding between micro-fibrils and the implication is that the lateral cohesion between micro-fibrils of the secondary wall is less than between cells [11]. In [12] and [13] it is mentioned that rupture occurs at the cellulose-lignin interface (because of the preferentially staining with lignin stains).
Besides bond rupture (as follows from the increased chemical reactivity with dilute acid) micelle distortion occurs. There is a sequential development in types of dislocations (being permanent crinks of the fibrils) with increasing stress. Trust lines, being local thickenings of the cell wall by small fibril deformation, develop into slip planes which grow to bands of slip planes (creases) leading to failure with considerable buckling and delaminating of the cell walls. Slip planes develop at about 25% loading level and the number increases about linearly with stress level. At a level of about 50 to 65% creases (bands of more than 2 slip lines) are formed increasing parabolic with stress level. At 80 to 100% level, gross buckling of the cell walls occur containing about 40% of the total failure strain.
The development of these micro-failures is related to time at a given stress level. At relatively high moisture content, or when deformations develop slowly at low stress levels, the micro deformations are widely distributed through the specimen. Creep tests on wood show that after long time, depending on the stress level, the deformation may increase at a higher rate indicating the development of creases after long times.
At low moisture contents and rapid stressing at high stress levels the micro deformations are fewer in number and localized preferentially at rays.

For high compression perpendicular to the fiber direction, wherefore the modulus of elasticity of about one-tenth of the modulus in longitudinal direction, side-ways distortion of cells occur. The whole shape of the cell changes. When failure does take place separation occurs between the layers S_1 and S_2 of the secondary wall. The greater strength in radial direction than in tangential direction is due to support from the rays.

2.3.3 Failure of the ultra-structure

Two components of the fine or chemical structure have a profound influence on the strength and stiffness. The first consists of matrix material, the lignin-hemicellulose complex, and the second is the cellulose fiber material. Wood behaves as a reinforced material. To investigate the failure mechanism of the cellulose chains, Ifju [7] reported the effect of reducing the cellulose chain length by gamma irradiation. The degree of polymerization of the cellulose was reduced from 5000 down to about 200 by successive higher doses of radiation. If slippage of the chains is a cause of failure it can be expected that there will be a critical chain length where below failure is caused by slippage and where above failure is by primary bond breaking of the chain itself and is independent on the chain length (thus independent of the degree of polymerization). Based on an assumed very high activation energy of breaking of the -C-O-C- linkage and a very low activation energy of breaking of the lateral hydrogen bonds it was calculated that this critical length is reached at a degree of polymerization of about 70. The experiments however did show a decrease of the strength at any reduction of the degree of polymerization. The conclusion that slippage at a degree of polymerization of 5000 is between micelles or fibrils through the "loosely" amorphous cellulose (with very few side bonds) is surely not right, because this expected long range interaction would indicate an early occurrence of rubbery behavior. The stiffness is however not proportional to the absolute temperature, as is necessary for rubbery behavior, and also the transition with temperature is different (Arrhenius equation) and the molecular models show only a very localized slip of about a cellobiose unit.
Thus the basis of the calculated critical chain length is more complicated than assumed. This can be seen by the bonding model of cellulose of Giles as e.g. discussed in chapter 4 of [8] where a special type of bonding is assumed in order to explain the high experimental stiffness of cellulose.

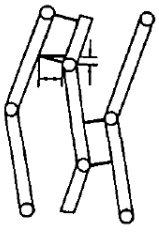

fig. 2.3 Scheme of a cellulose chain linked by hydrogen bonds

Straightening of the cellulose chain causes lateral stretching of the hydrogen bonds causing a four- to six- fold stiffness increase of the chain. Thus, if a chain is stretched, the hydrogen bonds may fail, reducing the stiffness of the chain and thus the stress on the chain. If within the crystalline region 4 successive hydrogen bonds have failed, the maximum reduction of the force is reached. The activation energy for this will be less than 4 x 6 = 24 kcal/mol, while for primary bond breaking the activation energy will be about 60 to 80 kcal/mol. This doesn't mean that a type of dislocation propagation by cooperative bond breaking of 4 bonds is the necessary failure mechanism. Also possible is e.g. the breaking

of 1 hydrogen bond with a rotation of 4 to 5 bonds of the glucose-rings (activation energy less than: 6 + 5x3.2 = 22 kcal/mol, to relieve a high chain force. Also for other polymers the flipping of the ring between two isomeric chair forms, is supposed to be a deformation mechanism. There is steric possibility for this movement [14] in cellulose. This mechanism, of breaking of one hydrogen bond, is in accordance with the measured first order reaction and the measured activation energy and volume of the bond breaking. Further the in [7] measured dependence of the strength on the logarithmic value of the degree of polymerization (being a measure of the logarithmic value of the numbers of cuts of the chain or the number of sources of dislocations) can be explained now by the in [1] developed molecular model. As shown later the flow-stress is:

$$\sigma = \frac{1}{\phi}\cdot\ln\left(\frac{2\dot{\varepsilon}}{A}\right) = \frac{1}{\phi}\cdot\ln\left(\frac{2\dot{\varepsilon}}{A'\rho}\right) = C_1 + \frac{1}{\phi}\cdot\ln(D)$$

where $\dot{\varepsilon}$ is the strain rate in a constant strain rate test, $A = A'\rho = \rho\cdot\nu\cdot\exp(-E/kT)$ is proportional to the flow unit density ρ, and D is the degree of polymerization being inversely proportional to the number of cuts, and thus inversely proportional to ρ. This leads to the expression:

$$\frac{\sigma_1}{\sigma_2} = 1 + \frac{1}{\phi\sigma_2}\cdot\ln\left(\frac{D_1}{D_2}\right)$$

By regression analysis, it can be shown that $1/\phi\sigma_2$ is constant, independent of temperature and moisture content and is about 0.11 for latewood and 0.17 for early-wood (coefficient of variation: 0.45). The values of this constant, $1/\phi\sigma_2$, indicate a different failure mechanism by irradiation than occurs normally in wood (showing values of about 0.03).

The change in molecular arrangement in the ordered, crystalline regions of the micelles by loading can be measured with the X-ray diffractometer [15]. Truly elastic behavior is due to chain straightening, orientation of crystallites or reorganization of the less ordered regions. Constant loading tests in tension show immediate orientation by loading and no increase in crystallinity with time (within 24 hours). Because X-ray diffraction shows only ordered regions of molecules, these regions only show elastic behavior. The alignment by loading gives some increase of the length of the crystallites and thus of the degree of crystallinity. At unloading (independent of the loading time) some alignment remains, indicating also some plasticity, increasing with increasing stress level (some of the new bonds recover at a not noticeable low rate by the low internal stress after unloading).

Time dependent molecular orientation activity in the amorphous regions can be observed by the infrared polarization technique. This was done in [16] for balsam fir tissues strained parallel to the fiber axis. The chosen adsorption bands in [16] contained no crystalline band with almost immediate orientation representing the elastic behavior. Thus the recorded bands gave the activity in the amorphous regions. In the chosen bands for lignin, hemicellulose and cellulose, only quick time dependent processes of orientation were recorded. The main slow stress relaxation process was not given. The explanation, given in [16], of the short periodic processes of loading and unloading as a result of the ability of the lignin network to act as an energy sink and to control the energy set up of the stressing is not probable. Obvious all components will be loaded on quick straining and because of the shorter retardation time of the lignin, the stress will be transmitted from the lignin to the cellulose chains instead of in the reversed direction. More probable is therefore that a type of dynamic crystallization occurs like in metals. Also in partly crystallized polymers this may occur if the degree of crystallinity increases during the straining. Thus a process of crystallization, flow and recrystallization may occur. A strong indication for this supposition is that the time of the process is dependent on the kinetics of crystallization and not on

the rate of straining or the viscoelastic properties and also that the stress of the relaxation test decreases during the orientation because like in the mentioned polymers the crystallization lowers the stress on the ends of the amorphous strands. This mechanism is however of minor importance, and need not be described, because the crystallization process in wood is very small so that it results only in a small wavy form of (or around) the main stress relaxation line. It can be concluded that there is a lack of the measurement of the main slow overall relaxation by this method.

2.4 References

[1] Concrete, Timber and Metals. J.M. Dinwoodie a.o. 1979, Van Nostrand Rheinhold Company, New York.
[2] Principles of Wood Science and Technology. F.F.P. Kollmann, W.A. Cote 1968, Springer-Verlag, Berlin New york.
[3] Recent progress in the study of the rheology of wood, A.P. Schniewind, Wood Science and Techn. Vol. 2)1968) p. 188-206.
[4] Berekeningsmodel voor horizontaal gelamineerde balken. T.A.C.M. van der Put, Rapport 4-83-16 GKH 6, 1983 Stevin-laboratorium Delft.
[5] Vingerlasverbindingen in horizontaal gelamineerd hout, T.A.C.M. van der Put, Rapport 4-76-5 VL5, 1976, Stevin-laboratorium Delft.
[6] Wood fibers in tension. B.A. Jayne, Forest Prod. J., 1960, 316-322.
[7] Tensile strength behavior as a function of cellulose in wood. G. Ifju, Forest Prod. J., 14, 1964, 366-372.
[8] Theory and Design of Wood and Fiber Composite Materials. B.A. Jayne Editor, pg. 83-95, 1972, Syracuse Wood Science Series, 3.
[9] Cell Wall Mechanics of Tracheids, R.E. Mark, 1967, Yale University Press, New Haven.
[10] Morphology and mechanics of wood fracture, G.R. Debraise, A.W. Porter, R.E. Pentoney, Mater. Res. Std., 6, 1966, 493-499.
[11] The anatomy and fine structure of wood in relation to its mechanical failure, A.B. Wardrop, F.W. Addo-Ashong, Proc. Tewksbury Symp. Melbourne, 1964, 169- 200.
[12] Failure in timber part II, The angle of shear through the cell wall during longitudinal compression stressing, J.M. Dinwoodie, Wood Science and Technology, Vol. 8, 1974, 56-67.
[13] Failure in timber part I, Microscopic changes in cell-wall structure associated with compression failure, J.M. Dinwoodie, Journal of the institute of wood science 21, 1968, 37-53.
[14] Ueber die Gestalt und die Beweglichkeit des Molekuls der Zellulose. P.H. Hermans, Kolloid Zeitsschrift, 102, Heft 2, 1943, 169-180.
[15] Cell-Wall Crystallinity as a Function of Tensile Strain. W.K. Murphy Forest Prod. J., April 1963.
[16] Molecular Rheology of Coniferous Wood Tissues, S. Chow, Transactions of the Soc. of Rheology 17:1, 1973, 109-128.
[17] Reaction kinetics of bond exchange of deformation and damage processes in wood, T.A.C.M. van der Put, Proc. IUFRO-conference Firence Italy, Sept. 1986.

3. Discussion of the basic principles of the theory of molecular deformation kinetics

3.1 Introduction

For plastic flow in a material, it is necessary to have "holes" into which the material may move, and a lowered energy potential (energy barrier) by the presence of this hole (with a bond strength of about a quarter of the bond strength in a perfect region for all materials). Thus the number of mobile molecules or mobile segments are determined by the number of these holes (called flow units).

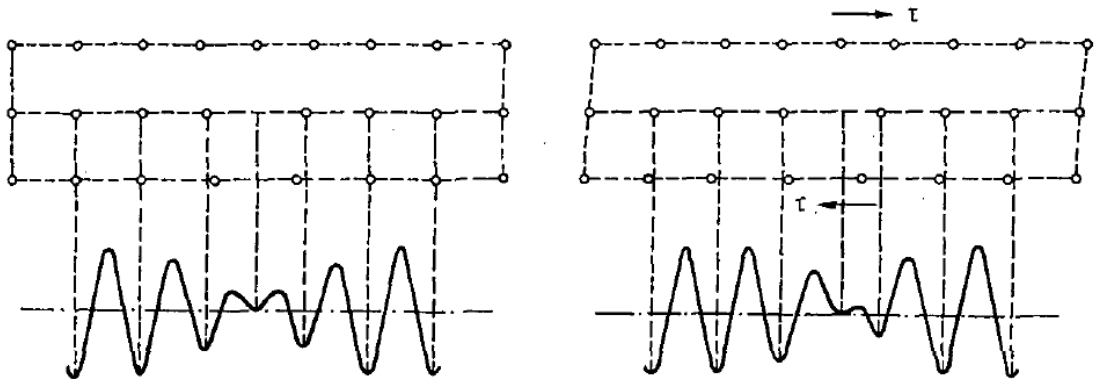

Fig. 3.1. Energy surface across an edge dislocation

The rate of flow is determined similarly as the chemical reaction rate of bond breaking and some aspects of this theory will be discussed to clarify the physical meaning of the constants of the basic equations that will be used for the derivation of a creep and damage model. The starting points on the reaction order, thermodynamics of the free energy change and parameters of the flow units are derived for use in the derivations of the next chapter 4.

3.2 Theory of reaction rates for plastic deformation in solids.

The basic concept of this theory is to regard plastic flow as a special form of a chemical reaction (like isomerization, where the composition remains constant but the bond structure of the molecules changes), because flow is a matter of molecular bond breaking and bond reformation in a shifted position.
An elementary form of the reaction rate equation is:

$$\frac{d\rho_2}{dt} = -\frac{d\rho_1}{dt} = \rho_1 \cdot C_f - \rho_2 \cdot C_b \qquad (3.2.1)$$

where ρ is the concentration of flow units, that may be kinks and holes in the polymers or vacancies and dislocation segments in the crystalline regions.
$C = \nu \cdot \exp(-E/kT)$ (where ν is a frequency) with:

E= the activation energy
k= Boltzmann's constant
T= the absolute temperature
Because there is a forward reaction into the product state and a backward reaction into the reactant state, there are two rate constants:

$$C_f = \nu \cdot \exp(-E_f / kT) \qquad (3.2.2)$$

$$C_b = \nu \cdot \exp(-E_b / kT) \qquad (3.2.3)$$

The molecules occupy equilibrium positions and are vibrating about the minimum of the free energy potential. Every position of the molecules with respect to each other determines a point of the potential energy surface. The molecules must reach an activated state on this potential surface in going from the reactant to the product state. The thermal energy is not equally divided among the molecules and it is a matter of chance for a molecule to get high enough energy to be activated and to be able to break bonds.

The explanation of the form of the rate constants C_i above is given by Bolzmann statistics.

$C = (kT/ h)\exp(-E/ kT)$,

$\upsilon = kT/ h$ can be approximated to the Debye frequency (about 10^{-13}) being the number of attempts per second of a particle to cross the barrier of height E. However, any attempt only succeeds when the energy of the particle exceeds E, and the probability of a jump per second is: $P = \upsilon.\exp(-E/ kT)$, where kT is the mean vibration energy of the particles (in that direction). Mostly not one group of reacting atoms is considered but a molar quantity. The molar free energy then is $E_m = N_m E$ and the Boltzmann constant k is replaced by the gas constant R, where $R = N_m k$ and N_m is Avogadro's Number. Thus:

$E /(kT) = N_m E/(N_m kT) = E_m /(RT)$.

$k = 8.616 \cdot 10^{-5}\ \mathrm{eVK^{-1}}$

$h = 4.135 \cdot 10^{-15}\ \mathrm{eV\,sec}$

$k/h = 2.084 \cdot 10^{10}\ \mathrm{sec^{-1}\,K^{-1}}$

$R = 1.9616\ \mathrm{cal\,K^{-1}mol^{-1}}$

$N_m = 6.02 \cdot 10^{23}$

1 Joule = 1Nm = $0.618 \cdot 10^{19}$ eV = 0.239 cal

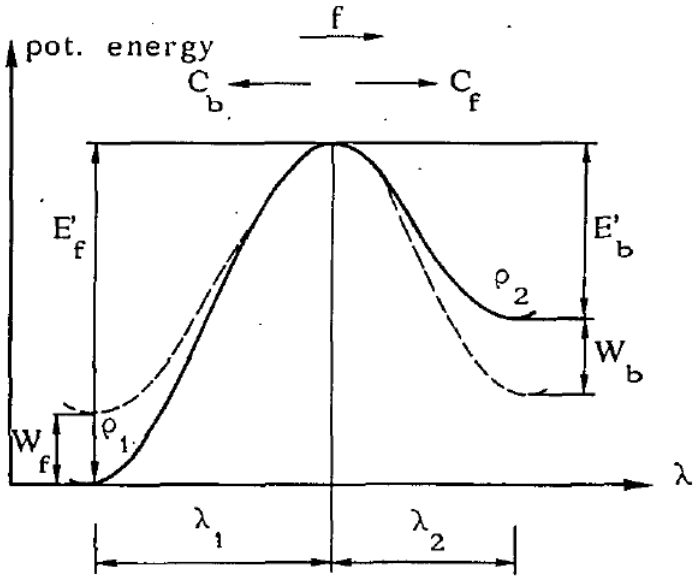

Fig. 3.2. Potential energy change for an elementary reaction [1].

The free energy of the activated complex consist of an enthalpy term, an entropy term and a work term due to the applied stress (see 3.4).

When the molecules are displaced from their equilibrium positions by an applied stress, the potential energy is increased. This means that the potential energy surface is changed,

making the reaction more probable, decreasing the barrier height with W_f in forward direction and increasing the barrier height with W_b in backward direction, where $W = W_f + W_b$ is the work of the external constraints. Thus:

$$C_f = \frac{kT}{h} \cdot \exp\left(\frac{-E_f^{'} + W_f}{kT} \right) \tag{3.2.4}$$

$$C_b = \frac{kT}{h} \cdot \exp\left(\frac{-E_b^{'} - W_b}{kT} \right) \tag{3.2.5}$$

3.3 Reaction order of deformation and fracture processes.

The first order reaction applies for solids, as is theoretical derived in § 2.4.1 of B(2005), also given in Section B.2: "Transformations of wood and wood like polymers". This is experimental confirmed for all processes in wood. This shows that there is one speed determining step and that there are no mechanisms with intermediate products. Further, the slightly lower value of the order than one, at higher concentrations, indicates that series reactions are acting (and not concurrent reactions).
Based on these results it is possible and convenient to obtain general solutions of the often complex reactions of transformations, by a sinus series expansion of the potential energy surface (as is discussed in Chapter 4). Based on the symmetry conditions of the orthogonal components there is a not changing, thus steady state, intermediate concentration in the successive steps causing a behavior like one elementary symmetrical reaction for each component. Even for the most complex reactions of decomposition of wood at high temperatures, the first order reaction applies, according to the "generalized flow theory", derived in Chapter 4 which is verified empirically in [2]: (with: W = weight loss; W_e = residual weight):

$$dW / dt = -\Sigma_i \, k_i \cdot (W - W_e) \tag{3.3.1}$$

The determining (slowest) bond breaking processes must be of first order in this case, because the overall reaction has an order close to one (at the highest rate), as follows from theory and from thermographic experiments [3].

3.4 Thermodynamics

The thermodynamic system is chosen to be a small volume around the dislocations (i.e. around the deformation- or fracture- site). This volume is surrounded by elastic material containing the effective stress (applied and internal stresses), and the temperature dependence of the elastic constants of this surrounding material has to be regarded separately. The local internal stresses σ at the sites act as external stresses on this closed system. The first law of thermodynamics, for a closed system, can be given in the differential relation of the change of the internal energy U of a process at constant pressure P, temperature T and stress σ.

$$dU = \delta Q - PdV + \delta W, \tag{3.4.1}$$

where δQ is the heat absorbed by the system; PdV is the work against pressure P by an increase of the total volume dV, and δW the other reversible work done by the system. $dQ = TdS$ is the change of entropy S by changes in volume, vibration spectrum and segment orientation. δW can be split here in the work done by the constant external stress σ, by a jump $d\lambda$ of a segment at activation, shifting the volume with $Ad\lambda$ (A is the area of

the cross section of the segment) and by other work terms. Thus: $\delta W = \sigma A d\lambda$.
Eq.(3.4.1) can now be written:
$dU - TdS + PdV = \sigma A d\lambda$. (3.4.2)
In this equation is $dU + PdV = dH$ called the change of enthalpy H, and $dH - TdS = dG$ is called the change of Gibbs free energy G, both under conditions of constant P and T. Thus eq.(3.4.2) becomes:
$dG = \delta W$, (3.4.3)
making it possible to calculate ΔG for an assumed mechanism. For a process in which only work is done by pressure, or $\delta W = 0$, eq.(3.4.1) gives:
$dH = \delta Q$, or $\Delta H = Q$. (3.4.4)
Thus for a process at constant pressure the heat exchanged between the system and the surroundings is the difference between the initial and final enthalpy of the system. A further consequence of eq.(3.4.4) is that the heat capacity at constant pressure C_p is:

$$C_p = \left(\frac{\delta Q}{\partial T}\right)_P = \left(\frac{\partial H}{\partial T}\right)_P \quad (3.4.5)$$

or:

$$\Delta C_p = \left(\frac{\partial \Delta H}{\partial T}\right)_P \quad (3.4.6)$$

Thus, the change of the heat of a reaction is directly related to the differences between the heat capacity of the products and that of the reactants (Kirchhoff's law), and depending on the sign of ΔC_P, the reaction is exo- or endothermic. If $\Delta C_P = 0$, the reaction is thermally neutral.
Because the energy change of a system, passing from one state to another, is independent of the particular course followed, the reaction may be split in different chemical steps if pressure, temperature and crystalline form are the same (Hess' law). The same can be done with other state properties e.g. volume or energy. As a consequence of this law, it is possible to expand the total potential energy curve into sinus series, as is done in the next chapter. Except for the first expanded term, this results in parallel rows of symmetrical barriers. Because, at zero stress, the forward and backward activation energy is the same for each barrier of the row, the reaction is neutral and the enthalpy change is constant independent of the temperature for the total row and because, at constant temperature and pressure, $\Delta C_P = T(\partial \Delta S / \partial T) = 0$, is also the entropy change ΔS constant during passage of the row. Thus the row acts as one process with a specific enthalpy and entropy, (both independent of the temperature) and with a specific activation volume.
If mass is added to the, above mentioned, closed system, for instance by absorbing moisture, the energy equation (3.4.1) becomes for zero δW:
$dU = \delta Q - PdV + \omega d\mu$, (3.4.7)
where ω is here the relative moisture content, or $\omega = 1$ at saturation of all bonds, and μ is the chemical potential or $d\mu$ is the change of the internal energy by saturation with water.
To find the potential energy change for a single process, thus without structural changes and other variations of the energy, a general thermodynamic potential E can be chosen in the determining variables T, λ and ω. The pressure P doesn't perform work for flow at constant volume and can be regarded to be constant.
$dE = d(H - TS - \sigma A\lambda - \mu\omega) = dH - TdS - SdT - \sigma A\, d\lambda - A\lambda\, d\sigma - \mu\, d\omega - \omega\, d\mu$ (3.4.8)
At equilibrium, or when P, T, λ and ω are constant, $dE = 0$, or:
$0 = dH - TdS - A\lambda\, d\sigma - \omega\, d\mu$ (3.4.9)
giving the first law of thermodynamics. Subtraction of eq.(3.4.9) from eq.(3.4.8) gives:

$$dE = -SdT - \sigma A d - \mu\, d\omega = \frac{\partial E}{\partial T}dT + \frac{\partial E}{\partial \lambda}d\lambda + \frac{\partial E}{\partial \omega}d\omega, \qquad (3.4.10)$$

being the second law.
As seen before, the enthalpy and entropy are constant with respect to T, (at zero stress), and thus $\partial E/\partial T$ is constant, and E is linear in T (by ST).
From the Maxwell relations: $\partial^2 E/\partial T\partial\lambda = \partial^2 E/\partial\lambda\partial T$, and so on, it can be found that:

$$-\frac{\partial S}{\partial \lambda} = -A\frac{\partial \sigma}{\partial T}; \quad A\frac{\partial \sigma}{\partial \omega} = \frac{\partial \mu}{\partial \lambda}; \quad \text{and} \quad \frac{\partial S}{\partial \omega} = \frac{\partial \mu}{\partial T}. \qquad (3.4.11)$$

If now the potential energy curve E, as function of λ (T, ω constant), is replaced by an equivalent straight line, then, in the first expression of eq(3.4.11) is $dS/d\lambda$ constant, independent on λ and T. Then S or E is linearly dependent on λ giving:

$$S = \lambda f_1(\omega) + f_2(\omega), \qquad (3.4.12)$$

and the stress σ will be, according to this first Maxwell relation:

$$\sigma A = Tf_1(\omega) + f_3(\omega,\lambda) \qquad (3.4.13)$$

Because E has the form: $E = -ST + f_4(\omega,\lambda,T)$,

$$E = -\lambda T f_1(\omega) - T f_2(\omega) + f_4(\omega,\lambda,T) \qquad (3.4.14)$$

Also E has the form: $E = -\sigma A\lambda + f_5(\omega,\lambda,T)$, or:

$$E = -\lambda T f_1(\omega) - \lambda f_3(\omega,\lambda) + f_5(\omega,\lambda,T). \qquad (3.4.15)$$

Because eq.(3.4.14) and eq.(3.4.15) has to be identical, *E* has the form:

$$E = -\lambda T f_1(\omega) - \lambda f_3(\omega,\lambda) - T f_2(\omega) + C \qquad (3.4.16)$$

where C is a constant. This equation satisfies the other Maxwell relations of eq.(3.4.11) and can be written:

$$E = C - \sigma\lambda A - T f_2(\omega). \qquad (3.4.17)$$

Thus E is linearly dependent on λ, σ and T. The value $\sigma\lambda$ is a function of ω and can be linearly dependent of T.

To determine the relations of ω, E can be regarded as function of the variables: ω, σ and T, or:

$$dE = -SdT - \lambda A\, d\sigma - \mu\, d\omega, \qquad (3.4.18)$$

giving the Maxwell relations:

$$\frac{\partial S}{\partial \sigma} = A\frac{\partial \lambda}{\partial T}; \quad A\frac{\partial \lambda}{\partial \omega} = \frac{\partial \mu}{\partial \sigma}; \quad \text{and} \quad \frac{\partial S}{\partial \omega} = \frac{\partial \mu}{\partial T}. \qquad (3.4.19)$$

The expansion of wood with moisture content is linear, thus $d\lambda/d\omega$ is constant and λ is linear dependent on ω. Also is λ linear dependent on T, (indicating a constant thermal expansion coefficient of λ up to activation). Thus $d\lambda/dT$ is linear with ω and also $dS/d\sigma$ and S. Further also μ is linear dependent on σ, ω and T, the same as S.
It is now shown that E can be assumed to be linear dependent on, σ,T and ω.

$$E = a_1 + a_2\omega + a_3 T + a_4\omega T + \sigma(a_5 + a_6\omega + a_7 T + a_8\omega T), \qquad (3.4.20)$$

and the energy change on activation has the same form:

$$\Delta E = \Delta a_1 + \Delta a_2\omega + \Delta a_3 T + \Delta a_4\omega T + \sigma(\Delta a_5 + \Delta a_6\omega + \Delta a_7 T + \Delta a_8\omega T). \qquad (3.4.21)$$

This can be given by a stress independent change of enthalpy H' and entropy S' denoted by a slash ', and a stress dependent part according to::

$$\Delta E = \Delta H' - \Delta S' T - \sigma V_a \qquad (3.4.22)$$

where V_a is the activation volume λA.
Leaving out the Δ – sign, because misunderstanding is not possible, is further used:

$E = H' - S'T - \sigma V_a = E' - \sigma V_a = E' - W,$ (3.4.23)

In this equation is, with the moisture content ω:

$H' = H_0 - \omega/\omega_m, \qquad S' = S_0 + S_1\omega/\omega_m, \qquad V_a = V_0 + (\omega/\omega_m)\left(V_1 T/T_m + V_2\right) + V_3 T/T_m,$

where T_m is a scaling temperature and ω_m the moisture content of saturation.

This thermodynamic law for activation parameters applies necessarily for all processes.

From tests of [4], it can be deduced that, for fracture processes, $H_1 = S_1 = 0$ and V_a is constant with respect to T for $\omega = 0$ (see later). Thus $V_3 = 0$ in that case.

3.5 Parameters of the flow units

For choosing an equilibrium system, as a limit analysis equilibrium solution, the reaction equations have to be expressed in the dimensions of the flow units. The total applied external stress: $\sigma_t = \sigma_e + \sigma$, where σ_e is the stress on the elastic material of the cross section and σ the stress on the mobile sites of the cross section (to be found by curve fitting).

If a segment is moving upwards, the hole 2λ in fig.3.5 is moving downwards. The activation volume V is 2λ times A, and the work, when moving over a barrier, of one unit is: $f \cdot V/2 = f \cdot A\lambda$, where f is the stress on the unit and A is the area. This can be expressed in the part of the mean stress on the flow units σ in the material by: σ = N.f.A where N is the number of elements per unit area. Thus the force per element, is the force per unit area divided by the number of elements per unit area. λ_1 is the length of the flow segment or the distance between flow-points. Thus the concentration of flow units ρ being the number of activated volumes per unit volume, can be written: $\rho = N2\lambda A/\lambda_1$.

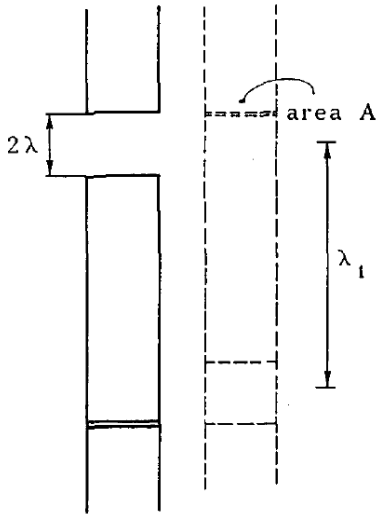

Fig. 3.5 Moving space

3.6 References

[1] Deformation kinetics. A.S. Krausz, H. Eyring 1975 John Wiley & Sns.
[2] Influence of Heat on Creep of Dry D.-Fir. E.L. Schaffer For. Prod. Lab. Madison, Wisconsin.
[3] Thermogravimetric Analysis of Pulps. Wood Science and Techn. V10-2 1976
[4] Ueber die Abhangigkeit der Festigk. d. Holzes v. d. Feuchte. J.M. Ivanov Holztechnologie 22 1981 1.

4. Derivation of a creep and damage limit analysis theory based on the theory of deformation kinetics

4.1. Introduction

In this chapter the mathematical derivation is given of a general creep- and damage- model that is solely based on the reaction equations of the bond-breaking and bond-reformation processes at the deformation sites due to the local stresses in the elastic material around these sites. The model doesn't contain the hidden suppositions of the other known models and is able to explain the phenomenological laws.

4.2. Basic reaction rate equations.

In this paragraph the reaction rate equations of [1] are given with all the steps of the derivation in order to see the modifications made in 4.3 to derive a generalized flow theory. Most models are based on the simple form of the reaction rate equation eq.(3.2.1) (for activation over a single potential energy barrier):

$$\text{Rate} = \frac{d\rho_2}{dt} = \rho_1 C_{1f} - \rho_2 C_{1b} = \frac{\rho_1 - \rho_2 C_{1b}/C_{1f}}{1/C_{1f}} \qquad (4.2.1)$$

being a poor approximation of eq.**Fout! Verwijzingsbron niet gevonden.** and eq.**Fout! Verwijzingsbron niet gevonden.** and will lead to variable activation parameters in different circumstances.
This is the case, because for larger, noticeable, plastic deformations, the reaction occurs over a system of energy barriers and systems of consecutive and parallel barriers have to be regarded.
For a two barrier system (fig.4.2) there is an intermediate stage of units being in steady state concentration. Thus:

$$\frac{d\rho_2}{dt} = 0 = -\rho_2\left(C_{2f} + C_{1b}\right) + \rho_{1f} C_{1f} + \rho_3 C_{2b} \qquad (4.2.2)$$

The net numbers of units crossing the two barrier system is thus:

$$\text{Rate} = \rho_2 C_{2f} - \rho_3 C_{2b} = C_{2f} \cdot \frac{\rho_1 C_{1f} + \rho_3 C_{2b}}{C_{2f} + C_{1b}} - \rho_3 C_{2b} =$$

$$= \frac{\rho_1 - \rho_3 \cdot \left(C_{1b}/C_{1f}\right) \cdot \left(C_{2b}/C_{2f}\right)}{1/C_{1f} + C_{1b}/\left(C_{1f} C_{2f}\right)} \qquad (4.2.3)$$

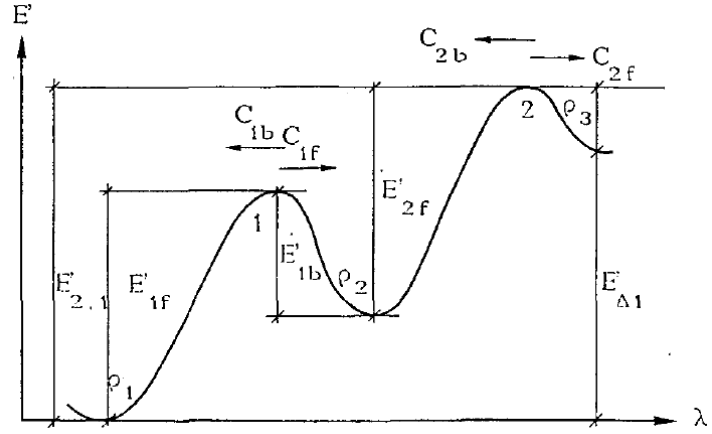

fig. 4.2. Two consecutive barriers [1]

For each obstacle i we have:

$$C_i = \kappa_i \frac{kT}{h} \exp\left(-\frac{E_i}{kT}\right) \tag{4.2.4}$$

or:

$$\frac{C_{ib}}{C_{i+1,f}} = \exp\left(\frac{E_{i+1,f} - E_{ib}}{kT}\right) \tag{4.2.5}$$

and:

$$\frac{C_{1b}}{C_{2,f}C_{1,f}} = \frac{h}{\kappa kT}\exp\left(\frac{E_{2f} - E_{1b} + E_{1f}}{kT}\right) = \frac{h}{\kappa kT}\exp\left(\frac{E_{2,1}}{kT}\right) = \frac{1}{C_{2,1}} \tag{4.2.6}$$

Similarly:

$$\frac{C_{1b}C_{2b}}{C_{1f}C_{2f}} = \exp\left(\frac{E_{1f} - E_{1b} - E_{2b} + E_{2f}}{kT}\right) = \exp\left(\frac{E_{\Delta 1}}{kT}\right) \tag{4.2.7}$$

Thus the rate becomes: (with E = E' - W)

$$\text{Rate} = \frac{\rho_1 - \rho_3 \cdot \exp\left(\frac{E'_{\Delta 1} - W_{\Delta 1}}{kT}\right)}{1/C_{1,1} + 1/C_{2,1}}, \tag{4.2.8}$$

with:

$$C_{1,1} = \kappa \frac{kT}{h}\exp\left(-\frac{E'_{1,1} - W_{1,1}}{kT}\right) \tag{4.2.9}$$

$$C_{2,1} = \kappa \frac{kT}{h}\exp\left(-\frac{E'_{2,1} - W_{2,1}}{kT}\right) \tag{4.2.10}$$

and

$$\begin{aligned} E_{\Delta 1} &= \left(E' - W\right)_{1f} - \left(E' + W\right)_{1b} - \left(E' + W\right)_{2b} + \left(E' - W\right)_{2f} = \\ &= \left(E'_{1f} - E'_{1b} - E'_{2b} + E'_{2f}\right) - \left(W_{1b} + W_{1f} + W_{2b} + W_{2f}\right) = E'_{\Delta 1} - W_{\Delta 1} \end{aligned} \tag{4.2.11}$$

$$\begin{aligned} E_{2,1} &= E_{1f} - E_{1b} + E_{2f} = \left(E' - W\right)_{1f} - \left(E' - W\right)_{1b} + \left(E' - W\right)_{2f} = \\ &= E'_{1f} - E'_{1b} + E'_{2f} - \left(W_{1f} + W_{2f} + W_{1b}\right) = E'_{2,1} - W_{2,1} \end{aligned} \tag{4.2.12}$$

$$C_{1,1} = C_{1f}$$

In the same way is for n obstacles in series:

$$\text{Rate}_n = \frac{\rho_1 - \rho_{n+1}\exp\left(E_{\Delta 1}/kT\right)}{\sum_{i=1}^{n}\left(1/C_{i,1}\right)} \tag{4.2.13}$$

with:

$$C_{i,1} = \kappa \frac{kT}{h}\exp\left(-\frac{E_{i,1}}{kT}\right) \tag{4.2.14}$$

For m processes parallel:

$$\mathrm{Rate}_{m,n} = \sum_{j=1}^{m}\left(\frac{\rho_1 - \rho_{n+1}\exp\left(E_{\Delta 1}/kT\right)}{\sum_{i=1}^{n}\left(1/C_{i,1}\right)}\right) \qquad (4.2.15)$$

4.3. Derivation of a general creep- and damage- model by series expansion

The general equations can be simplified to suitable forms for solutions of the rate equations as will be shown in the following.
It is possible to expand the total potential energy curve into (Fourier-) series and regard the process as a parallel acting system of symmetrical consecutive barriers.
Except of the first term, (see fig. 4.3.1) which is only symmetrical at loading to W_0, (see eq.(4.3.14), is in all series $E'_{\Delta 1} = 0$ (see fig.4.2) and because of the symmetry of the barriers in the series, all $E_{i,j}$'s and all $W_{i,j}$'s are equal.

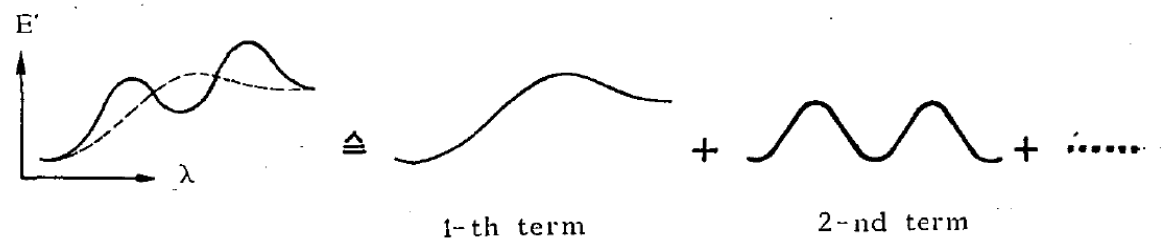

fig. 4.3.1 Series approximation of E'

By eq.(4.2.9): $C_{1,1} = \kappa\frac{kT}{h}\exp\left(-\frac{E'-W}{kT}\right)$ (4.3.1)

By eq.(4.2.10): $C_{2,1} = \kappa\frac{kT}{h}\exp\left(-\frac{E'-3W}{kT}\right)$ (4.3.2)

Eq.(4.2.14) becomes: $C_{i,1} = \kappa\frac{kT}{h}\exp\left(-\frac{E'-(2i-1)W}{kT}\right)$ (4.3.3)

Thus:

$$\sum\frac{1}{C_{i,1}} = \frac{1}{\kappa\frac{kT}{h}\exp\left(\frac{-E'}{kT}\right)}\cdot\left(\frac{1}{\exp\left(\frac{W}{kT}\right)} + \frac{1}{\exp\left(\frac{3W}{kT}\right)} + \ldots + \frac{1}{\exp\left(\frac{(2i-1)W}{kT}\right)}\right) =$$

$$= \frac{1}{\kappa\frac{kT}{h}\exp\left(\frac{-E'}{kT}\right)}\cdot\left(\frac{1}{\exp\left(\frac{W}{kT}\right)} + \frac{1}{\left(\exp\left(\frac{W}{kT}\right)\right)^3} + \ldots + \frac{1}{\left(\exp\left(\frac{W}{kT}\right)\right)^{2i-1}}\right) =$$

$$= \frac{1}{\kappa \frac{kT}{h} \exp\left(\frac{-E'}{kT}\right)} \cdot \left(\frac{\frac{1}{\exp(W/kT)}\left(1 - \left(\frac{1}{\exp(W/kT)}\right)^{2i}\right)}{1 - 1/\left(\exp(W/kT)\right)^2} \right) =$$

$$= \frac{1}{\kappa \frac{kT}{h} \exp\left(\frac{-E'}{kT}\right)} \cdot \left(\frac{1 - \exp(-2iW/kT)}{\exp(W/kT) - \left(\exp(W/kT)\right)^{-1}} \right) =$$

$$= \frac{1 - \exp(-2iW/kT)}{\kappa \frac{kT}{h} \left(\exp\left(\frac{-E'}{kT}\right)\right) \cdot 2\left(\sinh\left(\frac{W}{kT}\right)\right)} \qquad (4.3.4)$$

The rate is from eq.(4.2.11) and (4.2.13), with $E_{\Delta 1} = E'_{\Delta 1} - W_{\Delta 1} = -W_{\Delta 1} = -2iW$:

$$\text{Rate} = \frac{\left(\rho_1 - \rho_{n+1} \cdot \exp\left(-2iW/kT\right)\right) \cdot \left(2\kappa\left(kT/h\right)\exp\left(-E'/kT\right) \cdot \sinh\left(W/kT\right)\right)}{1 - \exp\left(-2iW/kT\right)} =$$

$$= 2\kappa \frac{kT}{h} \rho_1 \cdot \exp\left(\frac{-E'}{kT}\right) \cdot \sinh\left(\frac{W}{kT}\right). \qquad (4.3.5)$$

Equilibrium (Rate= 0) is only possible for W= 0 for these barriers and from symmetry of $E = E_f = E_b$, ρ_1 has to be equal to ρ_{n+1}.

Calling: $1/((\kappa kT/h)\exp(-E'/kT)) = t_i$, the relaxation time of the i-th expanded term, eq.(4.3.5) can be written like a chemical reaction equation:

$$\frac{d\rho_{n+1}}{dt} = -\frac{d\rho_1}{dt} = \frac{2\rho}{t_i} \sinh\left(\frac{W_i}{kT}\right) \qquad (4.3.6)$$

Now the work W, of a flow unit with area $\lambda_2 \cdot \lambda_3$ moving over a barrier over a distance 2λ, is (see § 3.5):

$W = f \cdot \lambda_2 \cdot \lambda_3 \cdot \lambda = f \cdot V/2 = \sigma \cdot \lambda / N$,

where V is the activation volume and N is the number of activated flow units per unit area. The concentration of flow units, or the number of activated volumes per unit volume, is:

$\rho = N \cdot \lambda_2 \lambda_3 \cdot 2\lambda / \lambda_1$.

Eq.(4.3.6) can now be written (with $\phi_i = \left(\lambda / NkT\right)_i$):

$$\frac{d}{dt}\left(\frac{N\lambda\lambda_2\lambda_3}{\lambda_1}\right) = \frac{2N\lambda_2\lambda_3\lambda}{t_i\lambda_1} \cdot \sinh\left(\sigma_i\phi_i\right). \qquad (4.3.7)$$

or, for a constant structure, by constant $N \cdot \lambda_2 \cdot \lambda_3$, this becomes:

$$\frac{d}{dt}\left(\frac{\lambda}{\lambda_1}\right) = \frac{2\lambda}{t_i\lambda_1} \cdot \sinh\left(\sigma_i\phi_i\right), \qquad (4.3.8)$$

or because λ/λ_1 is a plastic strain ε:

$$\frac{d\varepsilon}{dt} = \dot{\varepsilon} = \frac{\varepsilon'_0}{t_i} \cdot \sinh\left(\sigma_i\phi_i\right) = \frac{1}{t'_i} \cdot \sinh\left(\sigma_i\phi_i\right),$$

with the apparent relaxation time $t'_i = t_i / \varepsilon'_0$ ($\varepsilon'_0 = 1$ is assumed for cellulose materials).

Thus eq.(4.3.6) gets the form for no structural change:

$$\dot{\varepsilon} = \frac{1}{t_i}\sinh\left(\sigma_i \phi_i\right). \tag{4.3.9}$$

The form of the first expanded term of the series (see fig. 4.3.1) should be symmetrical for the expanded W. Thus from eq.**Fout! Verwijzingsbron niet gevonden.**:

$$\text{Rate} = \kappa\frac{kT}{h}\left(\rho_1 \cdot \exp\left(-\frac{E'_{1f} - W_1}{kT}\right) - \rho_{n+1} \cdot \exp\left(-\frac{E'_{1b} + W_1}{kT}\right)\right) \tag{4.3.10}$$

For a creep process, it may be expected that the rate is zero for no external force (equilibrium) or $W_1 = 0$. Thus eq.(4.3.10) becomes:

$$\rho_1 \cdot \exp\left(-\frac{E'_{1f}}{kT}\right) = \rho_{n+1} \cdot \exp\left(-\frac{E'_{1b}}{kT}\right) \tag{4.3.11}$$

and eq.(4.3.10) can be written:

$$\text{Rate} = 2\kappa\frac{kT}{h}\rho_1 \cdot \exp\left(-\frac{E'_{1f}}{kT}\right) \cdot \sinh\left(\frac{W_1}{kT}\right)$$

or: $\dot{\varepsilon} = \frac{1}{t_1}\sinh\left(\sigma_1 \phi_1\right)$ (4.3.12)

For structural changes, as in crack propagation, the crack extension force must overcome the thermodynamic "surface" energy. Further energy is needed to change the material near the crack surface (the new surface contains more defects) and to fracture strong ordered areas of bonds, crossing the surface, that cannot be broken by thermal activation at normal temperatures. Thus, calling these energies W_0, the crack is in an equilibrium state with zero velocity when W = W_0. Eq.(4.3.10) then gives:

$$\rho_1 \cdot \exp\left(-\frac{E'_{1f} - W_0}{kT}\right) = \rho_{n+1} \cdot \exp\left(-\frac{E'_{1b} + W_0}{kT}\right)$$

and eq.(4.3.10) can be written:

$$\text{Rate} = \kappa\frac{kT}{h}\rho_1 \cdot \exp\left(-\frac{E'_{1f} - W_0}{kT}\right) \cdot \left(\exp\left(\frac{W_1 - W_0}{kT}\right) - \exp\left(-\frac{W_1 - W_0}{kT}\right)\right) =$$

$$= 2\kappa\frac{kT}{h}\rho_1 \cdot \exp\left(-\frac{E'_{1f} - W_0}{kT}\right) \cdot \sinh\left(\frac{W_1 - W_0}{kT}\right) \tag{4.3.13}$$

or, for a steady state process ($\rho_1 \approx$ constant):

$$\dot{\varepsilon} = \frac{1}{t_1} \cdot \sinh\left(\frac{W_1 - W_0}{kT}\right) \tag{4.3.14}$$

with:

$$\frac{1}{t_1} = \kappa\frac{kT}{h}\rho_1 \cdot \exp\left(-\frac{E'_{1f} - W_0}{kT}\right) \qquad \left(\approx \kappa\frac{kT}{h}\exp\left(-\frac{E'_{1f} + E'_{1b}}{2kT}\right)\right)$$

and:

$$W_0 = \left(E'_{1f} - E'_{1b}\right)/2 - kT\ln\left(\sqrt{\rho_1/\rho_{n+1}}\right) \approx \left(E'_{1f} - E'_{1b}\right)/2.$$

For higher stress levels is:

$$\sinh\left((W_1 - W_0)/kT\right) \approx 0.5 \cdot \exp\left((W_1 - W_0)/kT\right).$$

and:

$$\dot{\varepsilon} = \kappa \frac{kT}{h} \cdot \exp\left(-\frac{E_{1f}' - W_0}{kT} \right) \cdot \sinh\left(\frac{W_1 - W_0}{kT} \right) \approx \kappa \frac{kT}{2h} \cdot \exp\left(\frac{-E_{1f}' + W_1}{kT} \right) \approx$$

$$\approx \kappa \frac{kT}{h} \cdot \exp\left(-\frac{E_{1f}'}{kT} \right) \cdot \sinh\left(\frac{W_1}{kT} \right)$$

This is assumed for the next equations.

If there are different kinds of flow units acting together, the total applied stress is the sum of these components. Thus:

$$\sigma = \sum_i \sigma_i$$

where σ_i is the part of the total stress acting on the i-th group of units.

With $W_i = \sigma_i \phi_i$ is:

$$\sigma = \sum_i \frac{1}{\phi_i} \cdot \operatorname{arcsinh}(t_i \dot{\varepsilon}),$$

or:

$$\frac{\sigma}{\dot{\varepsilon}} = \sum_i \frac{t_i}{\phi_i} \cdot \frac{\operatorname{arcsinh}(t_i \dot{\varepsilon})}{t_i \dot{\varepsilon}} \tag{4.3.15}$$

For the terms with $t_i \dot{\varepsilon} << 1$ is: $\operatorname{arcsinh}(t_i \dot{\varepsilon}) / t_i \dot{\varepsilon} = 1$

and for terms with $t_i \dot{\varepsilon} >> 1$ is: $\operatorname{arcsinh}(t_i \dot{\varepsilon}) / t_i \dot{\varepsilon} = 0$.

Thus there remain a limited number of terms:

$$\frac{\sigma}{\dot{\varepsilon}} = \sum \frac{t_i}{\phi_i} + \sum \frac{1}{\phi_i \dot{\varepsilon}} \operatorname{arcsinh}(t_i \dot{\varepsilon}_i) \tag{4.3.16}$$

The first term of (4.3.16) can be expressed in a mean value:

$$\sum \frac{x_i t_i}{\varphi_i} = t_1 \sum \frac{x_i}{\varphi_i} = t_1 \sum \frac{x_i t_i}{\varphi_i} = t_1 x_1 \sum \frac{1}{\varphi_i} = t_1 x_1 / \varphi_1 \tag{4.3.17}$$

and eq.(4.3.16) gets the form of the generalized flow theory [1] consisting of separate symmetrical elements:

$$\frac{\sigma}{\dot{\varepsilon}} = \frac{x_1 t_1}{\varphi_1} + \frac{x_2 t_2}{\varphi_2} \frac{\operatorname{arcsinh}(t_2 \dot{\varepsilon})}{t_2 \dot{\varepsilon}} + \frac{x_3 t_3}{\varphi_3} \frac{\operatorname{arcsinh}(t_3 \dot{\varepsilon})}{t_3 \dot{\varepsilon}} \tag{4.3.18}$$

Thus, by series expansion, the assumptions of this generalized flow theory have now been proven:

a) The flow unit spectrum exists as expanded terms and may be approximated by a limited number of elements with distinct average relaxation times. (As experimentally found [2], less than 3 groups are sufficient for a description of most materials).

b) The deformation rate of all units is the same (in accordance with the observations that there are no structural changes due to rate differences during flow).

The first term of eq.(4.3.18) represents Newtonian behavior. The others are non-Newtonian, or Newtonian in the low strain rate range.

The physical meaning of the expansion of the potential energy curve is to regard the total process as a result of parallel acting simple processes. For instance, a dislocation may meet different kinds of obstacles and the mean waiting time per obstacle at the end of the process is the mean of the waiting times at the different obstacles. At higher stresses these waiting times may change differently for the different obstacles and the apparent activation energy and volume may be stress dependent. Expansion means that groups of dislocations are supposed to meet only one type of obstacle. Each group meets another type of the same

obstacles in succession, resulting in a number of parallel acting simple reactions. In elementary reactions, (as the damage process in wood) the activation parameters (enthalpy, entropy) are constant (for temperature) as follows from thermodynamics § 3.4, so that a simple description of the total rate process becomes possible.

An experimental verification (by relaxation tests) of this behavior follows from [3] for metals. Those metals that where described with single barrier mechanisms, often had a stress dependent activation energy or volume. This was not the case for the metals which

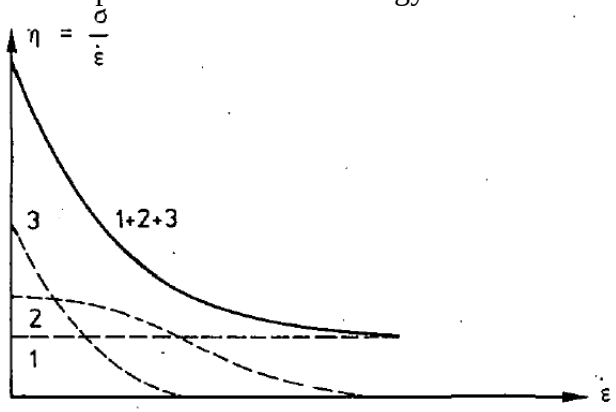

fig. 4.3.2 Viscosity-strain rate relation [1]

were described by two (thus more than one) parallel symmetrical barriers. The enthalpy and entropy were also constant, (as follows from thermodynamics theory given in § 3.4). The same has be done for wood by preliminary tests of B(1989a) and for cotton in [4] (that has a similar structure as wood). The two symmetrical barriers had constant, stress independent activation parameters.

4.4. Basic equations for fracture.

Eq.(4.3.18) applies for the steady state process, (as creep) when the structure and bond density do not change. Crack initiation and propagation occur when the rate of bond breaking exceeds the rate of bond re-establishment, leading to structural changes. For this case, eq.(4.3.6) does not lead to the constant structure eq.(4.3.8), but takes the form:

$$\frac{d}{dt}\left(\frac{N\lambda}{\lambda_1}\right)=\frac{2N\lambda}{\lambda_1 t_r}\sinh\left(\frac{\sigma\lambda}{NkT}\right), \qquad (4.4.1)$$

where the change of N may be due to primary bond breaking. If λ_1 can be regarded as a constant length of the flow segment, as can be expected if there is no change in flow unit density, then N can also be interpreted as the number of bonds along the flow segment and a change of N will be the change of the number of bonds along the segments. Thus N or λ may change in eq.(4.4.1) whether bond density changes (N) or change in free volume (λ) is expected to cause fracture. Both models give the same results because eq.(4.4.1) is for constant $\lambda=\lambda_0$ (and decreasing N), according to eq.(4.3.6):

$$-\frac{dN_1}{dt}=\frac{2N_1}{t_r}\sinh\left(\frac{\sigma\lambda_0}{N_1kT}\right),$$

or:

$$-\frac{d\left(1/N_1\right)}{dt}=\frac{1}{N_1}\frac{2}{t_r}\sinh\left(\frac{\sigma\lambda_0}{N_1kT}\right) \qquad (4.4.2)$$

For constant $N_1 = N_{n+1} = N$ and variable, increasing λ, eq.(4.3.6) leads to:

$$\frac{dN_{n+1}\lambda}{dt} = \frac{2N_1\lambda}{t_r}\sinh\left(\frac{\sigma\lambda}{N_1kT}\right)$$

or:

$$\frac{d\lambda}{dt} = \frac{2\lambda}{t_r}\sinh\left(\frac{\sigma\lambda}{NkT}\right) \tag{4.4.3}$$

Thus, eq.(4.4.2) in 1/N is exactly the same as eq.(4.4.3) in λ. The choice is thus possible to regard λ as a constant (as done for crystals and metals, (where λ is taken to be equal to the Burger's vector) or to take N as constant (when slip of the chains is expected to cause failure).

A third possibility for fracture is the change of λ_1 (by the part of the change of bond density along the segment or change in flow unit density that doesn't decrease the stressed area). Then eq.(4.4.1) becomes:

$$-\frac{d\left(1/\lambda_1\right)}{dt} = \frac{1}{\lambda_1}\frac{2}{t_r}\sinh\left(\frac{\sigma\lambda}{NkT}\right) \tag{4.4.4}$$

In the following it will be shown that both models eq.(4.4.2) and eq.(4.4.4) may give the same results. So that the simplest equation (4.4.4) can be used for applications.

Because fracture occurs at higher stresses, eq.(4.4.2) can be written:

$$-\frac{dN_1}{dt} = \frac{2N_1}{t_r}\sinh\left(\frac{\sigma\lambda_0}{N_1kT}\right) = \frac{N_1}{t_r}\exp\left(\frac{\sigma\lambda_0}{N_1kT}\right), \tag{4.4.5}$$

or for constant stress σ:

$$\int_{\sigma\lambda/N_0kT}^{\infty}\left(\frac{dN_1^{-1}}{N_1^{-1}}\exp\left(\frac{\sigma\lambda}{kT}N_1^{-1}\right)\right) = \frac{t_f}{t_r} \tag{4.4.6}$$

where t_f is the lifetime of the specimen subjected to a constant stress. The integral, in eq.(4.4.6), is the exponential integral: $-E_i\left(x\right)$ reducing for larger values of the variable to:

$$-E_i\left(-\frac{\sigma\lambda}{NkT}\right) \approx \frac{\exp\left(-\lambda\sigma/N_0kT\right)}{\lambda\sigma/N_0kT}, \tag{4.4.7}$$

Thus eq.(4.4.6) becomes:

$$t_f = t_r\frac{N_0kT}{\sigma\lambda}\exp\left(-\frac{\lambda\sigma}{N_0kT}\right) = \frac{N_0h}{\kappa\lambda\sigma}\exp\left(\frac{E'}{kT} - \frac{\lambda\sigma}{N_0kT}\right), \tag{4.4.8}$$

or:

$$\ln\left(t_f\right) = \ln\left(\frac{N_0h}{\kappa\sigma\lambda}\right) + \frac{E'}{kT} - \frac{\lambda\sigma}{N_0kT} \tag{4.4.9}$$

In the same way eq.(4.4.4) can be integrated:

$$\int_{1/\lambda_{10}}^{1/\lambda_{1m}} d\left(\ln\left(1/\lambda_1\right)\right) = \frac{t_f}{t_r}\exp\left(\frac{\sigma\lambda}{N_0kT}\right) = \ln\left(\frac{\lambda_{10}}{\lambda_{1m}}\right), \tag{4.4.10}$$

or:

$$t_f = \frac{h}{\kappa kT}\ln\left(\frac{\lambda_{10}}{\lambda_{1m}}\right)\cdot\exp\left(\frac{E'}{kT} - \frac{\sigma\lambda}{N_0kT}\right)$$

or:

$$\ln\left(t_f\right)=\ln\left(\frac{h}{\kappa kT}\ln\left(\frac{\lambda_{10}}{\lambda_{1m}}\right)\right)+\frac{E'}{kT}-\frac{\sigma\lambda}{N_0kT}=\ln\left(t_0\right)+\frac{E'}{kT}-\frac{\sigma\lambda}{N_0kT} \tag{4.4.11}$$

giving the same form as eq.(4.4.9). Eq.(4.4.11) gives a strain criterion for failure:

$$t_0=\frac{h}{\kappa kT}\ln\left(\frac{\lambda_{10}}{\lambda_{1m}}\right) \tag{4.4.12}$$

or:

$$\frac{\lambda_{10}}{\lambda_{1m}}=\frac{\varepsilon_m}{\varepsilon_0}=\exp\left(\frac{\kappa kT}{h}t_0\right). \tag{4.4.13}$$

From tests [5] it is found that t_0 in eq.(4.4.11) or eq.(4.4.9) has a definite value for the many materials tested, being the reciprocal of the natural oscillation frequency of atoms in solids. It is seen that t_0 is not constant in eq.(4.4.9) being the error of integrating with a constant (mean value) λ_1. This error diminishes when T approaches zero as can be seen in eq.(4.4.13): $\lambda_1\to\lambda_{1m}$ when $T\to 0$.

It follows that the bond breaking model in this form, changing only the value of N, only applies near absolute zero temperature for small values of E' and $\sigma\lambda/N_0$ (because $E'=\sigma\lambda/N_0=h/t_0$ for $T\to 0$), and thus for wood, which shows higher values of E' and $\sigma\lambda/N_0$, there will be always changes in $1/\lambda_1$ at failure.

To show the amount of change of N and, $1/\lambda_1$ eq.(4.4.1) can be written:

$$\frac{d\left(\lambda/N\lambda_1\right)}{dt}=\frac{2\lambda}{N\lambda_1t_r}\sinh\left(\frac{\sigma\lambda}{NkT}\right)\approx\frac{\lambda}{N\lambda_1t_r}\exp\left(\frac{\sigma\lambda}{NkT}\right) \tag{4.4.14}$$

$$\frac{d\left(\ln(\lambda/N)\right)}{dt}+\frac{d\left(\ln(1/\lambda_1)\right)}{dt}=\frac{1}{t_r}\exp\left(\frac{\sigma\lambda}{NkT}\right)- \tag{4.4.15}$$

$$\left(1+A\right)\frac{d\left(\ln(1/\lambda_1)\right)}{dt}=\frac{1}{t_r}\exp\left(\frac{\sigma\lambda}{NkT}\right) \tag{4.4.16}$$

where A is the mean value of: _

$\frac{d\left(\ln(1/\lambda_1)\right)/dt}{d\left(\ln(\lambda/N)\right)/dt}$ and: A = 0, when λ_1 is constant.

$$\int_{\lambda/N_0}^{\infty}\frac{d\left(\ln\left(\lambda/N\right)\right)}{\exp\left(\sigma\lambda/NkT\right)}=\int_0^{t_f}\frac{dt}{\left(1+A\right)t_r}\to E_1\left(\frac{\sigma\lambda}{N_0kT}\right)=\frac{t_f}{\left(1+A\right)t_r}\to$$

$$\frac{\exp(-\sigma\lambda/N_0kT)}{\sigma\lambda/N_0kT}\approx\frac{t_fkT}{\left(1+A\right)h}\exp\left(-\frac{E'}{kT}\right) \tag{4.4.17}$$

Or with $\upsilon=1/t_0$:

$$\exp\left(\frac{E'}{kT}-\frac{\sigma\lambda}{N_0kT}\right)=\frac{1}{\left(1+A\right)}\frac{t_f}{t_0}\frac{kT}{h\upsilon}\frac{\sigma\lambda}{N_0kT}\to$$

$$\frac{E'}{kT}-\frac{\sigma\lambda}{N_0kT}=\ln\left(\frac{t_f}{t_0}\right)+\ln\left(\frac{kT}{h\upsilon}\frac{\sigma\lambda}{N_0kT}\frac{1}{\left(1+A\right)}\right)$$

According to the measurements, see fig. 4.4.1, is, with $kT/h\upsilon \approx 1$,

$$\ln\left(\frac{\sigma\lambda}{N_0 kT}\frac{1}{(1+A)}\right) = 0 = \ln(1) \rightarrow 1 + A = \frac{\sigma\lambda}{N_0 kT} \qquad (4.4.18)$$

Because $\sigma\lambda / N_0 kT$ (≈ 34) >> 1 for wood, is: A >> 1 and the change of $1/\lambda_1$ dominates the change of N, and N may be regarded as constant when a maximum strain condition is used for the end state.

The improbable results of the bond breaking model eq.(4.4.9) shows that the change of N will be different. It is seen, that eq.(4.4.8) and eq.(4.4.11) contain N_0, the constant initial value of N and not a variable value of N. Thus the result of the process is not influenced by the path followed and it is possible to regard steps in the total process where $1/\lambda_1$ changes at constant N_0, followed by a step where $1/\lambda_1$ is constant and N changes. These steps may be infinitely small. Then t_f according to eq.(4.4.11) will be shortened by the bond-breaking process according to eq.(4.4.8), and the time to failure is determined by the difference of the times of both processes. The result of the subtraction of both equations gives:

$$t_f = \left(\frac{h}{\kappa kT}\cdot\ln\left(\frac{\lambda_{10}}{\lambda_{1m}}\right) - \frac{N_0 h}{\kappa\sigma\lambda}\right)\cdot\exp\left(\frac{E}{kT} - \frac{\sigma\lambda}{N_0 kT}\right).$$

Thus for this case:

$$t_0 = \frac{h}{\kappa kT}\cdot\ln\left(\frac{\lambda_{10}}{\lambda_{1m}}\right) - \frac{N_0 h}{\kappa\sigma\lambda}, \quad \text{or:}$$

$$\ln\left(\frac{\lambda_{10}}{\lambda_{1m}}\right) = \frac{\kappa kT t_0}{h} + \frac{N_0 kT}{\sigma\lambda}$$

and it follows that there is a necessary ultimate strain condition for failure, determined by the point where all bonds are failed. Because the value of $kTN_0/\sigma\lambda$ is small for wood, there is a minor difference with the strain condition eq.(4.4.13).

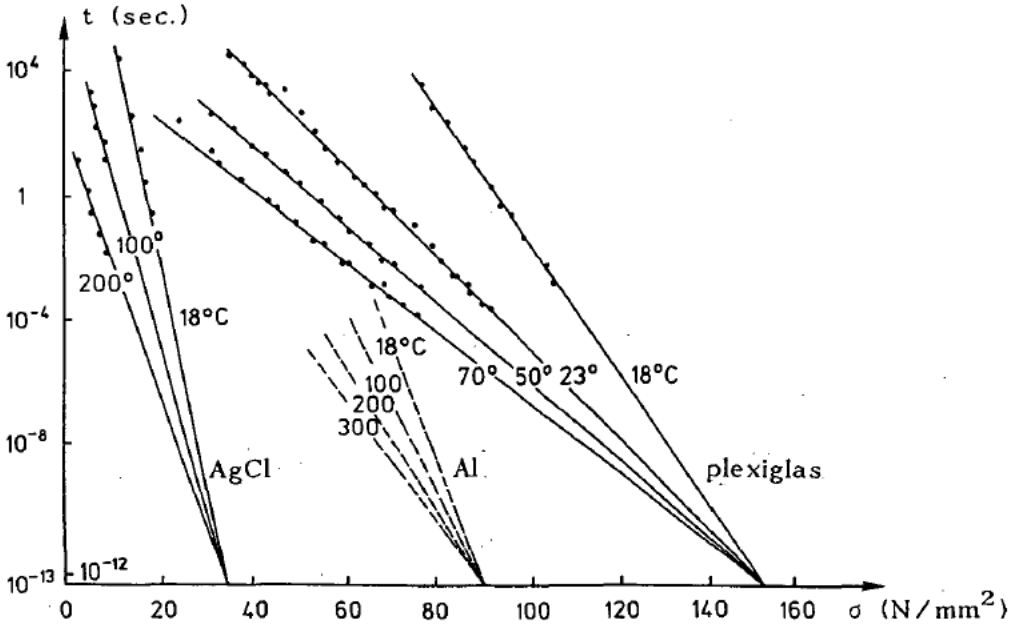

fig. 4.4.1 Stress and temperature dependence of the lifetime for some materials [5]

The derivations above are based on the relatively small initial value of $\lambda / N\lambda_1$. Wood and other structural materials also may show (at high local stress in the end state) a dominating process with a high initial value of $\lambda / N\lambda_1$ which doesn't change much with respect to the initial value, (thus determines a zero order reaction) and it is possible to regard a mean value of $\lambda / N\lambda_1$ in the right hand side of eq.(4.4.14). Integration then gives:

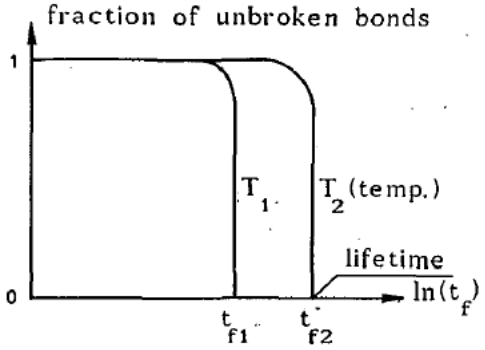

fig. 4.4.2 Lifetime of the bonds [8]

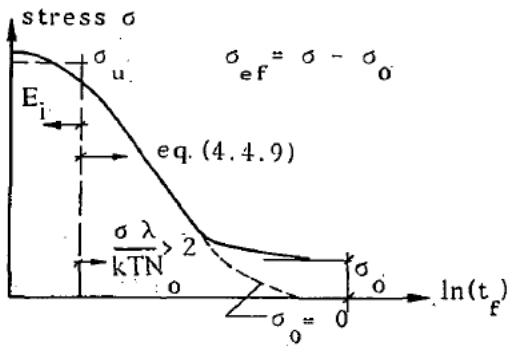

fig. 4.4.3 Long term strength

$$\frac{d}{dt}\left(\frac{\lambda}{\lambda_1 N}\right) \approx \frac{\lambda}{t_r \lambda_{10} N_0}\exp\left(\frac{\sigma\lambda}{N_0 kT}\right) \quad \rightarrow \qquad (4.4.19)$$

$$\frac{\lambda}{\lambda_1 N} = \frac{t_f}{t_r}\frac{\lambda}{\lambda_{10} N_0}\exp\left(\frac{\sigma\lambda}{N_0 kT}\right) + \frac{\lambda}{\lambda_{10} N_0} \quad \rightarrow$$

$$\left(\frac{\lambda}{\lambda_1 N_f} - \frac{\lambda}{\lambda_{10} N_0}\right)\frac{\lambda_{10} N_0}{\lambda} = \frac{t_f}{t_r}\frac{kT}{h\upsilon}\exp\left(-\frac{E'}{kT} + \frac{\sigma\lambda}{N_0 kT}\right) \quad \rightarrow$$

$$\frac{E'}{kT} - \frac{\sigma\lambda}{N_0 kT} \approx \ln\left(\frac{t_f}{t_0}\right) - \ln\left(\frac{N_0}{N_f} - 1\right) = \ln\left(\frac{t_f}{t_0}\right) - \ln\left(\frac{\varepsilon_f}{\varepsilon_0} - 1\right) \qquad (4.4.20)$$

According to fig.4.4.1, the left term of this equation is equal to: $\ln\left(t_f / t_0\right)$ leading to $N_f = 0.5 N_0$, as experimentally found for fracture (i.e. the crack length is about the crack distance, or the intact area has reduced to 0.5 times the initial area when instable crack propagation starts). This leads to the small crack merging model of fracture mechanics of Section C, which explains the measured mode I and mode II final softening behavior. Because λ / λ_1 is a strain, it is also possible to interpret this as an ultimate strain condition $\varepsilon_f / \varepsilon_0 = 2$ for a slip model. This slip model is the same as discussed in 4.3. In [6] this model was used and as has to be expected from the derivations above, it was found that a maximum shear strain condition has to be applied. This was compared by other tests [7] with the bonding-fracture model. Both models gave almost the same results as can be expected from the derivations above.

4.5. Fracture at constant loading rate and at creep loading

Numerical integration of the bond breaking eq.(4.4.2) [8] for constant loading rate is given in fig. 4.4.2, showing also the possibility to account for a constant value of N during the lifetime. This was also shown in § 4.4 and it is sufficient to use eq.(4.4.4). For a constant loading rate $\sigma = \dot{\sigma} \cdot t$ (with . $\dot{\sigma}$ = constant) this equation is:

$$\frac{d\left(\ln\left(1/\lambda_1\right)\right)}{dt} = \frac{2}{t_r}\sinh\left(\frac{\dot{\sigma}\lambda t}{NkT}\right) \tag{4.5.1}$$

or: $\ln\left(\frac{\lambda_{10}}{\lambda_{1m}}\right) = \frac{2NkT}{t_r\lambda\dot{\sigma}}\left(\cosh\left(\frac{\dot{\sigma}\lambda t_f}{NkT}\right)-1\right) \approx \frac{NkT}{t_r\lambda\dot{\sigma}}\exp\left(\frac{\dot{\sigma}\lambda t_f}{NkT}\right)$

for higher stresses. With $\dot{\sigma}t_f = \sigma_u$ this is:

$$\ln\left(\frac{h}{\kappa kT}\cdot\frac{\sigma\lambda}{NkT}\cdot\ln\left(\frac{\lambda_{10}}{\lambda_{1m}}\right)\right) = -\frac{E}{kT}+\frac{\sigma\lambda}{NkT} \tag{4.5.2}$$

Thus:

$$\ln\left(\frac{h}{\kappa kT}\cdot\frac{\sigma\lambda}{NkT}\cdot\ln\left(\frac{\lambda_{10}}{\lambda_{1m}}\right)\right) = -\frac{E}{kT}+\frac{\sigma\lambda}{NkT}$$

$$\ln\left(t_f\frac{NkT}{\sigma_u\lambda}\right) = \ln\left(\frac{h}{\kappa kT}\cdot\ln\left(\frac{\lambda_{10}}{\lambda_{1m}}\right)\right)+\frac{E}{kT}-\frac{\sigma\lambda}{NkT} = \ln\left(t_0\right)+\frac{E}{kT}-\frac{\sigma_u\lambda}{NkT} \tag{4.5.3}$$

This equation is the same as eq.(4.4.11). Thus the short-term failure time t_s is equivalent to a creep failure at level σ_u and life-time t_c:

$$t_c = t_s\cdot\frac{NkT}{\lambda\sigma_u} = \frac{NkT}{\lambda\dot{\sigma}}$$

The normalized creep strength creep strength divided by the short-term strength σ_s) is:

$$\frac{\sigma}{\sigma_s} = \frac{\frac{E'N}{\lambda}-\frac{NkT}{\lambda}\ln\left(\frac{t_f}{t_0}\right)}{\frac{E'N}{\lambda}-\frac{NkT}{\lambda}\ln\left(\frac{t_c}{t_0}\right)} = 1-\frac{\ln\left(t_f/t_c\right)}{\frac{E'}{kT}-\ln\left(\frac{t_c}{t_0}\right)} = 1-\frac{NkT}{\sigma_s\lambda}\ln\left(\frac{t_f}{t_c}\right) \tag{4.5.4}$$

For wood, eq.(4.5.4) is one line (see e.g. [9]) for different wood species, moisture contents, stress states(bending, shear, compression etc.) and types of loading, indicating the common strength determining mechanism determined by molecular deformation kinetics.
Another reason is possibly that there is one common strength determining element. This then will be the cellulose because the structure of cellulose is the same for all species.
Thus $\sigma_s\lambda / NkT = n$ has to be constant, independent of the density and moisture content.
According to thermodynamics, § 3.4, applies for the strength of wood polymers:
$t_0^{'} = t_0\exp\left(-S_0/k\right)$ and $E' = H' - S'T$ with $H' = H_0 - c\omega$ and $S' = S_0 + b\omega$, giving:

$$\sigma\lambda = NH_0 - Nc\omega - Nb\omega T - NkT\ln\left(t_f/t_0\right) \tag{4.5.5}$$

Extrapolation of eq.(4.5.4) to σ = 0, at $t_f = t_{f,m}$, shows that $t_{f,m}$ is constant because t_c is constant. Because t_s is a chosen time of the constant short term strength, is $t_c = t_s / n$ also constant. Extrapolation of eq.(4.5.5) to σ = 0 gives:

$$NH_0 - NkT\ln\left(t_{fm}/t_0^{'}\right) = Nc\omega + Nb\omega T$$

Because the left side of this equation is independent of the moisture content c and b must

be zero (Thus there is equilibrium for the stress independent part of the free energy due to equilibrium of moisture content $\Delta H'_\omega = T\Delta S'_\omega$).
The measured value [9] of the slope of the line, eq.(4.5.4) for t ≈ 3 sec.,(and not too long lifetimes at 20 ^{0}C) is:

$$\frac{d(\sigma/\sigma_s)}{d(\ln(t_s))} = \frac{NkT}{\sigma_s\lambda} = \frac{1.03}{17.1\ln(10)} = \frac{1}{38.2}.$$

Thus: $n = \frac{\sigma_s\lambda}{NkT} = 38$ (4.5.6)

This is comparable with the measured value of [10], if the equation is transformed to the 5 min. strength, giving the right measured value of 34 then.
As shown before, the main influence of a change of the content is the change of the activation volume of wood, which is shown to be linear dependent on the moisture content ω as confirmed by tests in [11].
Eq.(4.5.5) can now be written:

$$\sigma_u\lambda = \sigma_u(\lambda_0 + \lambda_{0,1}(T - T_0)) = NH' - NkT\ln(t_f / t_0) \quad (4.5.7)$$

in accordance with § 3.4 and the data of [11]. See fig. 4.5.2, where the modified activation volume V = λ / N is given.
A first estimate of the numerical values of T_0 and C_0/ω_m in:

$$\frac{V}{V_0} = 1 + C_0\frac{\omega}{\omega_m}(T - T_0) \quad (4.5.8)$$

are: (taken from the picture of [11] without the possibility of correction of the times to failure, that are not given and are probably not the same in all tests):
$T_0 = 265K$ and $C_0/\omega_m = 0.145$.
With these values, the lines in fig. 4.5.1, given by eq.(4.5.7), are:

$$\sigma_u = \frac{HN - NkT\ln(t_f / t'_0)}{\lambda_0\left(1 + C_0\frac{\omega}{\omega_m}(T - T_0)\right)} = \frac{193 - 0.35T}{1 + 0.145\omega(T - 265)} \quad (4.5.9)$$

showing that the straight line for $\omega = 0$, as well as the curved line for $\omega = 0.3$, can be given by one equation.
If it is assumed that the time of the short term tests is about 10 minutes, giving an equivalent step strength of about 20 sec, then:
$(NR/\lambda_0)\ln(20/10^{-13}) = 0.35$, or: NR/λ_0 = 1.06 10^{-2} and the enthalpy is:

H' = $193\lambda_0 / N$ = 193·1.987.10^{-3}/1.06.10^{-2} = 36 kcal/mol. (4.5.10)

n = $\sigma\lambda_0 / NRT \approx$ 93/(1.06.10^{-2}.293) = 30. (4.5.11)

According to [9] and [11], $t'_0 = t_0$, or S' = 0 is assumed.
The form of the equation of V = λ / N indicates a transition temperature of:
T_0 = 265 K = - 8 ^{0}C. (4.5.12)
Below this temperature is V = V_0 for tension, in agreement with the reported values of the tensile strength in [12] at low temperatures showing no influence of temperature and moisture content. For dry wood, $\omega = 0$, this transition disappears(and is not noticeable at low m.c.). Information about the mechanism that is determining for compression at low temperatures can be obtained by a fit of the measured values of e.g. [12]. The steep descent of the strength curves for $\omega = \omega_m$, indicates a small value of λ_0 / N and therefore λ_0 / N can be neglected as a first approximation. (For T $\rightarrow$ 0, this is not allowed).

With $\lambda / N = \sigma\lambda_{01} T / N$, eq.(4.5.2) becomes with $\omega = \omega_m$:

$$\sigma_u = \frac{H'N}{\omega_m \lambda_1 T} + \frac{Nk}{\omega_m \lambda_1} \ln\left(t_0' \frac{\omega_m \lambda_1 \sigma}{Nk} \right) \tag{4.5.13}$$

or scaled with respect to 20 ^{0}C or 293 K (Kelvin):

$$\sigma_u = \frac{H'N}{\omega_m \lambda_1 293} + \frac{Nk}{\omega_m \lambda_1} \ln\left(t_0' \frac{\omega_m \lambda_1 \sigma}{Nk} \right) + \frac{H'N}{\omega_m \lambda_1 T} - \frac{H'N}{\omega_m \lambda_1 293} =$$

$$= \sigma_{u,20} \left(1 + \frac{H'N}{\sigma_{u,20} \lambda_1 \omega_m} \left(\frac{1}{T} - \frac{1}{293} \right) \right) \tag{4.5.14}$$

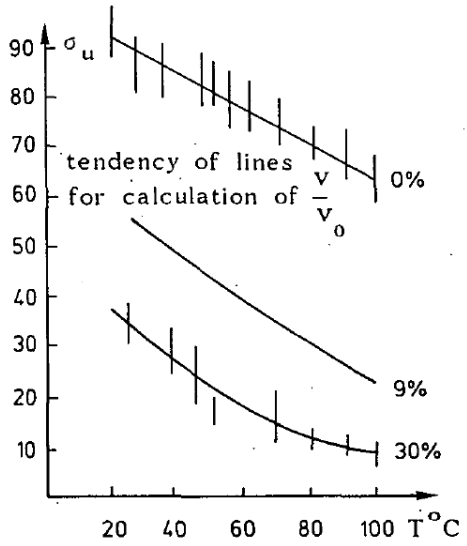

fig. 4.5.1 Compression strength of oak [11]

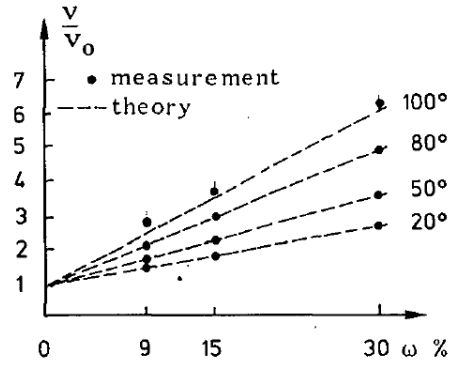

fig. 4.5.2 Activation volume

From the data of [12], the compression strength parallel to the grain of saturated wood is, (see fig. 4.5.3):

$$\frac{\sigma_u}{\sigma_{u,20}} = 1 + 845\left(\frac{1}{T} - \frac{1}{293} \right).$$

Thus:

$$\frac{H'N}{\sigma_{u,20} \omega_m \lambda_1} = 845 \qquad \text{or:} \qquad \frac{H'N}{\sigma_{u,20} \omega_m \lambda_1 293} = 2.88$$

Eq.(4.5.3) becomes:

$$\frac{\sigma_u \lambda}{H'N} = 1 + \frac{kT}{H'} \ln\left(\frac{t_0'}{t_f} \frac{\sigma_u \lambda}{NkT} \right) \rightarrow \frac{1}{2.88} = 1 + \frac{2 \cdot 0.29}{H'} \ln\left(\frac{t_0'}{t_f} \cdot \frac{H'}{2 \cdot 0.293 \cdot 2.88} \right) \tag{4.5.15}$$

giving a value of H' of about 30 kcal/mole, (if $t_0 / t_f = 10^{-13} / 600$ is a reasonable estimate). For dry wood, λ / N is constant and eq.(4.5.4) is nearly a straight line with respect to T because the influence of the temperature on t_c is small in the ln-function (see fig. 4.5.4). The enthalpy H' is about 36 kcal./mol, as found before.

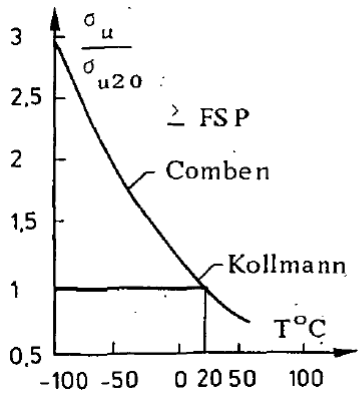

fig. 4.5.3 Saturated wood

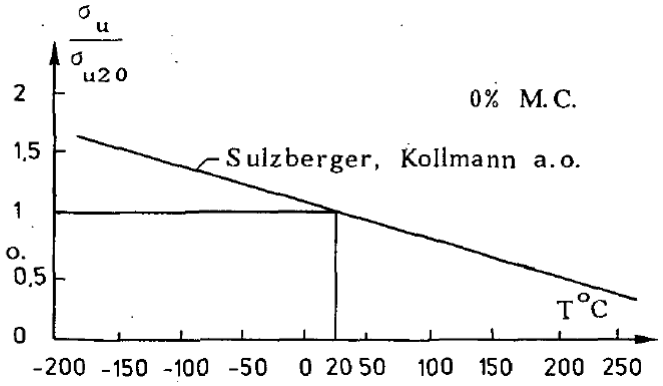

fig. 4.5.4 Dry wood

4.6 Power approximation of the rate equations.

As shown in 4.3, a range of successive processes can be given by eq. (4.3.5):

$$\text{Rate} = 2\kappa\frac{kT}{h}\rho_1 \exp\left(\frac{-E'}{kT}\right)\sinh\left(\frac{W}{kT}\right) \tag{4.6.1}$$

or for higher values of W (thus for higher stresses, in the neighborhood of σ_1):

$$\dot{\varepsilon} = \dot{\varepsilon}_0 \exp\left(\frac{W}{kT}\right) \quad \rightarrow \quad \frac{\dot{\varepsilon}}{\dot{\varepsilon}_1} = \exp\left(\frac{\sigma\lambda}{NkT} - \frac{\sigma_1\lambda}{NkT}\right) \approx 1 + \frac{\sigma\lambda}{NkT} - \frac{\sigma_1\lambda}{NkT} \tag{4.6.2}$$

The experimental power equation, as used in fracture mechanics, is:

$$\frac{\dot{\varepsilon}}{\dot{\varepsilon}_1} = \left(\frac{\sigma}{\sigma_1}\right)^n . \tag{4.6.3}$$

This can be written similar to eq.(4.6.2.), for high enough stresses:

$$\frac{\dot{\varepsilon}}{\dot{\varepsilon}_1} = \left(1 - \frac{\sigma_1 - \sigma}{\sigma_1}\right)^n \approx 1 - n\frac{\sigma_1 - \sigma}{\sigma_1} = 1 - n\left(1 - \frac{\sigma}{\sigma_1}\right) \tag{4.6.4}$$

Thus: $$n = \frac{\sigma_1\lambda}{NkT} \tag{4.6.5}$$

It is shown in § 4.5 that $\sigma_1\lambda / NkT$ is constant (for constant T), but is dependent on the scaling (i.e. the choice of the 1-sec.-strength or the 5-min.- short term strength). It is now shown that the empirical power form of the rate equation (4.6.3), is identical to the theoretical expression for activation over consecutive barriers if n is not too low, see also eq.(5.3.8). If there is a lower bound of stress σ_0, where flow can be ignored: $\dot{\varepsilon} = 0$, then the effective stress $\sigma - \sigma_0$, has to be taken in eq.(4.6.3).

Structural changes can be given by adding a linear term in ε in eq.(4.6.3). This is in conformity with dislocation mobility studies and other experiments. Then eq.(4.6.3) becomes:

$$\dot{\varepsilon} = (C + B\varepsilon)\left(\frac{\sigma - \sigma_0}{\sigma_1}\right)^n \tag{4.6.6}$$

For wood two main processes act at longer times:

$$\dot{\varepsilon} = C_1(1 + B_1\varepsilon)\left(\frac{\sigma - \sigma_0}{\sigma_1}\right)^n + C_2(1 + B_2\varepsilon)\left(\frac{\sigma - \sigma_0}{\sigma_1}\right)^m \tag{4.6.7}$$

In the first process then, the term $B_1C_1\varepsilon$ is small and for the second process $B_2C_2\varepsilon$ dominates and eq.(4.6.7) becomes:

$$\dot{\varepsilon} = C_1\left(\frac{\sigma-\sigma_0}{\sigma_1}\right)^n + C_2B_2\varepsilon\left(\frac{\sigma-\sigma_0}{\sigma_1}\right)^m \qquad (4.6.8)$$

Because the damage δ is proportional to the plastic deformation ε, this can be written:

$$\frac{d\delta}{dt} = C_1\left(\frac{\sigma-\sigma_0}{\sigma_1}\right)^n + C_3\delta\left(\frac{\bar{\sigma}-\sigma_0}{\sigma_1}\right)^m \approx C_1\left(\frac{\sigma-\sigma_0}{\sigma_1}\right)^n + C_4\delta \qquad (4.6.9)$$

where the constant mean internal stress $\bar{\sigma}$ acts in the second process. Then eq.(4.6.9) is the damage model of [13]. For creep-to-failure tests (σ = constant), a fit of the data of [13] gives n = 36 assuming $\sigma_0 = 0$. For $\sigma_0 = 0.48\sigma$, n = 34 is found in [10], giving about the same value of n. This is in accordance with the previous mentioned values (eq.(4.5.6)) confirming this interpretation of the power law.

Short term behavior is also determined by two main processes, as follows from the experiments of [14], where two values of n are given: n ≈ 62 for controlled crack growth tests, to n ≈ 65 in constant strain rate tests, and n ≈ 30 in constant (high) load tests to failure. In other experiments also values of n = 25 to 39 are mentioned. The variable value of n shows that more than two processes are acting at the same time and 2 values of n should have been found. Analyzing the creep values of [15] in [16], the existence of two parallel barriers was clearly demonstrated. The quick process had a high internal stress (forward activation only) and an activation energy of approximate 50 kcal/mole. The slower process was approximately symmetrical and had an activation energy of about 21 kcal/mole.

The activation energy of this process is comparable with values found in [17], where from creep tests at different temperatures for bending: H'= 22 kcal/mole to 24.4 kcal/mole, depending on the temperature range, have been found. From normal-to-grain relaxation tests 23 kcal/mole was reported for wet beech-wood in [18]. This energy is often regarded to be the energy of cooperative hydrogen bond breaking. The activation energy of 50 kcal/mole is high enough for cooperative C-O--bond or C-C-bond rupture.

The estimated value of H' of about 36 kcal/mole in 4.5, may be the result of a mixture of primary and secondary bond breaking at the same apparent activation volume.

Because the density of the cell wall is about 1.6/.35 times higher than the mean density of wood, an estimate of the real stress on the sites is:

f = (1.6/.35)·20 = 90 N/mm^2, and for n = 30 is,:

$\lambda\cdot\lambda_2\cdot\lambda_3 = 30\cdot kT/f = 30\cdot 1.39\cdot 10^{-20}\cdot 293/91 = 1.347\cdot 10^{-18}\,mm^3$.

Thus λ is of the order of: $(1.347.10^{-18})^{0.33} = 1.1.10^{-6}$ mm = 1.1 nm, or 1 cellobiose unit (see fig. 2.1.2). Processes wherefore n ≈ 60, thus may indicate an extend of the process to 2 cellobiose units.

Additional derivations of the theory of paragraphs 3, 4 and 5 are given in [19] to [24].

4.7 References

[1] Deformation kinetics. A.S. Krausz, H.Eyring 1975 John Wiley & Sns.
[2] Rheology, Theory and Applications. T.Ree, H. Eyring 1958 New York.
[3] Kinetics of stress relaxation in metals. J.F. Wilaon, N.R. Wilson, Transac. of the Soc. of Rheol. 1011, 399-418 1966.
[4] Mechanical Prop. of Textiles J.A.Lasater, E.L.Nimer, H.Eyring Text. Res. J. 23- 237-1953.

[5] Kinetic Concept of the strength of Solids S.N. Zhurkov Int.J.Fract. Mech.I, 311, 1965.
[6] J.Polym.Sci. 20,447 1956 B. Coleman.
[7] Int.J.Fract.Mech. 6,33 1970 and J.Fract.Mech. 5, 57,1969 C.B.Hen-derson P.H.Graham, C.N.Robinson.
[8] Influence of Heat on Creep of Dry D.-Fir. E.L.Schaffer For.Prod. Lab. Madison, Wisconsin.
[9] Bestimmung der Dauerfestigk. v. Holzkonstr… . J.M. Ivanov Holz-technol. 14-1973-4.
[10] Duration of Load Test Data Analysis R.O. Foschi, J.D. Barrett pap. G4 IUFRO-Meeting 1980 Oxford, England.
[11] Ueber die Abhängigkeit der Festigk. d. Holzes v. d. Feuchte. J.M. Ivanov Holztechnologie 22 1981 1.
[12] Effect of Moisture Content and Temperature. Gerhards Wood and Fib. Jan. 1982 14 1.
[13] First Int. Confer. on Wood Fracture. 1978 Banff, Alberta Canada R.O. Foschi and J.D. Barrett.
[14] Effect of Constant Deformation Rate on Strength O grain of D.-Fir. S. Mindess, Nadeau, Barrett, Wood Science 8 nr 4 1976.
[15] Creep and Stress relaxation in Wood during Bending. P.U.A. Gross-man, R.S.T. Kingston Austr.J.Appl.Sci., 1963,14,305-17.
[16] Time depend. Deformation of Wood etc. A. v.d.Wiel Report 4-84-4- Ha-17 Stevin Lab. Techn. Univ. Delft.
[17] Studies on Thermal Softening of Wood III O.Sawake, 1974, J.Jap. Wood Res.Soc. 20 (11):517-522.
[18] Studies on Rheological Properties of Wood. T.Yamada et al. 1961 J.Jap Wood Res. Soc. 7 (2):63 - 72.
[19] Theory of deformation processes and lifetime of wood T.A.C.M. van der Put, Rep. 4-85-5 HA-21 Stevin Lab. TU-Delft.
[20] A model of deformation and damage processes based on deformation kinetics, Lecture for the EC-meeting, Palaiseau, Oct. 1985. Rep. 4-85-9 HA-22, T.A.C.M. van der Put, Stevin Lab. TU-Delft.
[21] Reaction kinetics of bond exchange of deformation and damage processes in wood. Proceed. or the IUFRO S 5.02 Conf. Sept. 1986, Firenze, Italy. and Rep. 4-86-11 HA-28, T.A.C.M. van der Put, Stevin Lab. TU-Delft.
[22] Equations for parameter estimation for a deformation kinetics model EC-BOS-129-NL, Rep. 4-86-13, HA 29, T.A.C.M. van der Put, TUD.
[23] Investigation of a lifetime theory based on thermodynamics, Lect. CEC-meeting Munchen april 1987, T.A.C.M. van der Put.
[24] A rheological model based on the theory of molecular deformation kinetics, T.A.C.M. van der Put, Delft Progress Report, Vol. 12, nr. 4, Delft Univers. Press. 1988.

5. Solution and discussion of the derived model-equation for different loading paths

5.1 Introduction

In 4, the mathematical derivation of a creep and damage model is given, solely based on the reaction equations of plastic deformation at the deformation sites and the transmission of stresses by the surrounding elastic material. Hereby, only the end state or the flow process is regarded where there is no more internal elastic stress redistribution among the parallel processes and only the last strength determining process has an influence. To describe the whole creep and damage history, the change of the elastic stresses on the sites has to be regarded.
This leads to the following equations (with an elastic part ε_e and a viscous part ε_v):

$$\frac{d\varepsilon}{dt} = \dot{\varepsilon} = \dot{\varepsilon}_{ei} + \dot{\varepsilon}_{vi} = \frac{\dot{\sigma}_i}{K_i} + \left(A_i + B_i\varepsilon_i\right)\sinh\left(\sigma_i\varphi_i\left(1 - C_i\varepsilon_i\right)\right) \qquad (5.1.1)$$

This can be visualized by a parallel system of Maxwell elements, where σ_i is the stress on element i; ε_{vi} is the strain of the non-linear dashpot and K_i is the spring constant. The terms with B_i and C_i give the structural changes. It appeared that $C_i\varepsilon_i$ is very small and can be neglected. Thus hardening is not due to this term but is due to the influence of the parallel processes and σ_i has the form of $\sigma_i = \sigma - M\cdot\varepsilon$, where M is proportional to the spring constants of the parallel elements and $M\cdot\varepsilon >> C_i\varepsilon_i$. Thus M is measured in stead of a possible C_i. The term $A_i + B_i\varepsilon_i$ represents the always occurring first order reactions. A_i applies for high, hardly changing concentration, acting as zero order reaction. $B_i\varepsilon_i$ gives a first order reaction of a structural change process with a very long delay time (see e.g. fig. 5.9). Wood always shows such coupled zero- and first order processes, which should be treated as 2 separate parallel acting processes, because each process may dominate in different time ranges. The coupling then follows from the same time-temperature and same time-stress shift of both processes.

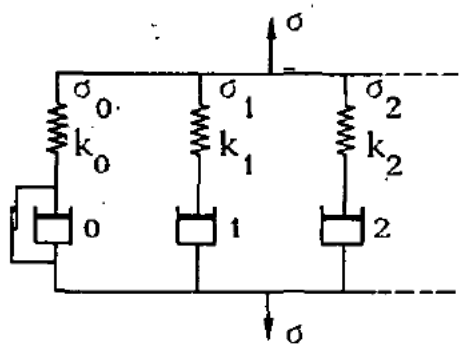

fig. 5.1 Parallel system of Maxwell units.

In most experiments, one of the processes controls the overall behavior and only three elements (free spring $K_0 + K_1$ and Maxwell element by spring K_2 with dashpot 2) have to be regarded (dashpots 0 and 1 are then rigid during the short loading time; see fig.5.1). During the deformation, the loading of the springs changes (transient flow) until all Maxwell elements flow. Then the behavior can be described by one equivalent single Maxwell element.

In the following the solutions of eq.(5.1.1) for the different loading histories will be given.

5.2 Constant strain rate test

In fig. 5.2, a three-element model is given of one dominating process controlling in the short term test. For the Maxwell unit at constant strain rate $\dot{\varepsilon} = \dot{\varepsilon}_e + \dot{\varepsilon}_v = c$. For the dominating short term process in wood, structural changes are negligible (B = C =0 in eq.5.1.1):

$$\dot{\varepsilon} = \dot{\varepsilon}_e + \dot{\varepsilon}_v = \frac{\dot{\sigma}_v}{K_1} + A \cdot \sinh(\varphi\sigma_v) \tag{5.2.1}$$

The solution of this equation is:

$$\sigma_v = \frac{1}{\varphi}\ln\left(\beta + \left(\sqrt{1+\beta^2}\right)\tanh\left(\frac{\sqrt{1+\beta^2}}{2} A\varphi K_1 (t - C)\right)\right) \tag{5.2.2}$$

with: $\beta = \frac{\dot{\varepsilon}}{A}$ and: $-\sqrt{1+\beta^2} \cdot \frac{A}{2} \cdot \varphi K_1 C = \operatorname{arctan h}\left(\frac{1-\beta}{\sqrt{1+\beta^2}}\right)$, (5.2.3)

if the initial value: $\sigma_{v0} = 0$.

In fig.(5.3), the stress - time relation of the model is given. For wood K_1 and σ_v are small and the line of fig. 5.3 can be approximated by a single straight line. This leads to a mean modulus of elasticity μ:

$$\mu = \frac{\sigma_m}{\varepsilon_m} = \frac{K_2}{\varepsilon_m} + \frac{\sigma_{v\infty}}{\varepsilon_m} = K_2 + \frac{1}{\varphi\varepsilon_m}\ln\left(\beta + \sqrt{1+\beta^2}\right) \approx K_2 + \frac{1}{\varphi\varepsilon_m}\ln(2\beta) \qquad \text{or:}$$

$$\mu = K_2 + \frac{1}{\varphi\varepsilon_m}\left(\ln(2/A) + \ln(\dot{\varepsilon})\right) \tag{5.2.4}$$

Thus the dependence of m on the strain rate $\dot{\varepsilon}$ is:

$$\mu = \mu_0\left(1 + \frac{1}{\mu_0\varphi\varepsilon_m}\left(\ln(\dot{\varepsilon}) - \ln(\dot{\varepsilon}_0)\right)\right), \tag{5.2.5}$$

with: $\mu_0\varphi\varepsilon_m = K_2\varphi\varepsilon_m + \ln(2\beta_0)$. (5.2.6)

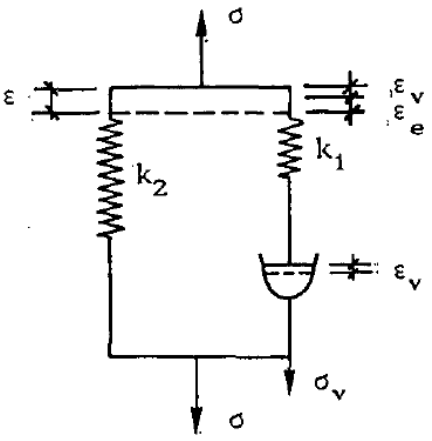

fig. 5.2. Three element model

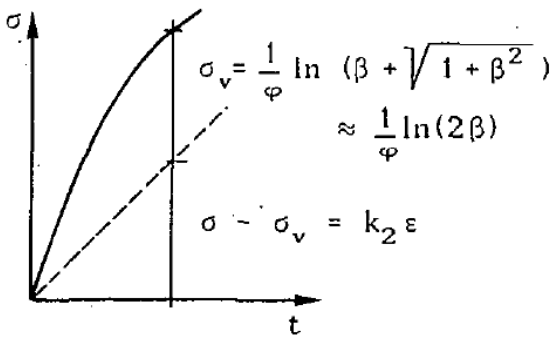

fig. 5.3. Early flow of wood

Eq.(5.2.5) is equal to the experimental equation given in [1]. Because $K_2\varphi\varepsilon_m$ dominates in

eq.(5.2.6), $K_2\varphi\varepsilon_m$ is approximately constant and φ is inversely proportional to $K_2\varepsilon_m$. Because $\mu_0\varphi\varepsilon_m \approx \sigma_m\varphi = n$, a value of $n \approx 12$ applies for green wood and $n \approx 36$ at 10 % m.c. as also has been found for fracture. It can be concluded that there is a small flow process in wood during loading at normal rates of loading.

Because usably β is much higher than 1, eq.(5.2.2) can be approximated by:

$\sigma_v\varphi \approx \ln\left(\beta + \beta\tanh\left(\beta A\varphi K_1 (t-C)/2\right)\right)$, or with $\gamma = \beta A\varphi K_1/2$ and

$\tanh(-\gamma C) = (1-\beta)/\beta$, this is:

$$\sigma_v\varphi \approx \ln\left(\beta + \beta\frac{\tanh(\gamma t)+\tanh(-\gamma C)}{1+\tanh(\gamma t)\cdot\tanh(-\gamma C)}\right) = \ln\left(\frac{1+\tanh(\gamma t)}{1+\frac{1-\beta}{\beta}\tanh(\gamma t)}\right) =$$

$$= \ln\left(\frac{\exp(2\gamma t)}{1+\frac{1}{2\beta}(\exp(2\gamma t)-1)}\right) \quad \rightarrow \quad \sigma_v\varphi \approx \ln\left(\frac{2\beta}{1+2\beta\exp(-2\gamma t)}\right) = \ln(2\beta\alpha) \qquad (5.2.7)$$

with: $1/\alpha \approx 1+2\beta\exp\left(-\beta A\varphi K_1 t_m\right) = 1+2\beta\exp\left(-\beta\sigma_{1e}\right)$,

because: $\beta A\varphi K_1 t_m = \dot{\varepsilon}\varphi K_1 t_m = \varphi K_1\varepsilon_m = \varphi\sigma_{1e}$

$\sigma_{1e} = K_1\varepsilon_m$ is the maximal possible potential elastic stress on element 1.

It is seen that the experimental law eq.(5.2.5) holds for relative long values of t_m when: $2\beta << \exp(\varphi\sigma_{1e})$, thus for relatively slow rates. For extremely high rates is: $\sigma_v\varphi \approx \sigma_e\varphi$.

Further: $\varphi(\sigma_v - \sigma_e) = \ln(1-\alpha)$, or: $\alpha = 1-\exp\left(\varphi(\sigma_v-\sigma_e)\right) = 1-\exp(\varphi\varepsilon_v K_1)$

When all Maxwell elements of fig. 5.1 flow, a description by a single (dominating) Maxwell element is possible (neglecting the small, almost constant, stress in K_1 in fig. 5.2). If B and C in eq.(5.1.1) are zero, then eq.(5.2.1) applies, represented by fig. 5.4.

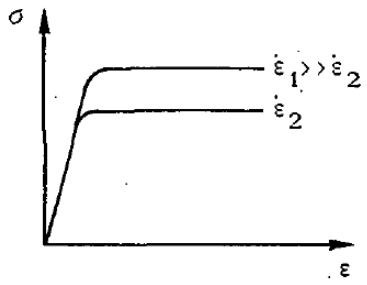

fig. 5.4 Non-linear Maxwell element

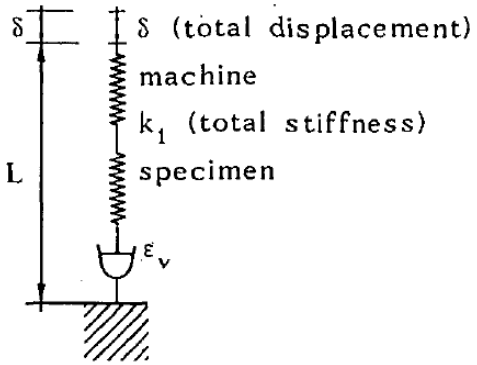

fig. 5.5 Flow of all elements

In general, when B and C in eq.(5.1.1) are not zero, the following applies. For a machine - specimen combination in a test, the crosshead displacement is (fig. 5.5):

$$\frac{\delta}{L} = \frac{\sigma}{K_1} + \varepsilon_v$$

and the constant crosshead rate $\dot{\delta} = c$ becomes:

$\dot{\delta} = L\left(\frac{\dot{\sigma}}{K_1} + \dot{\varepsilon}_v\right)$. Thus: $\dot{\varepsilon}_v = \frac{\dot{\delta}}{L} - \frac{\dot{\sigma}}{K_1} = \frac{\dot{\delta}}{L}\left(1 - \frac{L}{K_1}\frac{d\sigma}{d\delta}\right)$, or:

$$\frac{d\sigma}{d\delta} = \frac{K_1}{L} - \frac{K_1}{c}\dot{\varepsilon}_v = \frac{K_1}{L} - \frac{K_1}{L}A'T\left(\rho_0 + B'\left(\frac{\delta}{L} - \frac{\sigma}{K_1}\right)\right)\sinh\left(\varphi\sigma\left(1 - \frac{C\delta}{L} + \frac{C\sigma}{K_1}\right)\right) \qquad (5.2.8)$$

The analogues power equation for this case has the form:

$$\frac{d\sigma}{d\delta} = C_0 - \left(C_1 + C_2\delta - C_3\sigma\right)\cdot\left(\frac{\sigma + C_4\varepsilon_v}{\sigma_0}\right)^n. \qquad (5.2.9)$$

Both equations (5.2.8) and (5.2.9) cannot be integrated to a functional form. Results of numerical integration are shown in fig. 5.6 and 5.7. Clear wood in compression, parallel to the grain, shows a behavior like in fig. 5.4, indicating no hardening and no yield drop. Thus B' and C in eq.(5.2.8) may be neglected. For timber (with knots) in compression along the grain however there is a small yield drop, superposed on the behavior of the clear wood between the knots, indicating the acting of another Maxwell element (crack propagation by shear failure at the knots). Thus knots act as flow units with a low density. Hardening in compression by combined stresses is only possible as system hardening by confined dilatation as shown in D(2008a).

For wood in tension in grain direction, there is a high yield drop, indicating that B' in

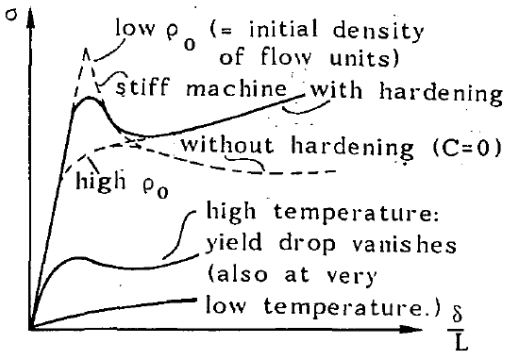

fig. 5.6 Yield drop eq.(5.2.8)

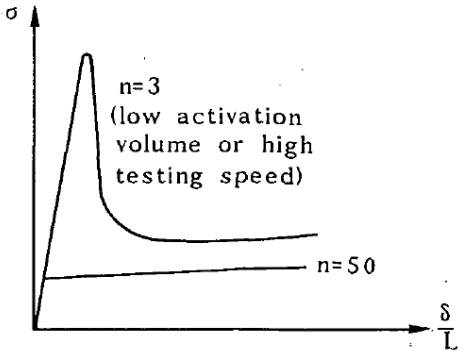

fig. 5.7 Influence of n, eq.(5.2.9)

eq.(5.2.8) is dominating by a low initial flow unit density ρ_0. Measurements show that this is not caused by a low value of n. There is also no indication of hardening so that the differential-equation for this case becomes:

$$\dot{\varepsilon} = \frac{\dot{\sigma}_v}{K_1} + B\varepsilon_v\sinh\left(\varphi\varepsilon_v\right) \qquad (5.2.10)$$

Taking the solution of this equation in the form: $\sigma_v = K_1\varepsilon - f(t)$, or: $\dot{\sigma}_v = K_1\dot{\varepsilon} - \dot{f}(t)$, then

$$\varepsilon_V = \varepsilon - \frac{\sigma_V}{K_1} = \varepsilon - \varepsilon + \frac{f}{K_1} = \frac{f}{K_1} \qquad (5.2.11)$$

and the differential equation is:

$\dot{f} - Bf\sinh\left(\varphi\left(K_1\varepsilon - f\right)\right) = 0$, or for higher stresses where f is noticeable:

$$\dot{f} - \frac{Bf}{2}\exp\left(\varphi\left(K_1\dot{\varepsilon}t - f\right)\right) = 0 \qquad (5.2.12)$$

or:

$$\exp\left(\varphi f\right)\cdot\frac{d\left(\ln\left(\varphi f\right)\right)}{dt} = \frac{B}{2}\cdot\exp\left(\varphi K_1\dot{\varepsilon}t\right) \qquad (5.2.13)$$

Now is: $\int_{x_0}^{x}\exp(x)d(\ln(x)) = \int_{-\infty}^{x}\exp(x)d(\ln(x)) - \int_{-\infty}^{x_0}\exp(x)d(\ln(x)) = E_i(x) - E_i(x_0)$, the exponential integrals. Thus eq.(5.2.13) has as solution:

$$E_i(\varphi f) - E_i(\varphi f_0) = \frac{B}{2\varphi K_1\dot{\varepsilon}}\left(\exp\left(\varphi K_1\dot{\varepsilon}t\right) - 1\right) \rightarrow \tag{5.2.14}$$

$$\frac{\exp(\varphi f)}{\varphi f} \approx \frac{B}{2\varphi K_1\dot{\varepsilon}}\left(\exp(\varphi K_1\dot{\varepsilon}t) - 1\right) + E_i(\varphi f_0) \approx \frac{B}{2\varphi K_1\dot{\varepsilon}}\left(\exp(\varphi K_1\dot{\varepsilon}t) - 1\right) + \frac{\exp(\varphi f_0)}{\varphi f_0}, \quad \text{or:}$$

$$\varphi f = \ln(\varphi f) + \ln\left(\frac{B}{2\varphi K_1\dot{\varepsilon}}\left(\exp\left(\varphi K_1\dot{\varepsilon}t\right) - 1\right) + \frac{\exp(\varphi f_0)}{\varphi f_0}\right) \approx$$

$$= \varphi f_0 + \ln\left(\frac{Bf\varphi}{2\varphi K_1\dot{\varepsilon}}\left(\exp\left(\varphi K_1\dot{\varepsilon}t\right) - 1\right)\exp(-\varphi f_0) + \frac{\varphi f}{\varphi f_0}\right) \approx$$

$$\approx \varphi f_0 + \ln\left(\frac{Bf}{2K_1\dot{\varepsilon}}\left(\exp\left(\varphi K_1\dot{\varepsilon}t\right) - 1\right)\exp(-\varphi f_0) + 1\right). \tag{5.2.15}$$

For larger values of time t, this approaches to:

$$\varphi f \approx \ln\left(\frac{Bf}{2\dot{\varepsilon}K_1}\cdot\exp\left(\varphi K_1\dot{\varepsilon}t\right)\right) = \varphi K_1\dot{\varepsilon}t - \ln\left(\frac{2\dot{\varepsilon}K_1}{Bf}\right), \quad \text{or:}$$

$$\sigma_v\varphi = \ln\left(2\beta\alpha\right), \qquad \text{with: } \beta = \dot{\varepsilon}/B \qquad \text{and: } \alpha = 1/\varepsilon_v \tag{5.2.16}$$

and the result is comparable with the case of initial high flow unit density, eq.(5.2.7). Because the process is small, showing only a very slight curvature of the loading line, parameter estimation is not possible with rate tests and a parabolic form of the line will be chosen as applies for all slightly curved lines.

For small values of φf, eq.(5.2.14) is approximately:

$$\ln(\varphi f) = \ln(\varphi f_0) + \frac{B}{2\varphi K_1\dot{\varepsilon}}\left(\exp(\varphi K_1\dot{\varepsilon}t) - 1\right) \tag{5.2.17}$$

or: $$\varepsilon_v = \varepsilon_{v0}\cdot\exp\left(\frac{B}{2\varphi K_1\dot{\varepsilon}}\left(\exp(\varphi K_1\dot{\varepsilon}t) - 1\right)\right) \tag{5.2.18}$$

For loading at a constant rate to a stress level σ_m, at a strain ε_m, this equation thus gets the form of: $$\varepsilon_v = \varepsilon_{v0}\cdot\exp\left(C\sigma_m\right) \tag{5.2.19}$$

when $\varphi\varepsilon_m$ is constant for different values of ε_m. Thus ε_v increases exponential with the stress. But the faint loading curve can be approximated by a parabola. Thus:

$\sigma = \left(K_1 + K_2\right)\varepsilon - K_1\varepsilon_v$ can be given by the parabola: $\sigma = E\varepsilon - c_1\varepsilon^2$. Thus: $\varepsilon_v = \left(c_1/K_1\right)\varepsilon^2$, a general property that is used later derivations. The parabolic loading line also can be given as: $\varepsilon = \sigma/E + c_2\sigma^2$, what represents the theoretical curve: $\varepsilon = \sigma/K + \left(K_1/K\right)\varepsilon_v$. Thus:

$\varepsilon_v = \left(Kc_2/K_1\right)\sigma^2 = c_3\sigma^2$. Thus:

$$\frac{\varepsilon_{va}}{\sigma_a} - \frac{\varepsilon_{vb}}{\sigma_b} = c_3\left(\sigma_a - \sigma_b\right) \tag{5.2.20}$$

5.3 Constant loading rate test

In this case is $\dot{\sigma}$ constant for the three-element model of fig. 5.2 and as shown before B_i and C_i of eq.(5.1.1) may be neglected for the dominating process in wood.

Because: $\sigma = K_2\varepsilon + \sigma_v$, is: $\dot{\varepsilon} = \dot{\sigma}/K_2 - \dot{\sigma}_v/K_2$, and eq.(5.2.1) becomes:

$$\frac{\dot{\sigma}}{K_2} = \dot{\sigma}_v\left(\frac{1}{K_1}+\frac{1}{K_2}\right) + A\sinh(\varphi\sigma_v) \tag{5.3.1}$$

having a similar form as eq.(5.2.1) and the solution has the identical form when β is taken to be:

$\beta = \dfrac{\dot{\sigma}}{AK_2}$ and: $\dfrac{1}{K_1}$ is replaced by: $\dfrac{1}{K} = \dfrac{1}{K_1}+\dfrac{1}{K_2}$. Thus:

$$\dot{\varepsilon} = \frac{\dot{\sigma}t}{K_2} - \frac{1}{\varphi K_2}\cdot\ln\left(\beta + \left(\sqrt{1+\beta^2}\right)\cdot\tanh\left(\frac{\sqrt{1+\beta^2}}{2}A\varphi K(t-C)\right)\right) \tag{5.3.2}$$

with the same value of C as given in eq.(5.2.3). The same approximation is possible as for the constant strain rate test. Thus:

$\sigma_v\varphi = \ln(2\beta)$.

Comparison of two stresses with different loading rates, at the same strain, gives:

$$\sigma_1 - \sigma_2 = K_2\varepsilon + \sigma_{v1} - K_2\varepsilon - \sigma_{v2} = \frac{1}{\varphi}\left(\ln(\beta_1) - \ln(\beta_2)\right) = \frac{1}{\varphi}\ln\left(\frac{\dot{\sigma}_1}{\dot{\sigma}_2}\right) =$$

$$= \frac{1}{\varphi}\ln\left(\frac{\dot{\sigma}_1 t_1}{\dot{\sigma}_2 t_2}\frac{t_2}{t_1}\right) = \frac{1}{\varphi}\ln\left(\frac{\sigma_1 t_2}{\sigma_2 t_1}\right) = \frac{1}{\varphi}\ln\left(\frac{t_2}{t_1}\right) + \frac{1}{\varphi}\ln\left(\frac{\sigma_1}{\sigma_2}\right)$$

or because the last term is negligible:

$$\frac{\sigma_1}{\sigma_2} = 1 + \frac{1}{\varphi\sigma_2}\ln(t_2) - \frac{1}{\varphi\sigma_2}\ln(t_1) \approx C_1 - C_2\ln(t_1) \tag{5.3.3}$$

This is equal to the experimental equation given in e.g. [2] and [3], suggesting failure at the same (ultimate) strain. This has to follow from the description of the end state. In that case, when all elements flow (fig. 5.5), the elastic strain rate is zero and the rate equation is:

$\dot{\varepsilon}_v \approx A\sinh(\phi\dot{\sigma}t)$, or integrated:

$$\varepsilon_v = \frac{A}{\dot{\sigma}\varphi}\left(\cosh(\phi\dot{\sigma}t) - 1\right),$$

For higher values of $\dot{\sigma}\varphi t$ this becomes:

$$\varepsilon_v = \frac{A}{\dot{\sigma}\varphi}\left(\frac{1}{2}\exp(\dot{\sigma}\varphi t) - 1\right) \tag{5.3.4}$$

or with $\sigma = \dot{\sigma}t$:

$$\sigma = \frac{1}{\varphi}\ln\left(2 + \frac{2\dot{\sigma}\varphi\varepsilon_v}{A}\right) \approx \frac{1}{\varphi}\ln\left(\frac{2\dot{\sigma}\varphi\varepsilon_v}{A}\right) \tag{5.3.5}$$

The strength is reached for $\varepsilon_v = \varepsilon_{vu}$. Thus σ_1 and σ_2, at the rates $\dot{\sigma}_1$ and $\dot{\sigma}_2$ are related by:

$$\sigma_1 - \sigma_2 \approx \frac{1}{\varphi}\ln\left(\frac{\dot{\sigma}_1}{\dot{\sigma}_2}\right) = \frac{1}{\varphi}\ln\left(\frac{\sigma_1 t_2}{\sigma_2 t_1}\right) \approx \frac{1}{\varphi}\ln\left(\frac{t_2}{t_1}\right) \quad \text{or:}$$

$$\frac{\sigma_1}{\sigma_2} = 1 + \frac{1}{\varphi\sigma_2}\ln(t_2) - \frac{1}{\varphi\sigma_2}\ln(t_1) = C_1 - C_2\ln(t_1)$$

what is equal to eq.(5.3.3) and gives an explanation of the experimental law given in [2], [3] etc., where $C_1 =$ 1.2 to 1.3 and $1/C_2 = n = 27$ for compression and n = 31 for bending.

If 1/n is approximately linear dependent on the moisture content as suggested in [1], then these values indicate a moisture content of 13%.

The same result is obtained by integration of eq.(5.3.6), where only the hardening term (C_i in eq.(5.1.1) is not acting. Thus:

$$\dot{\varepsilon}_v = (A + B\varepsilon_v)\sinh(\varphi\dot{\sigma}t) \qquad (5.3.6)$$

Only the ultimate strain ε_{vu} will have another value.

The alternative power representation becomes ($\dot{\sigma} =$ constant):

$$\dot{\varepsilon}_v = (A + B\varepsilon_v)\left(\frac{\dot{\sigma}}{\sigma_0}\right)^n t^n \qquad (5.3.7)$$

This is easy to integrate and the results are given in fig.(5.8).

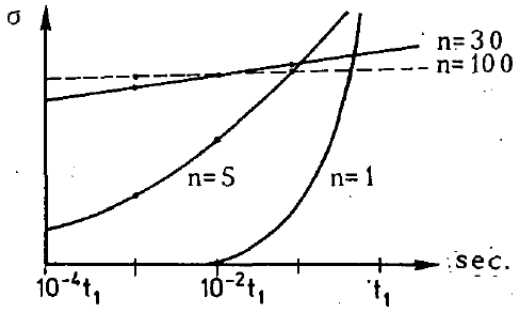

fig. 5.8 Influence of the rate of loading or time to loading to the same strain [4].

It can be seen from this figure, that for small values of n ($n \geq 1$), there is a strong influence of the loading rate on the level of the flow stress. For high values of n (e.g. $n \geq 30$ as for wood), there is only a small influence and there is a linear relation between the strength and log(time to failure) as is also derived before.

For small values of n, the derivation of n in 4.6, is not general enough. From:

$$\frac{\dot{\varepsilon}}{\dot{\varepsilon}_u} = \left(\frac{\sigma}{\sigma_u}\right)^n$$

it follows that : $\ln(\dot{\varepsilon}) = \ln(\dot{\varepsilon}_u) - \ln(\sigma_u^n) + n\ln(\sigma)$

Thus: $\dfrac{d(\ln(\dot{\varepsilon}))}{d(\ln(\sigma))} = n$

Applying this operation: $\dfrac{d(\ln(\dot{\varepsilon}))}{d(\ln(\sigma))}$ to: $\dot{\varepsilon} = A\sinh(\varphi\sigma)$ gives:

$$n = \frac{\sigma\varphi}{\tanh(\sigma\varphi)} \qquad (5.3.8)$$

Thus for small values of $\sigma\varphi$ is: n = 1, and for large values is $n = \sigma\varphi$. Thus for wood is:

$$n = \sigma\varphi \geq 1 \qquad (5.3.9)$$

For wood there is an empirical indication that there exists an element with a small value of n, as will be shown later. This is only noticeable at very high loading rates.

5.4 Creep and creep recovery

For the three-element model (fig.5.2), showing negligible structural changes, as applies for wood at common load levels, the force on the Maxwell element is determined by eq.(5.2.1). For the parallel spring K_2 is:

$$\dot{\varepsilon} = \frac{\sigma_2}{K_2} = \frac{1}{K_2}\frac{d(\sigma - \sigma_v)}{dt} = \frac{\dot{\sigma} - \dot{\sigma}_v}{K_2}$$

Because for creep $\dot{\sigma} = 0$, is: $\dot{\varepsilon} = -\frac{\dot{\sigma}_v}{K_2}$, and eq.(5.2.1) becomes:

$$\frac{\dot{\sigma}_v}{K_1} + A\sinh(\varphi\sigma_v) = -\frac{\dot{\sigma}_v}{K_2} \quad \text{or:}$$

$$\dot{\sigma}_v + KA\sinh(\varphi\sigma_v) = 0 \tag{5.4.1}$$

where $1/K = 1/K_1 + 1/K_2$

With the boundary condition: $\varepsilon_\infty = \frac{\sigma}{K_2}$, is: $\sigma_v = \sigma - K_2\varepsilon = K_2(\varepsilon_\infty - \varepsilon)$.

The solution of eq.(5.4.1) is:

$$\ln\left(\tanh\left(\frac{\varphi K_2}{2}(\varepsilon_\infty - \varepsilon)\right)\right) = -\varphi KAt + \ln\left(\tanh\left(\frac{\varphi K_2}{2}(\varepsilon_\infty - \varepsilon_0)\right)\right)$$

or, because arctanh(x) $= \frac{1}{2}\ln\left(\frac{1+x}{1-x}\right)$, this can be written as:

$$\varepsilon_\infty - \varepsilon = \frac{1}{\varphi K_2}\ln\left(\coth\left(-\frac{1}{2}\ln\left(\tanh\left(\frac{K_2\varphi}{2}(\varepsilon_\infty - \varepsilon)\right) + \frac{1}{2}K\varphi At\right)\right)\right) \tag{5.4.2}$$

In the early part of the test this reduces to the logarithmic form:

$$\varepsilon_\infty - \varepsilon = -\frac{1}{\varphi K_2}\ln\left(-\frac{1}{2}\ln\left(\tanh\left(\frac{K_2\varphi}{2}(\varepsilon_\infty - \varepsilon_0)\right) + \frac{1}{2}K\varphi At\right)\right) \tag{5.4.3}$$

or:

$$\varepsilon = \varepsilon_0 + \frac{1}{\varphi K_2}\ln\left(1 + \frac{K\varphi At}{\ln(\coth(\varphi\sigma_{v0}/2))}\right) \tag{5.4.4}$$

For sufficient large values of x is: ln(coth(x)) = 2arctanh(exp(-2x) $\approx$ 2exp(-2x).
Eq.(5.4.4) then becomes:

$$\varepsilon = \varepsilon_0 + \frac{1}{\varphi K_2}\ln\left(1 + \frac{K\varphi At\exp(\varphi\sigma_{v0})}{2}\right) \tag{5.4.5}$$

A fit of this equation is not found in literature. Tests of B(1989a) show however that the form of eq.(5.4.4) or (5.4.5) is right, also for small times. The fit in literature is always made for larger times (neglecting 1 in the last term) giving:

$$\varepsilon = C_1 + C_2\ln(t) \tag{5.4.6}$$

After longer times, the influence of a second mechanism with a long relaxation time is noticeable and because: ln(1 + cx) $\approx$ cx, for small values of cx, an additional term: C.t in eq.(5.4.6) is sometimes used to account for the influence of a slow process. According to eq.(5.4.5) is: $C \cdot t = K\varphi At \cdot \exp(\varphi\sigma_{v0})/(2\varphi K_2)$. However this only describes the beginning of the process. For the whole process at very long times and sufficient high values of $\sigma_{v0}\varphi/2$, as for wood, eq.(5.4.2) can be written:

$$\varepsilon_\infty - \varepsilon = \frac{1}{\varphi K_2}\ln(\coth(K\varphi At/2)) \approx \frac{2}{\varphi K_2}\exp(-K\varphi At) \quad \text{or:}$$

$$\varepsilon = \varepsilon_0 + \frac{2}{\varphi K_2}(1 - \exp(-K\varphi At)) \tag{5.4.7}$$

Thus the behavior becomes quasi Newtonian after long times. Eq.(5.4.1) can be expected to be quasi Newtonian for low stresses, because then sinh(x) = x. This equation then becomes:

$\dot{\sigma}_v + KA\varphi\sigma_v = 0$, with the solution: $\varepsilon - \varepsilon_0 = (\varepsilon_\infty - \varepsilon_0)\cdot\left(1-\exp\left(-KA\varphi t\right)\right)$

Also from the solution of eq.(5.4.1) this equation follows if the creep strain ε is very small. It is seen that test results, in not too long time ranges, can be fit by Newtonian equations as often is done. This, however will give an underestimation of the relaxation times because it is implicitly assumed that the creep is in the end state within the measuring time t or that the total creep strain is small.

For a structural change process, when $B_i\varepsilon_i$ dominates in eq.(5.1.1) and A_i can be neglected or regarded separately as parallel acting process, then eq.(5.2.1) of the three element model of fig.5.2 becomes:

$$\dot{\varepsilon} = \frac{\dot{\sigma}_v}{K_1} + B\varepsilon_v \sinh(\varphi\sigma_v) \tag{5.4.8}$$

Because: $\varepsilon = \frac{\sigma_2}{K_2} = \frac{\sigma-\sigma_1}{K_2} = \frac{\sigma}{K_2} - \frac{K_1}{K_2}\left(\varepsilon-\varepsilon_v\right)$, or: $\varepsilon_v = \frac{K_1+K_2}{K_1}\varepsilon - \frac{\sigma}{K_1}$, is:

$$\dot{\varepsilon}_v = \frac{K_1+K_2}{K_1}\dot{\varepsilon} - \frac{\dot{\sigma}}{K_1} = B\varepsilon_v\sinh(\varphi\sigma_v) \approx \frac{B\varepsilon_v}{2}\exp(\varphi\sigma_v) = \frac{B\varepsilon_v}{2}\exp\left(\varphi\left(\sigma - K_2\varepsilon\right)\right)$$

giving: $$(K_1+K_2)\dot{\varepsilon} = \dot{\sigma} + B\left((K_1+K_2)\frac{\varepsilon}{2} - \frac{\sigma}{2}\right)\exp\left(\varphi\left(\sigma - K_2\varepsilon\right)\right) \tag{5.4..9}$$

For creep is σ = constant, or $\dot{\sigma} = 0$, thus: $\dot{\varepsilon} = \frac{B}{2}\left(\varepsilon - \frac{\sigma}{K_1+K_2}\right)\exp\left(\varphi\sigma - \varphi K_2\varepsilon\right)$ or:

$$\frac{d\left(\varphi K_2\varepsilon\right)}{\varphi K_2\left(\varepsilon - \frac{\sigma}{K_1+K_2}\right)}\exp\left(\varphi K_2\varepsilon - \frac{\varphi K_2\sigma}{K_1+K_2}\right) = \frac{B}{2}\left(\exp\left(\varphi\sigma - \frac{\varphi\sigma K_2}{K_1+K_2}\right)\right)\cdot dt$$

having the form: $\int_{x_0}^{x}\frac{dx}{x}\exp(x) = \int_{-\infty}^{x}\frac{dx}{x}\exp(x) - \int_{-\infty}^{x_0}\frac{dx}{x}\exp(x) = E_i(x) - E_i(x_0)$

or: $$E_i\left(\varphi K_2\left(\varepsilon - \frac{\sigma}{K_1+K_2}\right)\right) - E_i\left(\varphi K_2\left(\varepsilon_0 - \frac{\sigma}{K_1+K_2}\right)\right) = \frac{Bt}{2}\exp\left(\frac{\varphi\sigma K_1}{K_1+K_2}\right) \tag{5.4.10}$$

Thus:

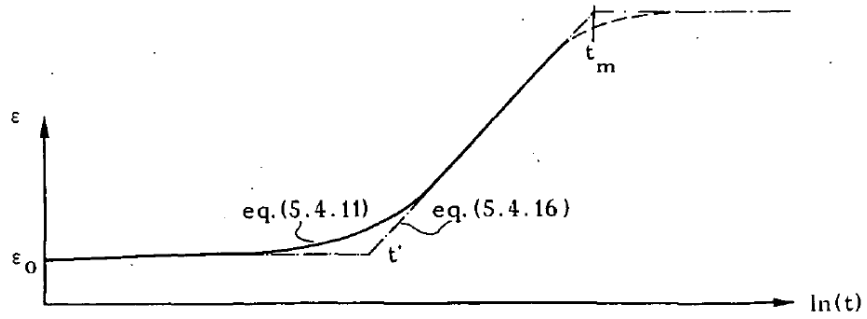

fig. 5.9 Irrecoverable creep (eq.(5.4.11))

$$\varepsilon - \frac{\sigma}{K_1+K_2} + \frac{1}{\varphi K_2}\cdot E_i^{-1}\left(\frac{Bt}{2}\exp\left(\frac{\varphi\sigma K_1}{K_1+K_2}\right) + E_i\left(\frac{\varphi\varepsilon_{v0}K_1K_2}{K_1+K_2}\right)\right) \tag{5.4.11}$$

For larger values of x is: $E_i(x) \approx \exp(x)$, and for small values is:
$E_i(x) \approx 0.577 + \ln(x)$. Thus for small times and small dislocation densities eq.(5.4.10) becomes:

$$\ln\left(\varphi K\varepsilon_v\right) = \frac{B}{2}\cdot t\cdot\exp\left(\frac{\varphi\sigma K}{K_2}\right) + \ln\left(\varphi K\varepsilon_{v0}\right) \qquad (5.4.12)$$

or: $$\varepsilon = \frac{\sigma}{K_1+K_2} + \frac{K\varepsilon_{v0}}{K_2}\exp\left(\frac{B}{2}\cdot t\cdot\exp\left(\frac{\varphi\sigma K_1}{K_1+K_2}\right)\right)$$

Thus there is a small exponential increase of the deformation during the first stage of the creep (delay time), as measured in e.g. [5], when the initial dislocation density is small (see fig. 5.9). At still smaller times eq.(5.4.12) can also be written:

$$\ln\left(\varepsilon_v/\varepsilon_{v0}\right) = \ln\left(\frac{\varepsilon_v-\varepsilon_{v0}}{\varepsilon_{v0}}+1\right) \approx \frac{\varepsilon_v-\varepsilon_{v0}}{\varepsilon_{v0}} = \frac{B}{2}\cdot t\cdot\exp\left(\frac{\sigma\varphi K}{K_2}\right)$$

and because $\left(\varepsilon_v-\varepsilon_{v0}\right)/\left(\varepsilon-\varepsilon_0\right) = c$, this is: $\varepsilon-\varepsilon_0 = \frac{\varepsilon_{v0}}{c}\cdot\frac{B}{2}\cdot t\cdot\exp\left(\frac{\sigma\varphi K}{K_2}\right)$ (5.4.13)

$\left(c = 1+K_2/K_1\right)$. Because ε_{v0} increases quadratic with σ at loading to the creep level, eq.(5.4.13) shows for shorter times a small initial quadratic increase of the creep with σ as measured in p.e. [6] ($\sigma\varphi$ is constant).
Eq.(5.4.10) becomes for larger times:

$$\frac{\exp\left(\varphi K_2\left(\varepsilon-\frac{\sigma}{K_2+K_1}\right)\right)}{\varphi K_2\left(\varepsilon-\frac{\sigma}{K_2+K_1}\right)} \approx \frac{B}{2}\cdot t\cdot\exp\left(\frac{\varphi\sigma K_1}{K_2+K_1}\right) + \ln\left(\varphi K_2\left(\varepsilon_0-\frac{\sigma}{K_2+K_1}\right)\right) \qquad \text{or:}$$

$$\varphi K_2\left(\varepsilon-\frac{\sigma}{K_2+K_1}\right) = \ln\left(\frac{\varphi K_1K_2\varepsilon_v}{K_2+K_1}\right) + \ln\left(\frac{B}{2}\cdot t\cdot\exp\left(\frac{\varphi\sigma K_1}{K_2+K_1}\right) + \ln\left(\frac{\varphi K_1K_2\varepsilon_{v0}}{K_2+K_1}\right)\right)$$

Thus for very small values of: $\varepsilon-\sigma/\left(K_1+K_2\right) = K_1\varepsilon_v/\left(K_1+K_2\right)$, the double log-plot applies in stead of the semi log-plot. For larger values, with $1/K = 1/K_1+1/K_2$ this equation becomes:

$$\varepsilon = \frac{\sigma}{K_2+K_1} + \frac{1}{\varphi K_2}\ln\left(\varphi K\varepsilon_v\right) + \frac{1}{\varphi K_2}\ln\left(\frac{B}{2}\cdot t\cdot\exp\left(\frac{\varphi\sigma K}{K_2}\right) + \ln\left(\varphi K\varepsilon_{v0}\right)\right) \qquad (5.4.14)$$

Because $\varphi K\varepsilon_{v0}$ is a small value, $\ln(\varphi K\varepsilon_{v0})$ is a high negative value. If this is replaced by the, during the initial creep stage, increased value ε_{v1} according to eq.(5.4.12), eq.(5.4.14) becomes:

$$\varepsilon = \frac{\sigma}{K_1+K_2} + \frac{1}{\varphi K_2}\ln\left(\varphi K\varepsilon_v\right) + \frac{1}{\varphi K_2}\ln\left(\frac{B}{2}\left(t-t_1\right)\exp\left(\frac{\varphi K\sigma}{K_2}\right) + \ln\left(\varphi K\varepsilon_{v1}\right)\right) \quad \text{or:}$$

$$\varepsilon = \frac{\sigma}{K_2} + \frac{1}{\varphi K_2}\ln\left(\frac{B}{2}\varphi K\bar{\varepsilon}_v\right) + \frac{1}{\varphi K_2}\ln\left(t-t_1+\frac{2}{B}\left(\ln\left(\varphi K\varepsilon_{v1}\right)\right)\cdot\exp\left(\frac{-\varphi\sigma K}{K_2}\right)\right) \qquad (5.4.15)$$

Because the second term on the right hand side is of minor importance, a mean value of ε_v can be applied and because:
$\sigma/K_2 = \varepsilon_0+\sigma_{v0}/K_2 = \varepsilon_0+\left(1/\varphi K_2\right)\ln\left(\exp\left(\varphi\sigma_{v0}\right)\right)$, the equation can be written:

$$\varepsilon = \varepsilon_0 + \frac{1}{\varphi K_2}\ln\left(1+\frac{\varphi K B\bar{\varepsilon}_v \exp(\varphi\sigma_{v0})}{2}\cdot(t-t')\right) \qquad (5.4.16)$$

where $t' = t_1 + \frac{2}{B}\exp(-\varphi\sigma_{v0})\cdot\left(\frac{1}{\varphi K\bar{\varepsilon}_v} - \ln(\varphi K\varepsilon_{v1})\right)$., is not far from t_1.

For long times $t >> t_1$, eq.(5.4.15) becomes:

$$\varepsilon = \frac{\sigma}{K_2} + \frac{1}{\varphi K_2}\ln\left(\varphi K B\bar{\varepsilon}_v\right) + \frac{1}{\varphi K_2}\ln(t) \qquad (5.4.17)$$

or: $-\varphi\sigma_1 = \ln(\varphi K B\varepsilon_v/2) + \ln(t)$

Thus the stress on element 1, σ_1, is zero at time: $t = t_m = 2/(\varphi K B\bar{\varepsilon}_v)$ and eq.(5.4.17) turns to:

$$\varepsilon = \varepsilon_m + \frac{1}{\varphi K_2}\ln\left(\frac{t}{t_m}\right) \qquad (5.4.18)$$

where $\varepsilon_m = \sigma/K_2$, when all the stress σ is on element 2 and the maximal strain is reached. (Of course ε is not the real strain for $t \to t_m$, but the extrapolation of the straight line approximation to ε_m, see fig.5.9).

For higher initial values eq.(5.4.10) becomes:

$$\frac{\exp(\varphi K\varepsilon_v)}{\varphi K\varepsilon_v} = \frac{\exp(\varphi K\varepsilon_{v0})}{\varphi K\varepsilon_{v0}} + \frac{B}{2}\cdot t\cdot\exp\left(\frac{\varphi K\sigma}{K_2}\right) \qquad (5.4.19)$$

or: $$\varepsilon = \varepsilon_0 + \frac{1}{\varphi K_2}\ln\left(\frac{\varepsilon_v}{\varepsilon_{v0}}\right) + \frac{1}{\varphi K_2}\ln\left(1+\frac{\varphi K\varepsilon_{v0}B}{2}\cdot t\cdot\exp(\varphi\sigma-\varphi K_2\varepsilon_0)\right)$$

or, because of the minor influence of the second term on the right hand side:

$$\varepsilon = \varepsilon_0 + \frac{1}{\varphi K_2}\ln\left(1+\frac{\varphi K\bar{\varepsilon}_v B}{2}\cdot t\cdot\exp(\varphi\sigma_{v0})\right) \qquad (5.4.20)$$

what is comparable with eq.(5.4.5) as can be expected for higher initial flow unit densities. The behavior according to fig. 5.9 is measured for wood. Because this is related to the cellulose, test results of dry summerwood fibers of pine holocellulose pulp [5], are also discussed. (holocellulose ≡ the wood structure without lignin).

In fig. 5.10, the average creep compliance of 50 fibre bundles is given for different initial stresses. As follows from the very different values of the initial compliances and from the not decelerating curves, flow without hardening must have been occurred. The kinked lines indicate two processes and a description is possible with two Maxwell elements. Because one process is slower than the other, a three-element model approach (one Maxwell element and one free spring) is initially possible. The line with the small slope is the quick process and as before, structural changes can be neglected (eq.(5.4.1)). The line with the steep slope, shows a strong delay time (see fig. 5.9) and follows exponential integral function of structural change processes, eq.(5.4.8).

As seen in fig. 5.11, the lines can be moved horizontally along the log(t) axis, to form one curve (giving the behavior after long times at the lowest given stress).

The line with the small slope is accordingly to eq.(5.4.4) and the line with the steep slope is given by eq.(5.4.16). It appears that in these equations, $1/\varphi\sigma K_2$ is constant or $1/\varphi K_2$ is proportional to σ, as also can be seen for creep of wood at lower stress levels. Thus $\varphi\sigma$ is constant, indicating that the number of creeping mechanisms per unit area increases with increasing initial stress. Except for cellulose materials, this property is also found in other

materials, like metals and rubbers [4].
The compliance according to eq.(5.4.4) is for longer times:

$$\frac{\varepsilon}{\sigma}=\frac{\varepsilon_0}{\sigma}+\frac{1}{\sigma\varphi K_2}\ln\left(\frac{K\varphi At}{2}\exp\left(\varphi\sigma_{v0}\right)\right)=\frac{\varepsilon_0}{\sigma}+\frac{1}{\sigma\varphi K_2}\ln\left(\frac{t}{t'}\right) \tag{5.4.21}$$

where $1/\sigma\varphi K_2$ is constant, independent of stress and temperature. Because of this, the

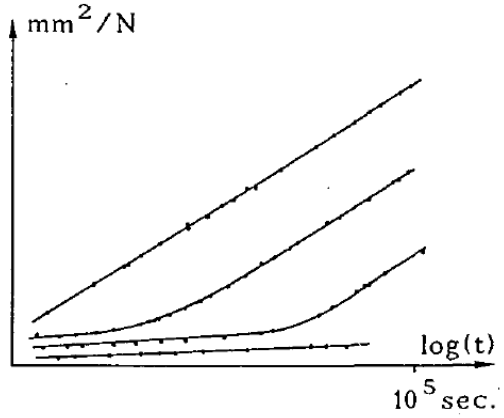

fig. 5.10 Creep compliance [5]

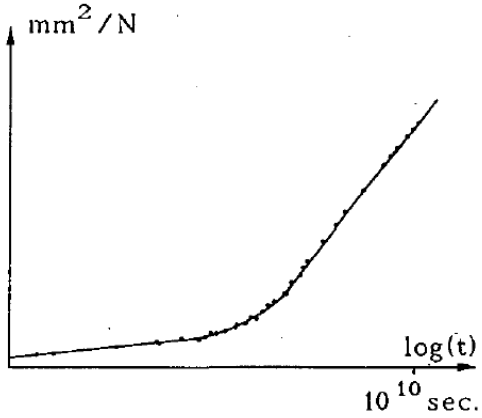

fig. 5.11 Master creep curve [5]

time temperature and time stress equivalence applies. According to this principle, for a horizontal shift of a creep equation along the time axis to an higher stress level $\sigma_a>\sigma_b$, is necessary that ε_b/σ_b at time t_b, has to be equal to ε_a/σ_a st time t_a. Thus it follows from eq.(5.4.21):

$$\frac{\varepsilon_a}{\sigma_a}-\frac{\varepsilon_b}{\sigma_b}=0=\frac{\varepsilon_{0a}}{\sigma_a}-\frac{\varepsilon_{0b}}{\sigma_b}+\frac{1}{\sigma\varphi K_2}\left(\ln\left(t_a\right)-\ln\left(t_b\right)-\ln\left(t'_a/t'_b\right)\right)$$

Thus:

$$\ln\left(t_a\right)-\ln\left(t_b\right)=-\frac{\sigma\varphi K_1K_2}{K_1+K_2}\left(\frac{\varepsilon_{v0a}}{\sigma_a}-\frac{\varepsilon_{v0b}}{\sigma_b}\right)-\ln\left(\frac{\varphi_b\exp\left(\varphi_b\sigma_{v0b}\right)}{\varphi_a\exp\left(\varphi_a\sigma_{v0a}\right)}\right)\approx-\sigma\varphi K\left(\frac{\varepsilon_{v0a}}{\sigma_a}-\frac{\varepsilon_{v0b}}{\sigma_b}\right)$$

because the neglected term is of lower order as follows from the following. According to eq.(5.2.7,) for loading to the creep level, this neglected term is:

$$\ln\left(\frac{\varphi_a 2\beta_a\alpha_a}{\varphi_b 2\beta_b\alpha_b}\right)=\ln\left(\frac{\varphi_a\dot{\varepsilon}_a\alpha_a}{\varphi_b\dot{\varepsilon}_b\alpha_b}\right)\approx\ln\left(\frac{\varphi_a}{\varphi_b}\right)$$

for loading at approximately the same strain rate $\dot{\varepsilon}$ ($\alpha\approx1$). Because $\sigma\varphi$ is constant is:

$$\ln\left(\frac{\varphi_a}{\varphi_b}\right)=\ln\left(\frac{\varphi_a\sigma_a}{\varphi_b\sigma_a}\cdot\frac{\sigma_b}{\sigma_a}\right)=\ln\left(\frac{\sigma_b}{\sigma_a}\right)=\ln\left(\frac{\bar{\varepsilon}K_2}{\sigma_a}\right)-\ln\left(\frac{\bar{\varepsilon}K_2}{\sigma_b}\right)<<\sigma\varphi K_2\left(\frac{\varepsilon_{0a}}{\sigma_a}-\frac{\varepsilon_{0b}}{\sigma_b}\right)$$

and thus negligible because $\sigma\varphi>>1$. Thus

$$\ln(t_a)-\ln(t_b)=-\sigma\varphi K\left(\frac{\varepsilon_{v0a}}{\sigma_a}-\frac{\varepsilon_{v0b}}{\sigma_b}\right) \tag{5.4.22}$$

with $\sigma\varphi=\sigma_a\varphi_a=\sigma_b\varphi_b$. Thus the shift is mainly dependent on the relative initial plastic strains. These strains arise during the loading to the creep level and because of the faint curved $\sigma-\varepsilon$ diagram, a parabolic approximation is possible (see above eq.(5.2.20)), leading to $\varepsilon_v=c_3\sigma^2$, which substituted in eq.(5.4.22), gives:

$$\ln(t_a)-\ln(t_b)=-\sigma\varphi Kc_3\left(\sigma_a-\sigma_b\right)=-C\left(\sigma_a-\sigma_b\right). \tag{5.4.23}$$

as also found empirically. The same time-temperature and time-stress equivalence applies for eq.(5.4.20) of the second mechanism, that occurs directly at creep, without a delay time, when loaded at a high stress level and leads to the same relation for the shift of the compliance along the ln(time) axis. The same can be stated for eq.(5.4.16). Because the shift of the second process is equal to that of the first process, there must be a critical value of the compliance, independent on the applied stress, where the second process starts. Thus it is probable that the first process creates the accumulation of flow units, for the second process. This also applies for wood (even for denser species as for instance Hinoki) and as can be seen in fig. 5.10 by the shift of the lines in proportion to the stress, the compliance increases linearly with the stress level (at a given time, as given in fig. 5.12 for wood).

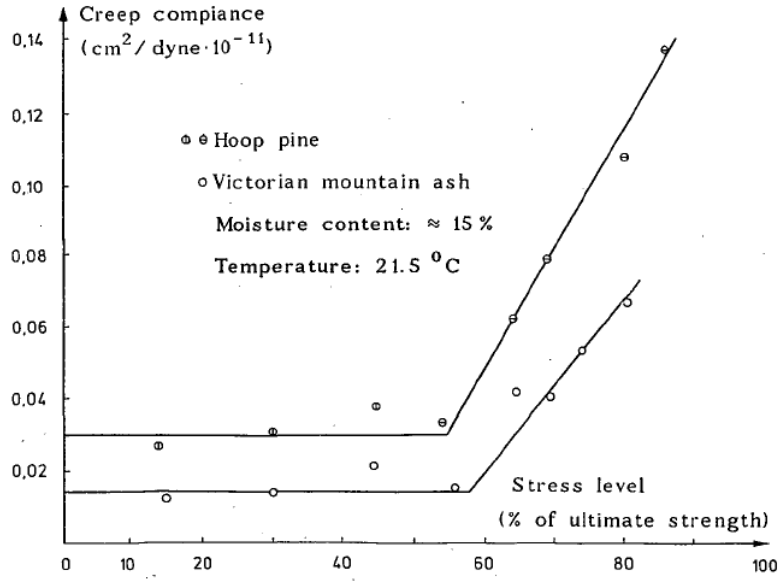

frig. 5.12 Dependence of the creep compliance on the stress level [7].

A fit by two lines with positive slopes would have been better in fig. 5.12 and the slope of the line at low stress levels is steeper [6] for dense species and higher moisture contents. However in the past, as a first approximation, the line for low stress levels was in practice often regarded as a horizontal line. This means that for this process ε_v is proportional to σ, and the behavior thus was regarded quasi linear. Thus for loading to ε:

$$\sigma_v = K_1(\varepsilon - \varepsilon_v) = \frac{1}{\varphi}\ln(2\beta\alpha) \qquad \text{or:} \qquad \varepsilon = \varepsilon_v + \frac{\varepsilon}{K_1\varphi\varepsilon}\ln(2\beta\alpha) \qquad \text{or:}$$

$\varepsilon_v = c''\varepsilon$ because: $K_1\varphi\varepsilon$ is constant

The parameter estimation for creep in [7], clearly shows the tendency of constant $\sigma\varphi$ at low stress levels, while the there estimated changing spring constants at higher stress levels is the indication of the occurrence of the mechanism with constant $\varphi\varepsilon^2$. This will be discussed later.

The constancy of $\sigma\varphi$ can be explained as follows. For compression the number of developing slip planes N is about linear proportional to the stress level σ at lower stress levels. Thus $\sigma/N = c$, and $\sigma\varphi = \sigma\lambda / NkT = \sigma\lambda' T / NkT = \sigma\lambda' / Nk = c\lambda' / k$ is constant. At a level of about 50 to 65% creases are formed, leading to the second mechanism of gross buckling of the cell walls where a constant buckling stress f may be expected. Thus $\sigma\lambda / N = f\lambda_2\lambda_3\lambda$ is constant, or σ / N is constant. Analogous is for crack propagation in tension the real stress f at a sharp crack at any stress level equal to the flow stress and is $f\lambda_2\lambda_3\lambda$ constant or is σ / N constant.

In the analysis above, it is assumed that the temperature is constant. To know the shift of the compliance along the time axis due to temperature, the same stress level has to be used in all tests at different temperatures. Then:

$\ln(t_a) - \ln(t_b) = E'/kT_a - E'/kT_b$

where E' is the activation energy. This is only true if $1/\sigma\varphi K_2$ is constant, independent of the temperature (e.g. for creep). If this is not constant, reduced strains are necessary to obtain the right activation energy.

If all Maxwell elements flow, one is determining for the overall rate in the end state and the power equation becomes for the general case:

$$\dot{\varepsilon} = A'(\rho_0 + B\varepsilon)\left(\frac{\sigma_a - M\varepsilon}{\sigma_0}\right)^n \tag{5.4.24}$$

This equation cannot be integrated. Numerical solutions show that the delay time is due to "dislocation multiplication" similar to yield drop, dependent on the initial flow unit density (see fig. 5.13). For creep recovery, after long time, the initial conditions are: $\sigma = 0$; $\varepsilon = \varepsilon_\infty$,

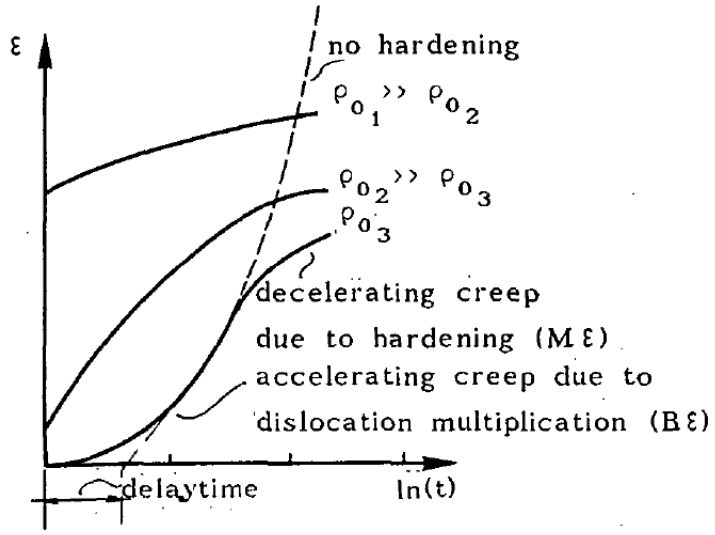

fig. 5.13 Creep dependent on model parameters

when t = 0, leading for the three-element model to:

$$\varepsilon = \frac{1}{\varphi K_2}\ln\left(\coth\left(-\frac{1}{2}\ln\left(\tanh\left(\frac{\sigma_{v0}\varphi}{2}\right) + \frac{K_1K_2A\varphi t}{2(K_1+K_2)}\right)\right)\right) \tag{5.4.25}$$

analogous to eq.(5.4.2).

5.5 Stress relaxation

The three element model (fig.5.2) loaded to σ_0 at strain ε_0 at time t_0 gets the stress $\sigma_0 - \sigma_{v0}$ on spring 2. This remains unchanged when by relaxation stress σ_v on spring 1 decreases. For the Maxwell element is: $\dot{\varepsilon} = 0$, or: $\dot{\sigma}_v = -K_1\dot{\varepsilon}_v$, or:

$$-\dot{\sigma}_v = K_1 A \sinh(\varphi\sigma_v) \tag{5.5.1}$$

Integration gives: $\ln\left(\tanh\left(\varphi\sigma_v/2\right)\right) = -A\varphi K_1 t + C$ or:

$$\sigma_v = \frac{2}{\varphi}\operatorname{arctanh}\left(\tanh\left(\varphi\sigma_{v0}/2\right)\cdot\exp\left(-A\varphi K_1 t\right)\right) \tag{5.5.2}$$

This equation can be written with: $a = \tanh(\sigma_{v0}\varphi/2)$ and $b = A\varphi K_1$:

$$\sigma_v = \frac{1}{\varphi}\ln\left(\frac{1+a\exp(-bt)}{1-a\exp(-bt)}\right) = \frac{1}{\varphi}\ln\left(\frac{\sqrt{a}\cdot\exp\left(bt/2-\ln\left(\sqrt{a}\right)\right)+\sqrt{a}\cdot\exp\left(-bt/2+\ln\left(\sqrt{a}\right)\right)}{\sqrt{a}\cdot\exp\left(bt/2-\ln\left(\sqrt{a}\right)\right)-\sqrt{a}\cdot\exp\left(-bt/2+\ln\left(\sqrt{a}\right)\right)}\right)$$

or: $\sigma_v = -\frac{1}{\varphi}\ln\left(\tanh\left(\frac{bt}{2}-\frac{1}{2}\ln(a)\right)\right)$ or:

$$\sigma_v = -\frac{1}{\varphi}\ln\left(\tanh\left(\frac{A\varphi K_1 t}{2}-\frac{1}{2}\ln\left(\tanh\left(\frac{\sigma_{v0}\varphi}{2}\right)\right)\right)\right) \qquad (5.5.3)$$

For the early part of the relaxation this is:

$$\sigma_v = -\frac{1}{\varphi}\ln\left(\frac{A\varphi K_1 t}{2}-\frac{1}{2}\ln\left(\tanh\left(\frac{\sigma_{v0}\varphi}{2}\right)\right)\right) \quad \text{or:}$$

$$\sigma_v = -\frac{1}{\varphi}\ln\left(\frac{A\varphi K_1}{2}\right)-\frac{1}{\varphi}\ln\left(t+\frac{2\,\mathrm{arccoth}\left(\sigma_{v0}\varphi\right)}{A\varphi K_1}\right) \qquad (5.5.4)$$

Except for very small times this will have the empirical form:

$\sigma_v = C_1 - C_2\log(t)$

The total stress on the specimen is: $\sigma = \sigma_0 - \sigma_{v0} + \sigma_v(t)$, or

$$\sigma = \sigma_0 - \ln\left(1+\frac{A\varphi K_1 t}{2\cdot\mathrm{arccoth}\left(\exp(\varphi\sigma_{v0})\right)}\right) \qquad (5.5.5)$$

or for not too small values of $\sigma_{v0}\varphi$:

$$\frac{\sigma}{\sigma_0} = 1-\frac{1}{\sigma_0\varphi}\ln\left(1+\frac{A}{2}\varphi K_1 t\cdot\exp\left(\sigma_{v0}\varphi\right)\right) = 1-\frac{1}{\sigma_0\varphi}\ln\left(1+\frac{t}{t'}\right) \qquad (5.5.6)$$

in agreement with the experiments in (1989a).

For longer times eq.(5.5.6) becomes:

$$\frac{\sigma}{\sigma_0} \approx 1-\frac{1}{\sigma_0\varphi}\ln\left(\frac{t}{t'}\right), \quad \text{with:} \quad t' = \frac{2}{A\varphi K_1\exp\left(\sigma_{v0}\varphi\right)} \qquad (5.5.7)$$

and for a horizontal shift of this relaxation line along the ln(t)-axis is:

$$\ln\left(t_a\right)-\ln\left(t_b\right) = \ln\left(t'_a\right)-\ln\left(t'_b\right) = \ln\left(\frac{\varphi_b}{\varphi_a}\right)+\frac{\sigma_{v0b}}{\sigma_{0b}}-\frac{\sigma_{v0a}}{\sigma_{0a}} \qquad (5.5.8)$$

For loading to the same stress level at different rates is $\varphi_a = \varphi_b$, and the shift is:

$$\ln\left(t_a\right)-\ln\left(t_b\right) = \ln\left(\frac{\dot{\varepsilon}_b\alpha_b}{\dot{\varepsilon}_a\alpha_a}\right) \qquad (5.5.9)$$

where $.\dot{\varepsilon}_i$ is the strain-rate for loading to the creep level.

This equation can be compared to the test results of [8] on micro-specimens of latewood and earlywood (Spruce and fir). The measured lines, given in fig.5 of [8], can be precisely described by eq.(5.5.6), giving a value of:

$1/\varphi\sigma_0 = 0.026$, for earlywood and: 0.032 for late wood. Thus a mean value of: 0.029 or:

$\varphi\sigma_0 = 34.5$, where t' is dependent on the rate of loading to the creep level, as predicted by the theory. The delay time t' is:

t' = 0.145 sec. for quick loading and is: 4.35 sec. for loading at the slow rate. Thus the shift of the line eq.(5.5.7) is:

$\ln(t_a)-\ln(t_b)=\ln(4.35/0.145)=\ln(30)=3.4$

According to eq.(5.9) is the shift, due to the difference of the rates of 0.002 and 0.208 mm/sec.:

$\ln(t_a)-\ln(t_b)=\ln(104\alpha_b/\alpha_a)$, indicating: $\alpha_b=0.29\alpha_a$.

$$\frac{\alpha_b}{\alpha_a}=\frac{1-\exp(-\varphi_b K_1\varepsilon_{v0b})}{1-\exp(-\varphi_a K_1\varepsilon_{v0a})}\approx\frac{\varphi_b K_1\varepsilon_{v0b}}{1}$$

when ε_{vob} is very small (fast loading) and ε_{voa} is sufficient large (slow loading). Thus:

$\varphi_b K_1\varepsilon_{v0b}=0.29$, with: $\varphi_b K_1\varepsilon_0\approx 0.2\sigma_0\varphi=0.2\cdot 34.5=6.9$, is:

$\varphi_b K_1\varepsilon_{v0b}=\varphi_b K_1\varepsilon_0-\varphi\sigma_{v0b}=6.9-\varphi\sigma_{v0b}=0.29$, or: $\varphi\sigma_{v0b}\approx 6.6$.

$$\ln\left(\frac{t'_a}{t'_b}\right)=3.4=\ln\left(\frac{\exp(\varphi\sigma_{v0b})}{\exp(\varphi\sigma_{v0a})}\right)=6.6-\varphi\sigma_{v0a},\ \text{giving: } \varphi\sigma_{v0a}\approx 3.2.$$

The values of $\varphi\sigma_{v0}$ are first estimates because the value of K_1 of: $K_1=0.2\cdot(K_1+K_2)$ is an estimate. Further, at the fast loading rate, there is a small influence of another very quick relaxing element that is not noticeable at the slow rate (see fig. 5.8). Accounting for this influence would lower the ratio of the strain rates in the analysis above. Nevertheless the data of [8] can be fully explained by the theory and the value of $n=\sigma_0\varphi=34$ is comparable with the values of other experiments.

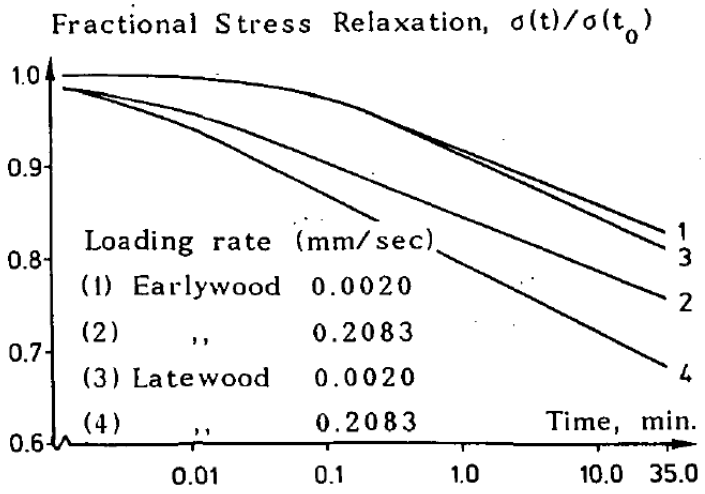

fig. 5.14 Typical curves for relaxation [8]

At relaxation of tropical wood, as measured in [9], there appears to be more plastic deformation increase than for relaxation of the species of [7] (different types of ash, hoop pine and blackbutt).

For parameter estimation in [9], it was assumed that all relaxation processes were finished at the same time (8 hours) independent of the stress level. The consequence of this assumption can be seen by the following equation. Eq.(5.5.7) can be written, with $A=B\varepsilon_{v0}$, for a structural change process:

$$\frac{\sigma}{\sigma_0}=1-\frac{\sigma_{v0}}{\sigma_0}-\frac{1}{\sigma\varphi_0}\ln\left(\frac{\varphi K_1 B\varepsilon_{v0}}{2}\cdot t\right)=\frac{K_2\varepsilon_0}{\sigma_0}-\frac{1}{\sigma\varphi_0}\ln\left(\frac{t}{t_m}\right)\qquad(5.5.10)$$

Extrapolation of this line to the stress value that is reached at the end of the relaxation:

$\sigma = K_2\varepsilon_0$, gives the intersect $t_m = 2/(\varphi\varepsilon_{v0}BK_1)$. Thus the assumption of equal times of total relaxation, is equivalent with the assumption that t_m is constant, or $\varphi\varepsilon_{v0}$ is constant (in stead of $\varphi\varepsilon_0$). Because ε_{v0} is proportional to ε_0^2 , it is assumed that $\varphi\varepsilon_0^2$ is constant. It can clearly be seen from the parameter estimation of [9] that $K_1\varphi\varepsilon_0$ is constant there and K_1 increases linearly with the strain. Because K_1 has to be constant, it follows that $\varphi\varepsilon_0^2$ is constant. This leads to the relaxation line (with $\varepsilon_{v0} = c\varepsilon_0^2$):

$$\frac{\sigma}{\sigma_0} = 1 - \frac{1}{\varphi\sigma_0}\ln\left(\frac{t}{t'}\right) = 1 - \frac{\varepsilon_{v0}}{\varphi\varepsilon_{v0}\sigma_0}\ln\left(\frac{t}{t'}\right) = 1 - \frac{c\varepsilon_0\ln(t/t')}{\varphi\varepsilon_{v0}(K_1+K_2)} \qquad (5.5.11)$$

and a plot of this equation for t = 8 hours is given in fig. 5.15. It is seen that also the second

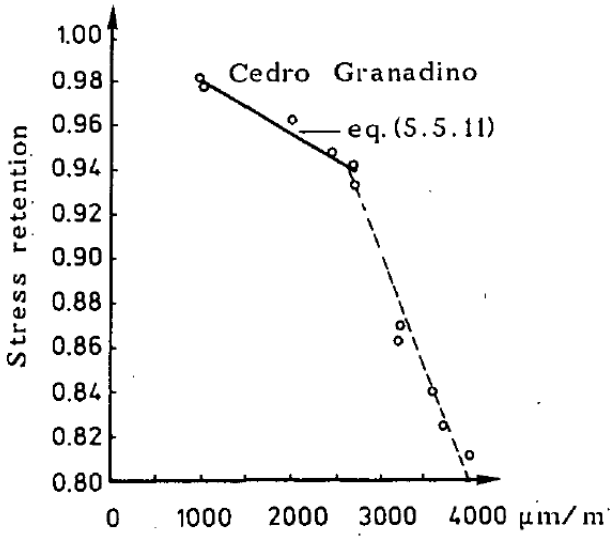

fig. 5.15 Relaxation for compression of tropical wood [9]

mechanism, above 2600 µm/m, has this dependency of φ . The constancy of $\varphi\varepsilon_{v0}$, which only occurs at high stresses for the species of [7], may also appear at low stresses in tropical species. On the other hand, the influence of the creep of the strain gauges is not known and it is possible that the creep of the glue is also measured. The same process lasted 28 hours in [7] (in stead of 8 hours in [9]) by using a very thin glue layer. Because this mechanism is different from those of wood tissues (cell walls), wood pulp (cellulose), and for fracture, and is dominating in dense lignin rich species, it may represent a flow mechanism of the lignin. For high stresses also another mechanism may occur with a constant φ , as measured for Blackbutt in [7], and as found for spruce in the B(1989a) investigation.
It may be supposed that the parabolic loading line, for loading up to the relaxation strain, may be due to a specter of mechanisms, or at least by two parallel processes. Then the relaxation equations for that case are:

$$\dot{\sigma}_1 + K_1A_1\sinh(\varphi_1\sigma_1) = 0$$

$$\dot{\sigma}_2 + K_2A_2\sinh(\varphi_2\sigma_2) = 0$$

with: $\sigma = \sigma_1 + \sigma_2$ (or, if there is a parallel spring: $\sigma = \sigma_1 + \sigma_2 + \sigma_3$ where: $\sigma_3 = K_3\varepsilon$ represents the parallel spring).
The solution of these equations are:

$$\sigma_1 = \sigma_{10} - \frac{1}{\varphi_1}\ln\left(1+\frac{t}{t'_1}\right) \qquad \text{and:} \qquad \sigma_2 = \sigma_{20} - \frac{1}{\varphi_2}\ln\left(1+\frac{t}{t'_2}\right)$$

or with: $\sigma_0 = \sigma_{10} + \sigma_{20}$ and for longer times:

$$\sigma = \sigma_0 - \frac{1}{\varphi_1}\ln(t) - \frac{1}{\varphi_2}\ln(t) + \frac{1}{\varphi_1}\ln(t'_1) + \frac{1}{\varphi_2}\ln(t'_2) = \sigma_0 - \left(\frac{1}{\varphi_1}+\frac{1}{\varphi_2}\right)\ln\left(\frac{t}{t'}\right) \qquad (5.5.12)$$

with: $t' = (t'_1)^{\varphi_2/(\varphi_1+\varphi_2)} \cdot (t'_2)^{\varphi_1/(\varphi_1+\varphi_2)}$ (5.5.13)

If one of these mechanisms is comparable with those of wood tissues and or wood pulp (cellulose), then for the first mechanism is: $\varepsilon_0\varphi_1 = c_1$ is constant or $\sigma_0\varphi_1$ is approximately constant and for the other is $\varphi_2\varepsilon_0^2 = c_2$ is constant. Then eq.(5.512) becomes:

$$\frac{\sigma}{\sigma_0} = 1 - \frac{1}{\sigma_0\varphi_1}\left(1+\frac{c_1\varepsilon_0}{c_2}\right)\ln\left(\frac{t}{t'}\right) \qquad (5.5.14)$$

and this equation doesn't approach the value $\sigma/\sigma_0 = 1$ for ε_0 approaching zero. This thus is not probable as can be seen in fig. 5.15.

The influence of temperature on stress relaxation is e.g. given in [10] for wet Hinoki wood. It appears that $\varphi\varepsilon$ is constant and is independent of the temperature below and above the transition temperature (about 50 ^{0}C), being smaller above the transition temperature.

For a horizontal shift of the line along the ln(t)-axis due to temperature difference is:

$$\left(\frac{\sigma}{\varepsilon}\right)_a - \left(\frac{\sigma}{\varepsilon}\right)_b = 0$$

leading to the so called Arrhenius equation. This is derived in 6.3, see eq.(6.3.14).

Thus: $\ln(v) = \ln(t_a) - \ln(t_b) = \ln(A_b/A_a) \approx (H/RT)_b - (H/RT)_a$ or:

$$\frac{d(\ln(v))}{d(1/T)} = \frac{H}{R} \qquad (5.5.16)$$

The shift of the relaxation lines have to be done for both slopes of the lines separately. If this is done on the data of [10] an apparent activation energy H of about 46 kcal/mol is found above and about 28 kcal/mol below transition (as also found for creep in [7]). In the transition region (between 40 ^{0} C and 60 ^{0} C) also vertical shifts are necessary for a precise fit because of the temperature dependence of $\varphi\varepsilon$ in this region. Thus there is a transition to a different mechanism with a smaller value of φ, or with an increased number of activated sites N and a higher activation energy.

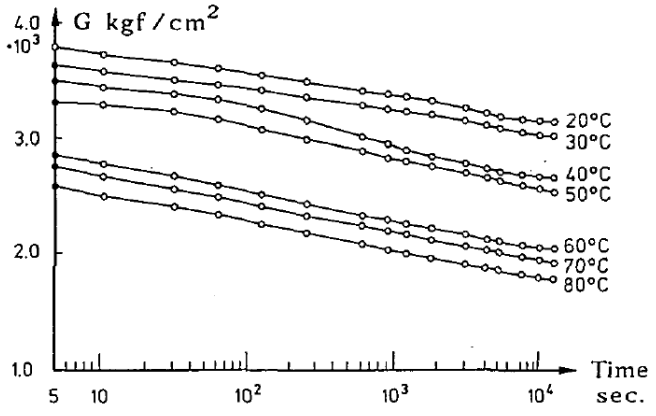

fig. 5.16 Stress relaxation curves for wet Hinoki [10] at various temperatures.

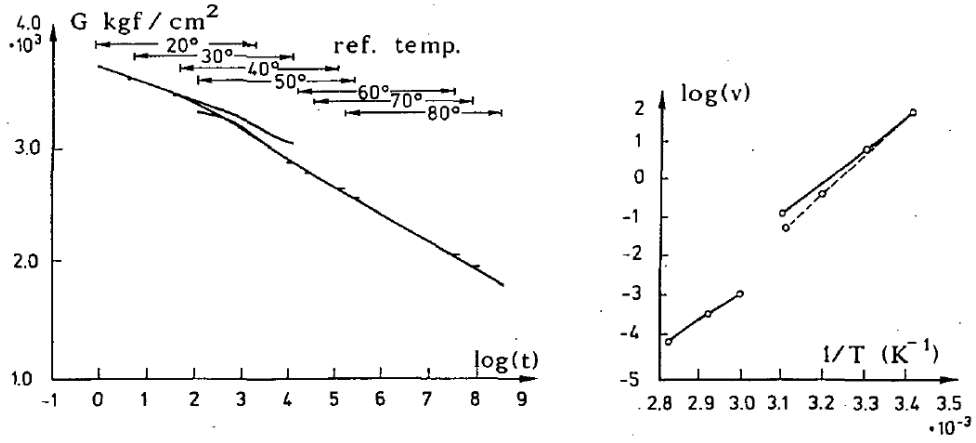

fig. 5.17 Master stress relaxation curves and shift diagram [10]

For the mechanism with a constant, stress independent value of φ, there is an indication that φ is also independent of the temperature as follows from the B(1989a) investigation. As mentioned before, the non-linearity of the time dependent behavior is not strong and there is no well defined point of flow at loading and the loading line can be regarded to be parabolic and the plastic strain ε_{v0} is therefor proportional to ε_0^2. In the following it will be shown that this is a possible approximation.
For loading up to the level of creep or relaxation is:

$$\sigma_v\varphi = \ln\left(\frac{2\dot{\varepsilon}}{B\varepsilon_v}\right) \quad \text{or:} \quad \varphi K_1\left(\varepsilon-\varepsilon_v\right) = \ln\left(2\beta/\varepsilon_v\right) \tag{5.5.17}$$

Substitution of: $\varepsilon_v = c\varepsilon^2$ gives:

$$\varepsilon = c\varepsilon^2 + \frac{\varepsilon}{\varphi K_1\varepsilon}\ln\left(\frac{2\beta}{c\varepsilon^2}\right) \quad \text{or:} \quad 1 = c\varepsilon + \frac{1}{\varphi K_1\varepsilon}\ln\left(\frac{2\beta}{c\alpha^2}\cdot\frac{\alpha^2}{\varepsilon^2}\right) \quad \text{or:}$$

$$1 = c\varepsilon + \frac{1}{\varphi K_1\varepsilon}\left(\ln\left(\frac{2\beta}{c\alpha^2}\right) - 2\ln\left(\frac{\varepsilon}{\alpha}\right)\right) \tag{5.5.18}$$

where α here is a constant, chosen in such way that $(\varepsilon-\alpha)/\alpha$ is sufficient small with respect to 1. Then:

$$\ln\left(\frac{\varepsilon}{\alpha}\right) = \ln\left(1+\frac{\varepsilon-\alpha}{\alpha}\right) \approx \frac{\varepsilon-\alpha}{\alpha} = \frac{\varepsilon}{\alpha} - 1 \tag{5.5.19}$$

Eq.(5.5.18) then becomes: $\varphi\varepsilon K_1 = \varphi\varepsilon K_1 c\varepsilon + \ln\left(2\beta/c\alpha^2\right) - 2\varepsilon/\alpha + 2$
In this equation the terms with ε have to disappear and because $\varphi\varepsilon$ is constant is:
$\varphi\varepsilon K_1 c\alpha = 2$ and; $\varphi\varepsilon K_1 - 2 = \ln\left(\beta\varphi\varepsilon K_1/\alpha\right)$
Thus an estimate for c is:

$$c = \frac{2\beta}{\left(\varphi\varepsilon K_1\right)^2}\exp\left(\varphi\varepsilon K_1 - 2\right) \tag{5.5.20}$$

The same can be done when $\varphi\varepsilon^2$ is constant. Eq.(5.5.18) then becomes:

$$\frac{1}{\varepsilon} = c + \frac{1}{K_1\varphi\varepsilon^2}\left(\ln\left(\frac{2\beta}{c\alpha^2}\right) + 2\ln\left(\frac{\alpha}{\varepsilon}\right)\right)$$

or with eq.(5.5.19):
$K_1\varphi\varepsilon^2/\varepsilon = cK_1\varphi\varepsilon^2 + \ln\left(2\beta/c\alpha^2\right) + 2\alpha/\varepsilon - 2$. Thus:

$$2\alpha = K_1\varphi\varepsilon^2 \quad \text{and:} \quad c = \frac{\left(K_1\varphi\varepsilon_v\right)^2}{8\beta}\exp(2 - K_1\varphi\varepsilon_v) \tag{5.5.21}$$

As mentioned in 5.4, there is also a possibility of an approximate linear relationship between ε_v and ε_v (influence of lignin). When α is close to 1, eq.(5.5.17) can be written:

$$\varepsilon_v = \varepsilon\left(1 - \frac{1}{\varepsilon\varphi K_1}\ln\left(\frac{2\dot{\varepsilon}}{A}\right)\right) = c\varepsilon \tag{5.5.22}$$

An example of this relationship is mentioned in 2.3.2, where the number of slip lines increases linearly with the stress level.
When φ is constant, the shift of the creep line (and not the compliance line) or the shift of the relaxation line (and not the line of relative relaxation) has to be regarded to see the dependency of ε_v on ε.

5.6 Conclusions

For many materials there is a dominating mechanism with a constant value of $\varphi\varepsilon_0$ (ndependent of the temperature and initial strain ε_0 at constant moisture content). Probably this is the case for slip-line formation, local buckling, and crack initiation and propagation, but it also applies for short segments movements of rubbers in the glassy state. Until now it was not recognized that this also applies for wood. Coupled to this mechanism is another mechanism with a lower value of $\varphi\varepsilon$ and a long delay time (flow unit increase) that occurs after some critical visco-elastic strain (0.4% [6]) of the first mechanism and possibly this first mechanism creates the room, or the flow units, for the second mechanism. The additional creep strain of this second mechanism is irreversible [6]. This mechanism did not occur in cell wall experiments, even not at high stress levels. Because in high loaded wood, the early-wood is higher loaded than in these cell wall experiments and thus flows, this mechanism can probably be related to flow of the early-wood and load transmission from the early-wood to the latewood.
The dependency of this mechanism on the moisture content ω follows from strain rate tests, where it was found that 1/n is proportional to ω (or the density of flow units N is proportional to ω). The same was found in creep tests.
Besides these dominating mechanisms, that are related to the cellulose and hemi-cellulose, there is a small mechanism with a low value of $\sigma\varphi$.
(n = 1) and a short relaxation time that is only noticeable at very high loading rates.
With the property of constant $\varphi\varepsilon_0$ (or constant n), it is possible to explain experimental laws as, for instance, the linear dependence of the stiffness on the logarithmic value of the strain rate in a constant strain rate test; the logarithmic law for creep and relaxation; the shift factor along the log- time axis due to stress and temperature; the different power models (of the stress and of the time) as the Forintek model and the Andrade and Clouser creep- equations; the constant of the WLF-equation and the height of the relaxation spectrum as shown later.
For clear wood in compression there in no indication of hardening and yield drop, showing the influence of a amorphous polymer (lignin). For wood in tension there is a high yield drop, showing the influence of a crystalline material (cellulose) dominated by a low initial flow unit density ρ_0. There is also no indication of hardening, showing that the change of one model-parameter (λ_1) dominates as also follows from the high value of $\sigma\varphi$.

The viscoelastic and viscous flow strain at loading to the creep or relaxation level, is approximately proportional to the quadrate of the strain: $\varepsilon_v \approx c\varepsilon^2$, for holocellulose (= wood structure without lignin) and for flow of the early-wood. For wood at low stresses ε_v is about linear dependent on ε and the viscoelastic behavior is quasi linear by the influence of the lignin wherefore $B\varepsilon_v \approx A$ is constant (by the high initial flow unit density and no structural change).
The existence of another mechanism in wood is reported in [7] and [9]. For this structural change mechanism, the relaxation time is independent of the stress level and thus it is not related to the holocellulose. It can be deduced that for this mechanism $\varphi\varepsilon_v$ or $\varphi\varepsilon_0^2$ is constant. Thus the number of creeping sites N increases with increasing plastic strain ($n = \sigma\lambda / NkT = \sigma(\lambda / \lambda_1) / kT(N / \lambda_1) = \sigma\varepsilon_{v0} / kTN'$, with $N' = N / \lambda_1$. being the number of flow units per unit volume). Half of the stress was relaxed in about 10 minutes in [9], but the process occurred only at high stress levels and lasted much longer in [7] (halve of the creep in about 3 hours). Possibly there is an influence of creep of the glue of the strain gauges. The thin glue layer of [7] may then explain the much longer relaxation time. However also measured in [7] are mechanisms with constant $\varphi\varepsilon$ at low stress levels and constant φ f at high stress levels (with $\varepsilon_v = c\varepsilon$) indicating a right behavior of the strain gauges. Thus a better explanation is that this is a mechanism in the lignin. Tropical woods are much denser and contain much more lignin (about twice as much) than the Nordic species. Especially the Nordic hardwoods have the less content of lignin and will not show this mechanism.
The constancy of $\varphi\varepsilon_v$ applies only for constant temperature and moisture content. Probably $1/\varphi\varepsilon_v$ is linear dependent on ω and T. In the B(1989a) investigation an approximate constant φ, independent of the temperature and moisture content, was found for high stress levels (and probably this is due to a dominant influence of diffusion on the creep by the small cycling humidity conditions as discussed in 7.2. In that case, the stress independent part of the activation energy is linear dependent on ω).

5.7 References

[1] Predicting the effect of specific gravity, moisture content, temperature and strain rate on the elastic properties of wood. L.C. Palka, Wood Science and Technology 7, 1973.
[2] For. Prod. Lab. Report No 1767, J.A. Liska, 1950.
[3] Bulletin of A.I.J. no 32, H. Sugiyame 1953.
[4] Deformation kinetics. A.S. Krausz, H.Eyring 1975 John Wiley & Sns.
[5] The creep behaviour of individual pulp fibers under tensile stress, R.L. Hill, Tappi 50, no 8 Aug. 1967.
[6] Creep and strain behaviour of wood, E.G. King, Forest Prod. Journ. Oct. 1957.
[7] Some aspects of the rheological behaviour of wood, R.S.T. Kingston, L.N. Clarke, Austr. Journ. of applied Science 12 no 2, 1961.
[8] On the fractional stress relaxation of coniferous wood tissues, E. Kirbach, L. Bach, R.W. Wellwood, J.W. Wilson, Wood and Fiber 8, no 2, 1976.
[9] Stress relaxation of wood at several levels of strain, H. Echenique Manrique, U.S.N. Office of Naval Research. Techn. Rep., 1967.
[10] The effect of temperature on torsional stress relaxation of wet Hinoki wood, H. Urakami and K. Nakato, Proc. of the 14th meeting of the J.W. Res. Soc. Tokyo, Apr. 1964.

6. Other aspects of the derived theory

6.1 Introduction

The derived general theory is able to explain the different empirical equations and to give a physical meaning to the constants of those equations. This will be discussed here for frequently used models.
As shown before, equations in the power of the stress, as the Forintek model and as used in fracture mechanics, can be explained. The same is possible with the relations containing the power of the time, as the Andrade and Clouser equations. It appears that the Clouser-type equation is equivalent to the theoretical logarithmic creep behavior.
The derived deformation kinetics theory also gives an explanation of the WLF-equation (Williams-Landel_Ferry is WLF) for the shift factor of the creep line at different temperatures along the log-time axis. The theory explains why this equation also applies for cross-linked polymers at transient creep.
Often, the nonlinear viscoelastic deformation problem is linearized by splitting up the contribution to the rigidity in numerous linear viscoelastic processes giving a relaxation spectrum. It is shown here that, on the contrary, by a special property of the activation volume, a single process explains the measured, broad, nearly flat spectra of glasses and crystalline polymers, giving a physical meaning to a spectrum.

6.2 Mathematical explanation of the Andrade creep equation or of the power model for creep

Power models are first approximations, regarding only one acting process. Application for more at the same time acting processes, needs a determination of the applied stress σ_1, σ_2, of each process, providing more than one power. The Andrade-type equation for the description of creep is often used for wood and wood-products. The "constants" of this equation depend on the chosen time scale. To explain this equation and this behavior, a derivation of the constants is given, showing the physical meaning of the "constants", by comparison with the theory of reaction kinetics as given in § 4. Andrade divided high temperature creep into three regions: primary or decelerating creep, secondary or steady state creep and tertiary or accelerating creep. For the description of low temperature creep, that is considered to have only a decelerated stage, Andrade suggested the following equation:

$$\gamma = \gamma_0 + c_1 t^{1/3} + c_2 t \qquad (6.2.1)$$

where γ is the deformation, c, c_1, c_2 are constants and t is the time. For the cross-linked polymers of wood c_2 is negligible and eq.(6.2.1) becomes:

$$\gamma = \gamma_0 + c t^{1/3} \qquad (6.2.2)$$

For wood, c is proportional to γ_0 (as will be discussed at the end of § 6.2) and eq.(6.2.2) can be expressed in the relative creep δ:

$$\delta = \frac{\gamma - \gamma_0}{\gamma_0} = C t^{1/3} \qquad (6.2.3)$$

or more general:

$$\delta = C t^m \qquad (6.2.4)$$

This equation is known as the "power-model" or "Clouser" equation. To explain the meaning of this empirical equation it will be compared with the theoretical equation for deceler-

ated creep behavior as given before in § 5.4. From this theory it appears that decelerating creep can be described by:

$$\gamma = c_1 - c_2 \ln\left(\coth\left(c_3 + c'_4\, t\right)\right) \tag{6.2.5}$$

where the constants c_i are known expressions in the molecular parameters. In the early part of the process this reduces to:

$$\gamma = \gamma_0 + c_2 \ln\left(1 + c_4 t\right) \tag{6.2.6}$$

or for not too short times, comparable with the range where eq.(6.2.1) is applicable, thus when: $1 << c_4 t$, is: $\delta = B\ln\left(t / t_1\right)$ (6.2.7)

Thus eq.(6.2.4) has to be compared with this expression. Eq.(6.2.4) can be written like:

$$\delta = A'\left(t / t_1\right)^m = A'\left(t / t_0\right)^m \left(t_0 / t_1\right)^m = A'\left(t_0 / t_1\right)^m \cdot \exp\left(m \ln\left(t / t_0\right)\right) \tag{6.2.8}$$

or in Taylor séries:

$$\delta = A'\left(t_0 / t_1\right)^m \left(1 + m\ln\left(t / t_0\right) + \frac{1}{2}\left(m\ln\left(t / t_0\right)\right)^2 + \frac{1}{6}\left(m\ln\left(t / t_0\right)\right)^3 + ... \right) =$$

$$= A'\left(t_0 / t_1\right)^m \left(1 + m\ln\left(t / t_0\right) + \psi\right) \tag{6.2.9}$$

where t_0 is a scaling time providing that $m \cdot \ln\left(t / t_0\right)$ will be smaller than 1 and ψ is the small influence of the higher order terms.

Eq.(6.2.7) can be written: $\delta = B\ln\left(t / t_0\right) + B\ln\left(t_0 / t_1\right)$

and comparing with eq.(6.2.9), the conditions to obtain the same values with both equations are:

$$mA'\left(t_0 / t_1\right)^m = B \quad \text{and:} \quad A'\left(t_0 / t_1\right)^m \left(1 + \psi\right) = B\ln\left(t_0 / t_1\right)$$

leading to:

$$1 + \psi = \ln\left(B / mA'\right) = m\ln\left(t_0 / t_1\right) \tag{6.2.10}$$

The value of ψ can be taken at some intermediate time t_b, between t_0 and the maximum time of observation t_m.

$$1 + \psi = \exp(m\ln\left(t_b / t_0\right)) = m\ln\left(t_b / t_0\right) = \left(t_b / t_0\right)^m - \ln\left(t_b / t_0\right)^m \tag{6.2.11}$$

or with aid of eq.(6.2.10):

$$\exp\left(1 + \psi\right) = \left(t_b / t_1\right)^m / \ln\left(t_b / t_1\right)^m \tag{6.2.12}$$

Now is m in eq.(6.2.13) not constant:

$$A'\left(t / t_1\right)^m = B\ln\left(t / t_1\right) \tag{6.2.13}$$

If in this equation m is regarded as a function of time then the change of m with time is minimal for B = A' and eq.(6.2.10) becomes:

$$1 = m \cdot \exp\left(1 + \psi\right) \tag{6.2.14}$$

or with negligible ψ:

$$1 = m.e \quad \text{or:} \quad m = 1/e = 0.368 \tag{6.2.15}$$

or better, if $q\,\psi = 0.1$ is chosen for curve fitting, then: m = 0.334 which is the exponent of Andrade.

From eq.(6.2.10) and eq.(6.2.12) it follows that $\psi = 0.1$, $t_0 / t_1 = 27$, $t_b / t_1 = 93$ and $t_m / t_1 \approx 195$ can be taken for not too high deviation at t_m. According to eq.(6.2.9) is $t_m / t_1 < 540$ to maintain convergence of the series. For larger time scales m will be different. For instance, if $t_b / t_1 = 100000$ to 1000000, than m is about: m = 0.2.

The meaning of the constants of the Andrade equation can now be given.
Because A' = B, is A' equal to the inverse of the initial creep stress times the activation volume parameter:

$$1/A' = \sigma V / RT \qquad (6.2.16)$$

where σ is the creep stress, V the activation volume, R the gas constant and T the absolute temperature. For not to high stress levels A` can be regarded to be constant because V is inverse proportional to σ. As measured in [1], C = 0.02 for m = 0.31 for timber, indicating a value of A' of about A' = 0.03. The value 1/A' has the same meaning as the exponent n (n = 1/A') of the experimental power law of the creep rate $\dot{\varepsilon} = c\sigma^n$.
The time t_1 is for wood the delay time of the main process where the creep levels off to higher rates. It is a function of the activation parameters and is dependent on the initial flow unit density.
It can be concluded that the Andrade-type equation is equivalent to the theoretical logarithmic creep behavior and that the constants accordingly have a special meaning and can be compared with the theoretical parameters. Because these "constants" are not really constant but functions of many parameters, it is necessary to use the logarithmic representation instead of the power-model for a real prediction of behavior after long times.

6.3 Derivation of the WLF-equation for the time-temperature equivalence above glass-rubber-transition

The derivation and explanation of B(1998a), of the WLF-equation (Williams-Landel-Ferry is WLF) for the time-temperature equivalence above glass-rubber transition temperature, is outdated and therefore not discussed here. The theory is renewed and extended in B(2010) and in B.3, leading to an important new vision, discussed in a separate section B.3.

6.4 Relaxation and retardation spectra

The nonlinear viscoelastic deformation problem is often linearized by splitting up the contribution to the rigidity in numerous linear viscoelastic processes. Thus the contribution: fdt to G(t) is associated with relaxation times in the range τ and $\tau + d\tau$. Mostly a logarithmic time scale is used and the contribution of the range ln(t), ln(t) + d(ln(t)) is H.d(ln(t)) with H = ft. The time dependent rigidity or relaxation modulus is then:

$$G(t) = G_\infty + \int_{-\infty}^{\infty} H \cdot \exp(-t/\tau) \cdot d\left(\ln(\tau)\right) \qquad (6.4.1)$$

Because a spectrum of relaxation times does not exist, as follows from the zero relaxation test, eq.(6.4.1) has no physical meaning, and is a mathematical representation of measured data by H, called relaxation spectrum. For the solution of H, the intensity function exp(-t/τ), having values between 0 and 1 for τ = 0 to $\tau = \infty$, can be approximated by a step function from 0 to 1 at τ = t, Thus:

$$G(t) = G_\infty + \int_{\ln(t)}^{\infty} H \cdot d\left(\ln(\tau)\right)$$

Differentiation of this equation with respect to the limit ln(t) gives:

$$-\left.\frac{d\left(G(t)\right)}{d\left(\ln(t)\right)}\right|_{t=\tau} = H(\tau) \qquad (6.4.2)$$

Thus the relaxation spectrum at $\tau = t$ is, as first approximation, the negative slope of the measured relaxation modulus. This approximation is accurate if H changes slowly with time. Except for the beginning and end of a kinetic process in wood, G(t) has the form:

$$G(t) = G_{\infty} - C \cdot \ln(t) \qquad (6.4.4)$$

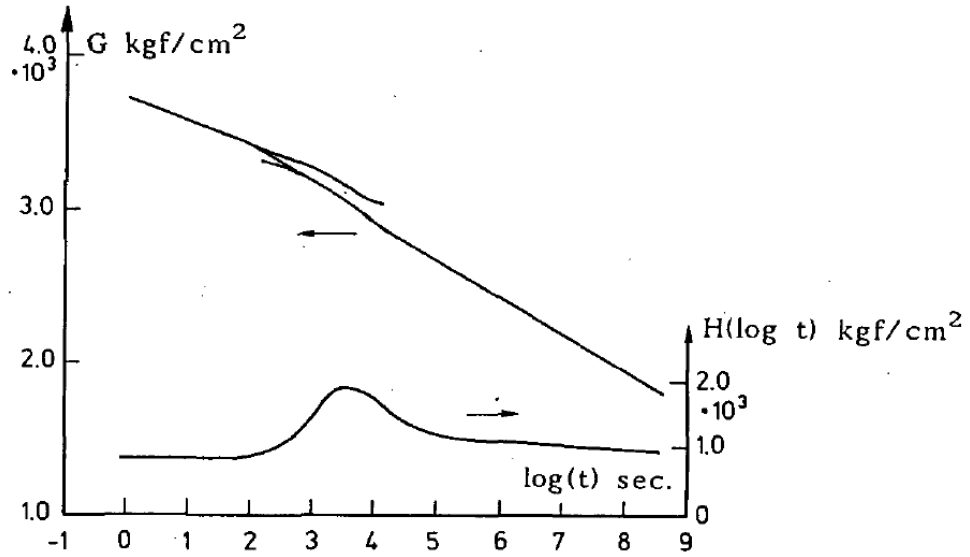

fig. 6.4 Master relaxation curve G(t) and relaxation spectrum of wood [8].

and H = C (where C is proportional to the slope of G(t)) in a wide time range due to a single acting process. This explains the measured, broad, nearly flat spectra of glasses and crystalline polymers.
As mentioned before a second process is starting in wood and in other highly crystalline polymers after a long delay time depending on the stress level. At the transition to this second process the change of H is not slow with time and H can be approximated by:

$$H(\tau) = -\frac{d(G(t))}{d(\ln(t))} + \frac{d^2(G(t))}{d(\ln(t))^2}\Bigg|_{t=2\tau} \qquad (6.4.5)$$

leading to the outline above of the relaxation spectrum for wood in fig. 6.4 that is due to two non-linear processes in stead of the assumed infinite number of impossible linear viscoelastic processes which are shown to be non-existent by the zero relaxation test discussed at § 8. The relaxation spectrum H thus is nothing more than an alternative mathematical expression of the measurements G(t).

6.5 Spectrum of energy loss at forced vibrations and fatigue behavior

For a forced vibration on a single Maxwell element by an applied strain: $\varepsilon = a \cdot \sin(2\pi\upsilon t)$, the stress is: $\sigma = b.\sin(2\pi\upsilon t + \theta)$ and the absorbed energy is:

$$Z = \int_0^{t_c} \sigma d\varepsilon = \pi ab \sin(\theta) \qquad (6.5.1)$$

where t_c is the period of the vibration $1/\upsilon$ and θ is the phase angle.
For the three element model at small values of $\phi\sigma_v$ applies:

$$\sigma = \sigma_v + \sigma_2 = \frac{\dot{\varepsilon}_v}{A\phi} + K_2\varepsilon \tag{6.5.2}$$

or also: $\sigma = K_1(\varepsilon - \varepsilon_v) + K_2\varepsilon$. (6.5.3)

Elimination of ε_v in the last two equations gives:

$$A\phi K_1\sigma + \dot{\sigma} = (K_1 + K_2)\dot{\varepsilon} + A\phi K_1 K_2\varepsilon \tag{6.5.4}$$

Substitution of the expressions for σ and ε gives:

$$A\phi K_1 b\sin(2\pi\nu t + \theta) + 2\pi\nu b\cos(2\pi\nu t + \theta) =$$
$$= (K_1 + K_2)2\pi\nu a\cdot\cos(2\pi\nu t) + A\phi K_1 K_2 a\cdot\sin(2\pi\nu t) \tag{6.5.5}$$

This must be true at any time, thus the sum of the terms containing cos(2 $\pi\nu$ t) has to be zero and also the sum of the terms containing sin(2 $\pi\nu$ t). This leads to:

$$b = \left(\frac{2\pi\nu(K_1 + K_2)}{A\phi K_1}\right)\cdot\left(\sin(\theta) + \frac{2\pi\nu}{A\phi K_1}\right)^{-1} \tag{6.5.6}$$

and:

$$\sin(\theta) = \frac{2\pi\nu a K_1^2 (A\phi)^{-1}}{bK_1^2 + 4\pi^2\nu^2 b(A\phi)^{-2}} \tag{6.5.7}$$

Thus from eq.(6.5.1) follows:

$$Z = \frac{2\pi^2\nu a^2 K_1^2 (A\phi)^{-1}}{K_1^2 + 4\pi^2\nu^2 (A\phi)^{-2}} \tag{6.5.8}$$

The energy of absorption is maximal at the frequency ν_n, where: $\partial Z/\partial\nu = 0$.

Thus: $\nu_n = K_1 A\phi/2\pi$.

For a relaxation time distribution:

$$Z = \pi a^2 \sum_i \frac{K_i\nu/\nu_i}{1 + (\nu/\nu_i)^2} \tag{6.5.9}$$

Usually this is given for an infinite number of processes as:

$$\int h(\tau)\cdot\frac{\omega\tau}{1 + \omega^2\tau^2}\,d(\tau),$$

where τ is the relaxation time:$1/\omega_n$ and $\omega = 2\pi\nu$.

The natural frequencies ν_n are far apart and it can be expected that Z between two natural frequencies ν_1 and ν_2 is mainly determined by these two processes:

$$Z = \pi a^2\left(\frac{K_1\nu/\nu_1}{1 + (\nu/\nu_1)^2} + \frac{K_2\nu/\nu_2}{1 + (\nu/\nu_2)^2}\right) \tag{6.5.10}$$

For $\nu = \nu_1$:

$$Z_1 = \frac{\pi a^2 K_1}{2}\left(1 + \frac{2K_2\nu_1/K_1\nu_2}{1 + (\nu_1/\nu_2)^2}\right) \approx \pi a^2 K_1\left(\frac{1}{2} + \frac{K_2\nu_1}{K_1\nu_2}\right) \tag{6.5.11}$$

because $\nu_1 \ll \nu_2$. In the same way, for $\nu = \nu_2$, $Z = Z_2$.

$$Z_2 \approx \pi a^2 K_2\left(\frac{1}{2} + \frac{K_1\nu_1}{K_2\nu_2}\right) \tag{6.5.12}$$

and because the spectrum is flat [6], or Z is about constant, is $Z_1 \approx Z_2$ and the stiffness must be equal or: $K = K_1 = K_2$. If for an intermediate value of ν, $\nu = (\nu_1 + \nu_2)/2$, Z is equal to Z_1 and Z_2, then $\nu_1 \approx 0.1\cdot\nu_2$. Thus there will be a range of relaxation times:

$t_i = (1/10)^i \cdot t_0$. Thus: $t_i / t_0 = \exp(E_i / RT - E_0 / RT) = (0.1)^i = \exp(-i \ln(10))$ or:

$$E_i = E_0 - RT \cdot i \cdot \ln(10) = E_0 - 1.35 \cdot i \qquad (6.5.13)$$

and there will be a long range of activation energies in kcal./mol. of for instance:
23 - 22 - 20 - 19 - 18 - 16 - 15 - 14 - 12 - 11 - etc. However measured by other methods are p.e. 23 and 11 kcal./mol. (β - mechanisms). Thus it is necessary that in eq.(6.5.8) in a wide range: $\phi / \nu = \text{constant} = c2\pi / KA = c2\pi t_r / K$ (6.5.14)

and the flat spectrum is determined by only one process with relaxation time t_r.

The analysis shows that ε_v is alternating and thus is reversible.

A particular solution of eq.(6.5.4) is:

$$\sigma = C \cdot \exp(-A\varphi K_1 t) = C \cdot \exp(2\pi\upsilon t), \qquad (6.5.15)$$

showing that a disturbance disappears within a part of the period. For instance in half the period time is $\sigma = C \cdot \exp(-\pi) = 0.04 \cdot C$.

For high loading:

$$\sigma_v = \frac{1}{\varphi} \ln\left(\frac{2\dot{\varepsilon}_v}{A}\right) = K_1(\varepsilon - \varepsilon_v) \quad \text{or:} \quad 2\dot{\varepsilon}_v = A \cdot e^{(\varphi K_1 \varepsilon - \varphi K_1 \varepsilon_v)} \quad \text{or:}$$

$$\left(\varphi K_1 e^{\varphi K_1 \varepsilon_v}\right) \cdot d\varepsilon_v = \left(e^{\varphi K_1 \varepsilon} \cdot \varphi K_1 A / 2\right) \cdot dt$$

Thus:

$$e^{\varphi K_1 \varepsilon_v} - e^{\varphi K_1 \varepsilon_{v0}} = \frac{n}{2} \int_0^{t_c} \varphi K_1 A e^{\varphi K_1 \varepsilon} \cdot dt = n \cdot C_1$$

where t_c is the time of high stress within the period and n is the number of cycles. Thus:

$$\varphi K_1 \varepsilon_v = \varphi K_1 \varepsilon_{v0} + \ln\left(1 + C_1 n \cdot e^{-\varphi K_1 \varepsilon_{v0}}\right) \qquad (6.5.16)$$

For higher values of n: $\ln\left(t + C_1 n \cdot e^{-\varphi K_1 \varepsilon_{v0}}\right) \approx \ln\left(C_1 n \cdot e^{-\varphi K_1 \varepsilon_{v0}}\right) = \ln(n / n_0)$ and eq.(6.5.16) becomes:

$$\varphi K_1 \varepsilon_v = \varphi K_1 \varepsilon_{v0} + \ln(n / n_0) \qquad (6.5.17)$$

Outside the high stress region the stress and ε_v resume quickly, according to eq.(6.5.15), the low stress values (as described by eq.(6.5.1) to (6.5.8)), but ε_v has increased according to eq.(6.5.17). At high frequencies this increase is small and ε_v is mainly determined by $\sin(\theta)$ of the low stress region. If, for comparison with static long term loading, mean values of stress and strain are regarded, then:

$$\bar{\sigma}(2/\pi) = (K_1 + K_2)\bar{\varepsilon}(2/\pi) - K_1 \bar{\varepsilon}_{v0}(2/\pi) - (1/\varphi)\ln(n/n_0) \quad \text{or:}$$

$$\frac{\bar{\sigma}}{\bar{\sigma}_0} = 1 - \frac{1}{\varphi \bar{\sigma}_0 (2/3)} \ln\left(\frac{n}{n_0}\right) \qquad (6.5.18)$$

This equation thus applies for high frequencies, empirically for frequencies above 1 Hz up to 10^4 Hz. For cases where peak-stresses play a role, as at knots, in particle board and at finger joints, it can be deduced from the regression lines, given in [7], that the empirical fatigue equation is:

$$\frac{\bar{\sigma}}{\bar{\sigma}_0} = 1.14 - 0.103 \cdot \log(n) \qquad (\leq 1 \text{ at the delay time at the start}) \qquad (6.5.19)$$

For low frequencies, $\sin(\theta)$ is small and the increase of ε_v is curvilinear and now also the factor $2/\pi$ on its top value applies, giving:

$$\frac{\bar{\sigma}}{\bar{\sigma}_0} = 1 - \frac{1}{\varphi\bar{\sigma}_0}\ln\left(\frac{n}{n_0}\right) \qquad (6.5.20)$$

This equation applies below about 0.1 Hz. for wood. Depending on the frequency, fracture may occur in a few cycles. However, this equation can be written in a total time to failure:

$$\frac{\bar{\sigma}}{\bar{\sigma}_0} = 1 - \frac{1}{\varphi\bar{\sigma}_0}\ln\left(\frac{\nu t}{\nu t_0}\right) = 1 - \frac{1}{\varphi\bar{\sigma}_0}\ln\left(\frac{t}{t_0}\right) \qquad (6.5.21)$$

and this equation is identical to the long duration strength of a specimen loaded by a constant load, equal to the top value of the fatigue loading. The empirical equation of this long duration strength is:

$$\frac{\bar{\sigma}}{\bar{\sigma}_0} = 1.17 - 0.070\ln(t) \qquad (\leq 1 \text{ at the delay time, at the start}) \qquad (6.5.22)$$

showing that the slope of the high frequency line is indeed about a factor 1.5 steeper. Or more precise: 0.103/.070 = 1.47. If there is a stress level where below there is no fatigue or no failure for long term loading, then the maximum strain condition predicts that this level will be a factor 1.47 lower for high frequency loading. Because the stress level for no damage at long term loading is supposed to be 0.5, the fatigue level is about 0.5/1.47 = 0.35. This is in agreement with the expectation from tests on rotor-blades (of NASA).

For very low frequencies (lower than about 10^{-6} Hz), recovery may occur at the period of unloading and only the sum of the loading times have to be taken for t in eq.(6.5.22). Thus it follows that at least half of the "permanent" strain at higher stress levels is recoverable.

For a small initial flow unit density: $A = B\varepsilon_v$, the analysis is comparable as done before and as done for static loading.

$$\sigma_v = \frac{1}{\varphi}\cdot\ln\left(\frac{2\dot{\varepsilon}_v}{B\varepsilon_v}\right) = K_1(\varepsilon - \varepsilon_v) \qquad \text{or:} \qquad 2\dot{\varepsilon}_v = B\varepsilon_v e^{\varphi K_1(\varepsilon-\varepsilon_v)} \qquad \text{or:}$$

$$\left(e^{\varphi K_1\varepsilon_v}\right)\cdot d\left(\ln\left(\varphi K_1\varepsilon_v\right)\right) = \left(\frac{B}{2}e^{\varphi K_1\varepsilon}\right)\cdot dt$$

Thus: $E_i\left(\varphi K_1\varepsilon_v\right) - E_i\left(\varphi K_1\varepsilon_{v0}\right) = \frac{n}{2}\int_0^{t_c} B\cdot e^{\varphi K_1\varepsilon}dt = n\cdot C_1$ or:

$$\varphi K_1\varepsilon_v = E_i^{-1}\left(n\cdot C_1 + 0.577 + \ln\left(\varphi K_1\varepsilon_{v0}\right)\right) \qquad (6.5.23)$$

and there is a delay time for fatigue. The fatigue line starts with a small slope and bends down at higher values of n to a straight line on log(n)-scale. Because for higher values of ε_v and n, this equation becomes:

$$\exp\left(\varphi K_1\varepsilon_v\right) = \varphi K_1\varepsilon_v\left(n\cdot C_1 + 0.577 + \ln\left(\varphi K_1\varepsilon_{v0}\right)\right) \qquad \text{or:}$$

$$\varphi K_1\varepsilon_v = \ln\left(\varphi K_1\varepsilon_v\right) + \ln\left(C_1\left(n - n_1\right)e^{-\varphi K_1\varepsilon_{v0}}\right) + \varphi K_1\varepsilon_{v0} \qquad \text{or:}$$

$$\varphi K_1\varepsilon_v = \varphi K_1\varepsilon_{v0} + \ln\left(\frac{n - n_1}{n_0}\right) \qquad (6.5.24)$$

the same fatigue equations occur as given before, however in a shifted position on the log(n)-axis.

A delay time is not to be expected for particle board, because of the high concentration of holes. Knots in timber act however as flow units with a low density, as can be seen by the strong yield drop in a constant strain rate test, and timber will show a delay time for fatigue.

6.6 References

[1] Rheology, Theory and Applications. T.Ree, H. Eyring 1958 New York.
[2] Influence of Heat on Creep of Dry D.-Fir. E.L.Schaffer For.Prod. Lab. Madison, Wisconsin.
[3] Studies on Dynamic Torsional Viscoelasticity of Wood, H. Becker, D. Noack, Wood Science and Technology Vol. 2 (1968) p. 213-230.
[4] Softening of fibre components in hot pressing of fibre mats, N. Taka-mura, Journ. Japan Wood Res. Soc. 14 (4) p. 75-79 (1968).
[5] R.J. Hoyle, M.C. Griffith, R.Y. Itany, 1985, Wood and Fiber Science, July 1985 V.17.
[6] Rheology and the study of wood, R.E. Pentoney, R.W. Davies, For. Prod. Journ. May 1962, p. 248.
[7] J.P. McNatt, Wood Science 11, 1979, 1.
[8] The effect of temperature on torsional stress relaxation of wet Hino-ki wood, H. Urakami, K. Nakato, Proc. of the 14 th meeting of the J.W. Res. Soc. Tokyo, Apr. 1964.

7. Explanation of the mechano-sorptive effect

Discussed are the derivations of B(1989a) and the further development in B(1989b). In B(1989a), part of the differential strain rate between the layers was defined as a separate mechano-sorptive strain. This however appeared to be superfluous and the straightforward exact derivation of B(1989b) is now retained in the following.

7.1 Small changes of moisture content at low stresses

At constant moisture content or moisture gradient, moisture acts as lubricant, reducing the relaxation time of wood. At changing moisture content, the behavior of adjacent layers can be very different because one layer may shrink and the other may elongate, with respect to the free volume change. The S_2 layer elongates in axial direction (by the steeper microfibril angle) and shrinks perpendicular to this direction at desorption while the other layers behave reversed from this with respect to the stress free expansions. This causes high internal stresses and extensive flow and shifts of the layers with respect to each other.
The kinetic equation of layer deformation is similar to that of a Maxwell element (a spring with a non-linear dashpot on top) with a parallel spring. When, in a stress relaxation test, this three-element model is loaded to σ_0 at strain ε_0 at time t_0, then the Maxwell element is loaded to σ_{v0} and the free parallel spring to $\sigma_0 - \sigma_{v0}$, what remains unchanged when by relaxation, the stress σ_v on the Maxwell element decreases.
For relaxation of this three-element model $\dot{\varepsilon} = 0$ and for the Maxwell element:

$$\dot{\varepsilon} = \dot{\varepsilon}_e + \dot{\varepsilon}_v = 0, \quad \text{or:} \quad \dot{\sigma}_v + K_1\dot{\varepsilon}_v = 0 \quad \text{or:} \quad \dot{\sigma}_v + K_1 A \sinh(\varphi\sigma_v) = 0 \tag{7.1}$$

At changing moisture content conditions there is a rapid reaction of water with the hydrogen bonds. Thus a low activation energy and activation volume can be expected and the equation for relaxation may be approximated to:

$$\dot{\sigma}_1 + K_1 A \sinh(\varphi\sigma_1) \approx \dot{\sigma}_1 + K_1 A' \omega\varphi\sigma_1 = 0 \tag{7.2}$$

as follows from the exact derivation of diffusion behavior in section B.2. The free overall swelling is subtracted because this has no influence on the stress.
Thus, in eq.(7.2) is $\sinh(\varphi\sigma_1) \approx \varphi\sigma_1$, $A = A'\omega$ (in accordance with thermodynamics and reaction order) and ω is the change in moisture content. Thus the starting equation is:

$$\dot{\sigma}_1 + K_1 A' \omega\varphi\sigma_1 = 0 \tag{7.3}$$

For creep, the same equation applies with K_1 replaced by K ($1/K = 1/K_1 + 1/K_2$).
The solution of eq.(7.3) is:

$$\ln\left(\frac{\sigma}{\sigma_0}\right) = -K_1 A\varphi t = -K_1 A' \omega\varphi t \tag{7.4}$$

where ω is the suddenly applied (step-) difference in moisture concentration.
This eq.(7.4) is based on the bond breaking process and can also be obtained by the rate equation of bond breaking:

$$\dot{\rho} = -k\rho\omega \tag{7.5}$$

where ρ is the concentration of mobile bonds, having as solution:

$$\ln\left(\frac{\rho}{\rho_0}\right) = -k\omega t \tag{7.6}$$

and it is seen that this result is identical to eq.(7.4). Thus the stress supported by the reactive bonds is proportional to the number of bonds and the ratio ρ / ρ_0 can be determined

from the stress relaxation test (or from creep tests).
These equations apply for very thin specimens, where the step-change is approximately possible. For thicker specimens, the moisture has to diffuse into the specimen. Diffusion is discussed and derived in B(2005) §2.3. From Fick's second law, (based on random walk of jumping elements only, thus applying for low or zero stresses only), the moisture concentration rate for a long, round specimen is:

$$\frac{d\omega}{dt} = D\left(\frac{\partial^2\omega}{\partial r^2} + \frac{1}{r}\frac{\partial\omega}{\partial r}\right) \tag{7.7}$$

The solution of this equation is [1]:

$$\frac{\omega}{\omega_0} = 1 - \frac{4}{d}\sum_{n=1}^{\infty}\frac{J_0(\psi_n r)}{\psi_n J_1(\psi_n d)}\exp\left(-\frac{4D\psi_n^2}{d^2}t\right) \tag{7.8}$$

where ω_0 is the concentration, surrounding the specimen; D is the diffusion coefficient; ψ_n is the n-th root of the zero-order Bessel function; d the diameter of the specimen and J_n is the Bessel function of the order n.

Because stress relaxation in tension or compression depends on the mean stress and strain in the specimen, only the mean concentration is of importance. Thus the average concentration therefore is:

$$\bar{\omega} = \frac{4}{\pi d^2}\int_0^{d/2} 2\pi\omega r dr = \omega_0\left[1 - \sum_{n=1}^{\infty}\frac{4}{\psi_n^2}\exp\left(-\frac{4D\psi_n^2}{d^2}t\right)\right] \tag{7.9}$$

Substituting $\bar{\omega}$ in eq.(7.3) or eq.(7.5) will give the measured stress- or bond decay. Because only the first term of the summation is of importance and the other terms may be neglected the equation becomes:

$$\ln\left(\frac{\rho}{\rho_0}\right) = -k\omega_0\left[t + \frac{d^2}{D\psi_1^4}\left\{\exp\left(-\frac{4D\psi_1^2}{d^2}t\right) + c_1\right\}\right] \tag{7.10}$$

or for the stress with $c_1 = -1$ as boundary condition:

$$\ln\left(\frac{\sigma}{\sigma_0}\right) = -K_1 A'\varphi\omega_0\left[t + \frac{d^2}{D\psi_1^4}\left\{\exp\left(-\frac{4D\psi_1^2}{d^2}t\right) - 1\right\}\right] \tag{7.11}$$

where $\psi_1 = 2.405$ is the first root of the Bessel function.

For longer times the exponential function is approximately zero, thus this line becomes:

$$\ln\left(\frac{\sigma}{\sigma_0}\right) = -K_1 A'\varphi\omega_0\left[t - \frac{d^2}{D\psi_1^4}\right] \tag{7.12}$$

The intercept of this line with the time axis thus is: $d^2 / D\psi_1^4$, showing the time lag due to diffusion. This equation applies exactly for e.g. human hair [1], where there is no swelling or shrinking during wetting and drying. At moistening the stress quickly dropped to about 1/3 of the applied value. At drying the stress totally restores to the initial level before wetting in the relaxation tests. Thus this work is due to the chemical energy of bond reformation (heat of fusion) as also applies for the slight restoring of the stress at moistening of wood. Tests with alkali hydroxide solutions on cotton, which has a comparable structure as wood, showed an instantaneous relaxation as rapidly as the solution could be added. After that, a slower process occurred of conversion of the crystalline regions into an amorphous structure. The instantaneous stress reduction indicates a very fast reaction where equilibrium is directly reached according to the reaction:

$\omega + \rho \underset{k_b}{\overset{k_f}{\rightleftarrows}} (\rho_0 - \rho)$ or: .

$$-\dot{\rho} = \rho\omega k_f - k_b(\rho_0 - \rho) = 0 \qquad (7.13)$$

or: $$\omega = \frac{k_b}{k_f} \cdot \frac{\rho_0 - \rho}{\rho} = \frac{k_b}{k_f} \cdot \frac{\Delta\rho / \rho_0}{1 - \Delta\rho / \rho_0} \qquad (7.14)$$

where $\Delta\rho / \rho_0 = (\rho_0 - \rho)/\rho_0$. Thus $\Delta\rho / \rho_0$ is about proportional to ω $(\Delta\rho / \rho_0 << 1)$, but this relation bends off to a limiting value at high values of ω according to the measurements [1] and eq.(7.14). The limiting value for alkali-hydroxides at high concentration seems to approach unity according to eq.(7.14), indicating that the structure of cotton may be completely accessible for alkali reagents. This reaction with both the amorphous and crystalline regions followed also from X-ray diffraction experiments. Because $\Delta\rho$ is not noticeable dependent on the temperature, the activation enthalpy will be small.

For strong acids $\Delta\rho / \rho_0$ approaches a limiting value well below 1, being of the same order as the quantity of disordered regions as follows from X-ray measurements. Thus $(\Delta\rho / \rho_0)_{lim}$ can be expected to be a direct measure of the accessibility of the amorphous regions. The linear increasing value of $(\Delta\rho / \rho_0)_{lim}$ with temperature, in concert with a negative entropy increase, which shows the equilibrium between ordered and disordered regions. The equilibrium constant K_c is:

$$K_c = \frac{k_f \omega_m}{k_b} = \frac{(\Delta\rho / \rho_0)_{lim}}{1 - (\Delta\rho / \rho_0)_{lim}} \qquad (7.15)$$

and the energy of cellulose conversion is: $E_f - E_b = -RT\ln(K_c)$, what was found to be 4 kcal/mol. The same can be expected for wood. Because acids effect only the amorphous regions and because the limiting value of the instantaneous reduction is far below 1, there is no cross section totally disordered and the ordered region is the continuous phase.

The nature of the reagents and the rapidity of the reactions indicate an attack of secondary hydrogen bonds between the cellulose chains. After removal of the reagents, some types of bonds are unable to move back against the force to assume their original positions, but combine with new neighbors in a relaxed position.

The influence of water on the hydrogen bonds is comparable with the influence of acids because only the amorphous regions are effected and $\Delta\rho / \rho_0$ will be proportional to ω.

Although there is an immediate reaction with water, there is no instantaneous stress drop in a relaxation test because the water has to diffuse into the structure and the rate of diffusion determines the reaction rate with the hydrogen bonds. There thus is an equilibrium and any change of moisture content gives a reaction close to the equilibrium at the rate of the moisture supply. For the reaction near equilibrium, eq.(7.13) becomes:

$$-\dot{\rho} = \rho\omega k_f - k_b(\rho_0 - \rho) = \rho k_f(\omega - \omega_0) \qquad (7.16)$$

where: $\omega_0 = k_b(\rho_0 - \rho)/(k_f\rho)$ is the equilibrium moisture content (where $\dot{\rho} = 0$).

Eq.(7.9), giving a moisture increase from zero to ω_0, is, for the first expanded term, with a rounding off to account for the other terms, approximately:

$$\bar{\omega} = \omega_s(1 - \exp(-at)), \qquad (7.17)$$

where $a = 4D\psi_1^2 / d^2 = 23D / d^2$, and ω_s is the saturation amount of adsorbed water.

For a loaded test specimen, with a moisture content ω_0, that is placed in a dry environment causing a moisture content of $\omega_0 - \omega_s$ after long time, eq.(7.17) modifies to:

$$\bar{\omega} = \omega_0 - \omega_s + \omega_s \exp(-at) \tag{7.18}$$

and the solution of eq.(7.5), which applies in the first stage, becomes:

$$\ln(\rho/\rho_0) = -k(\omega_0 - \omega_s)t + \frac{k}{a}\omega_s\left(\exp(-at) - 1\right) \tag{7.19}$$

or with eq.(7.18):

$$\ln(\rho/\rho_0) = \ln(\rho'/\rho'_0) - \frac{k}{a}(\omega_0 - \omega_s) \tag{7.20}$$

where: $\ln(\rho'/\rho'_0) = -k(\omega_0 - \omega_s)t$ is the relaxation (or creep) at the constant equilibrium moisture content $\omega_0 - \omega_s$. The same solution is obtained from eq.(7.3) and the equations can be read by replacing ρ by σ and with $k = K_1 A'\varphi$ for relaxation and $k = KA'\varphi$ for creep. Thus eq.(7.20) for desorption becomes:

$$\ln(\sigma/\sigma_0) = \ln(\sigma'/\sigma'_0) - \frac{k}{a}(\omega_0 - \omega) \tag{7.21}$$

It follows that: $\ln((\sigma'\sigma_0)/(\sigma'_0\sigma)) = c(\omega_0 - \omega)$, is a straight line, that is the same as given empirically in [2] and fig. 7.1. where: $(\omega_0 - \omega)$ is the amount of desorbed water.

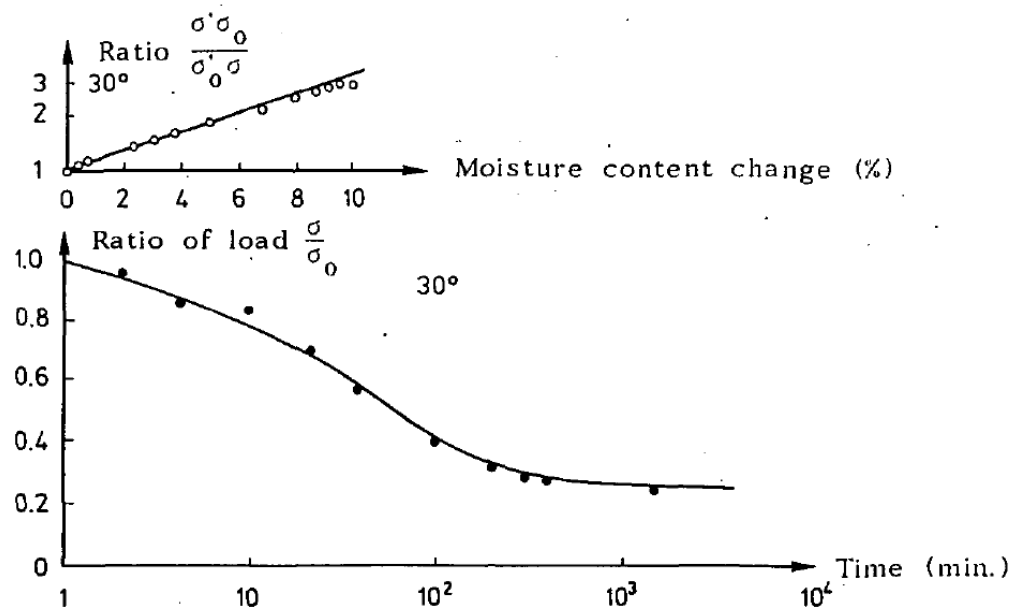

Fig. 7.1. Comparison of the theoretical equation (7.21) with measurements of [2]

For adsorption, when a loaded test specimen with a moisture content ω_0 is placed in a wet environment, causing a moisture content of ω_1 after long time, eq.(7.17) modifies to:

$$\bar{\omega} = \omega_1 - (\omega_1 - \omega_0)\cdot\exp(-at) \tag{7.22}$$

and the solution of eq.(7.5) is:

$$\ln(\rho/\rho_0) = -k\omega_1 t - \frac{k}{a}(\omega_1 - \omega_0)\cdot(\exp(-at) - 1) \tag{7.23}$$

or: $$\ln(\rho/\rho_0) = -k\omega_1 t + \frac{k}{a}(\omega - \omega_0) \tag{7.24}$$

or: $$\ln(\rho/\rho_0) = \ln(\rho'/\rho'_0) + \frac{k}{a}(\omega_0 - \omega) \tag{7.25}$$

where: $\ln(\rho'/\rho'_0) = -k\omega_1 t$, is the relaxation at constant maximum moisture content ω_1. This equation is identical to eq.(7.20) if the adsorbed amount: $\omega - \omega_0$ can be regarded as a negative desorption. Eq.(7.20) shows that there is an increase of deformation on drying and eq.(7.25) shows a restoring of the bond structure on rewetting. Thus there is at least one dominating element with an opposed behavior to other materials. These phenomena by sorption can explain the mechano-sorptive effect, which derivation is discussed in § 7.2, when not only hydrogen bond fail, but shifts of layers with respect to each other occur at high loading and high moisture content changes. This behavior can be described by two parallel Maxwell elements. The deviation at higher moisture changes shows that eq.(7.1) applies, thus a departure from the linear approach eq.(7.3) of simple hydrogen bond failure.

7.2. Influence of high stresses and moisture content changes

Interesting for mechano-sorptive effects is creep loading at sufficient high stresses, when flow and slip occurs, and sinh(x) can be approximated by (exp(x))/2. The strain rate equations are similar to those of two nonlinear Maxwell elements 1 and 2 (see Fig. 7.2) which are:

$$\dot{\varepsilon} = \frac{\dot{\sigma}_1}{K_1} + A'_1 \frac{\omega}{2} \exp(\varphi_1 \sigma_1) + \dot{\varepsilon}_m \tag{7.26}$$

$$\dot{\varepsilon} = \frac{\dot{\sigma}_2}{K_2} + A'_2 \frac{\omega}{2} \exp(\varphi_2 \sigma_2) - \dot{\varepsilon}_m \tag{7.27}$$

In these equations $\sigma_2 = \sigma - \sigma_1$ or: $\dot{\sigma}_2 = \dot{\sigma} - \dot{\sigma}_1 = -\dot{\sigma}_1$, because the total external stress σ is constant. The material thus is divided in two types of layers, one with mechano-sorptive slip ε_m at desorption and recovery at adsorption, and one with the more common reversed behavior. Elimination of $\dot{\varepsilon}$ from eq.(7.26) and eq.(7.27) gives:

$$\frac{\dot{\sigma}_1}{K} + A'_1 \frac{\omega}{2} \exp(\varphi_1 \sigma_1) - A'_2 \frac{\omega}{2} \exp(\varphi_2 \sigma_2) + 2\dot{\varepsilon}_m = 0 \tag{7.28}$$

where $1/K = 1/K_1 + 1/K_2$. $1/K = 1/K_1 + 1/K_2$ and $2\dot{\varepsilon}_m$ is the relative strain rate of the adjacent layers $\dot{\varepsilon}_r$. Because the process is a matter of side bonds breaking it has to be assumed that the sites of both parts are the same for the mechano-sorptive effect, or: $\varphi_1 = \varphi_2 = \varphi$, and eq.(7.28) becomes ($\sigma_2 = \sigma - \sigma_1$):

$$\frac{\dot{\sigma}_1}{K} + e^{\varphi\sigma/2} \omega \sqrt{A'_1 A'_2} \cdot \sinh\left(\varphi\sigma_1 - \varphi\sigma/2 + \ln\left(\sqrt{A'_1 A'_2}\right)\right) + 2\dot{\varepsilon}_m = 0 \tag{7.29}$$

The mechano-sorptive rate of bond-breaking has the form: $\dot{\varepsilon}_m = A\sinh(\varphi\sigma) \approx A\varphi\sigma$, for small stresses as used before. For high stresses is: $\dot{\varepsilon}_m = (A/2) \cdot \exp(\varphi\sigma)$.

This rate is zero for constant moisture content and is proportional to the rate of change of the moisture content. Thus $2\dot{\varepsilon}_m$ can be given in the form:

$$2\dot{\varepsilon}_m \approx \frac{\dot{\omega}}{a} \sqrt{A'_1 A'_2} \cdot \frac{1}{2} \exp\left(\frac{\varphi\sigma}{2}\right) \approx \frac{\dot{\omega}}{a} \sqrt{A'_1 A'_2} \exp\left(\frac{\varphi\sigma}{2}\right) \sinh(c) \tag{7.30}$$

With: $\omega = \omega_0 + (\omega_e - \omega_0) \cdot \left(1 - e^{-at}\right)$, is: $\omega = \omega_e - \dot{\omega}/a$ and eq.(7.29) can be split in a creep equation at the constant moisture content ω_e:

$$\frac{\dot{\sigma}_1}{K} + e^{\varphi\sigma/2} \cdot \omega_e \sqrt{A'_1 A'_2} \cdot \sinh\left(\varphi\sigma_1 - \varphi\sigma/2 + \ln\left(\sqrt{A'_1 A'_2}\right)\right) = 0 \tag{7.31}$$

and in a mechano-sorptive change:

$$\frac{\dot{\sigma}_1}{K} - e^{\varphi\sigma/2}\cdot\frac{\dot{\omega}}{a}\sqrt{A'_1 A'_2}\cdot\sinh\left(\varphi\sigma_1 - \varphi(\sigma/2) + \ln\left(\sqrt{A'_1 A'_2}\right)\right) + 2\dot{\varepsilon}_m = 0 \qquad (7.32)$$

the same as is done for small stresses in § 7.1, leading to the same equation with the same linear increase with time t for small stresses.

Substitution of eq.(7.30) in eq.(7.32) shows that a particular solution of eq.(7.32) is:

$$\varphi_1\sigma_1 = \frac{\sigma\varphi}{2} - \frac{1}{2}\ln\left(A'_1/A'_2\right) + c \qquad (7.33)$$

The general part of this equation is:

$$\frac{\dot{\sigma}_1}{K} - e^{\varphi\sigma/2}\cdot\frac{\dot{\omega}}{a}\sqrt{A'_1 A'_2}\cdot\sinh\left(\varphi\sigma_1 - \varphi(\sigma/2) + \ln\left(\sqrt{A'_1 A'_2}\right)\right) = 0$$

and integration of this equation has the form:

$$\int\frac{d(x)}{\sinh(x)} = -c\int\dot{\omega}d(t),$$

or with: $\omega = \omega_0 + (\omega_e - \omega_0)\left(1 - e^{-at}\right)$, where ω_e is the moisture content at the end, this is:

$$\ln\left(\tanh\left(x/2\right)\right) = C\left(\frac{\omega_0 - \omega_e}{a}e^{-at}\right) + C_1$$

or in terms of eq.(7.32) this becomes:

$$\ln\left(\tanh\left(\frac{\varphi\sigma_1}{2} - \frac{\varphi\sigma}{4} + \frac{1}{4}\ln\left(A'_1/A'_2\right)\right)\right) = C_1 - \varphi K e^{\sigma\varphi/2}\sqrt{A'_1/A'_2}\left(\frac{\omega_e - \omega_0}{a}e^{-at}\right) \qquad (7.34)$$

again similar to the equation of § 7.1 for small stresses.

Calling: $p = \varphi K e^{\sigma\varphi/2}\sqrt{A'_1/A'_2}\left(\frac{\omega_e - \omega_0}{a}e^{-at}\right) = \varphi K e^{\sigma\varphi/2}\sqrt{A'_1/A'_2}\cdot(\omega - \omega_e)$

eq.(7.34) becomes:

$$\frac{\varphi\sigma_1}{2} - \frac{\varphi\sigma}{4} + \frac{1}{4}\ln\left(A'_1/A'_2\right) = \operatorname{arctan}h(\exp(p + C_1)) \qquad (7.35)$$

and the total solution is:

$$\frac{\varphi\sigma_1}{2} - \frac{\varphi\sigma}{4} + \frac{1}{4}\ln\left(A'_1/A'_2\right) = \operatorname{arctan}h(\exp(p + C_1)) + \frac{c}{2} \qquad (7.36)$$

The value of C_1 follows from the initial value $\sigma_1 = \sigma_{10}$. For this case is:

$$\ln\left(\tanh\left(\frac{\varphi\sigma_{1,0}}{2} - \frac{\varphi\sigma}{4} + \frac{1}{4}\ln\left(A'_1/A'_2\right) - \frac{c}{2}\right)\right) - p_0 = C_1 \qquad (7.37)$$

Substitution of eq.(7.37) in eq.(7.36) gives:

$$\frac{\varphi\sigma_1}{2} - \frac{\varphi\sigma}{4} + \frac{1}{4}\ln\left(A'_1/A'_2\right) - \frac{c}{2} =$$

$$= \operatorname{arctan}h\left(\tanh\left(\frac{\varphi\sigma_{10} - \varphi\sigma_{20} + \ln\left(A'_1/A'_2\right) - 2c}{4}\right)\cdot e^{\varphi K\sqrt{A'_1/A'_2}\cdot\exp(\varphi\sigma/2)\cdot(\omega-\omega_0)/a}\right) \qquad (7.38)$$

Calling: $q = \frac{\varphi\sigma_1}{2} - \frac{\varphi\sigma}{4} + \frac{1}{4}\ln\left(A'_1/A'_2\right) - \frac{c}{2}$. then this equation becomes:

$$q = \operatorname{arctan}h\left(\tanh\left(q_0\right)\cdot e^{\varphi K\sqrt{A'_1/A'_2}\cdot\exp(\varphi\sigma/2)\cdot(\omega-\omega_0)/a}\right)$$

For small values of q_0 this becomes:

$$q = q_0\cdot e^{\varphi K\sqrt{A'_1/A'_2}\cdot\exp(\varphi\sigma/2)\cdot(\omega-\omega_0)/a} \qquad \text{or:}$$

$$\varphi\sigma_1 = \varphi\sigma_{10} + \frac{1}{2}\left(\varphi\sigma_{20} - \varphi\sigma_{10} - \ln\left(A'_1/A'_2\right) + 2c\right)\cdot(1-)\cdot\left(1 - e^{\varphi K\sqrt{A'_1/A'_2}\cdot\exp(\varphi\sigma/2)\cdot(\omega-\omega_0)/a}\right) \quad (7.39)$$

For high values of q is: $\tanh(q) \approx 1$, and: $q \approx \operatorname{arctanh}\left(e^{\varphi K\sqrt{A'_1/A'_2}\cdot\exp(\varphi\sigma/2)\cdot(\omega-\omega_0)/a}\right)$

and because: $\operatorname{arctan}h(e^x) = \frac{1}{2}\ln\left(\frac{1+e^x}{1-e^x}\right) = \frac{1}{2}\ln\left(\coth\left(-\frac{x}{2}\right)\right)$ is:

$$\frac{\varphi\sigma_1}{2} - \frac{\varphi\sigma}{4} + \frac{1}{4}\ln\left(A'_1/A'_2\right) - \frac{c}{2} = -\frac{1}{2}\ln\left(\tanh\left(\varphi K\sqrt{A'_1/A'_2}\cdot e^{\varphi\sigma/2}\left(\omega_0-\omega\right)/2\right)\right) \quad (7.40)$$

For not too high moisture changes this becomes:

$$\frac{\varphi\sigma_1}{2} - \frac{\varphi\sigma}{4} + \frac{1}{4}\ln\left(A'_1/A'_2\right) - \frac{c}{2} = -\frac{1}{2}\ln\left(\varphi K\sqrt{A'_1/A'_2}\cdot e^{\varphi\sigma/2}\left(\omega_0-\omega\right)/2\right) \quad (7.41)$$

and for high values of: $\varphi K\sqrt{A'_1/A'_2}\cdot e^{\varphi\sigma/2}\left(\omega_0-\omega\right)/2$, eq.(7.40) turns to:

$$\frac{\varphi\sigma_1}{2} - \frac{\varphi\sigma}{4} + \frac{1}{4}\ln\left(A'_1/A'_2\right) - \frac{c}{2} \approx 0 \quad (7.42)$$

This is also the limit of eq.(7.39) for high moisture changes at small stresses q_0.

According to eq.(7.30) is:

$$\frac{c}{2} + \frac{\sigma\varphi}{4} = \frac{1}{2}\ln\left(\frac{4\dot{\varepsilon}_m a}{\omega\sqrt{A'_1 A'_2}}\right) \quad (7.43)$$

and the maximal mechano-sorptive stress σ_1 of eq.(7.42) is:

$$\sigma_1\varphi = \ln\left(\frac{4\dot{\varepsilon}_m a}{\omega A'_1}\right) \quad (7.44)$$

For high moisture changes (p.e. ω_0 maximal and $\omega_e \approx 0$), this is ($\dot{\varepsilon}_r = 2\dot{\varepsilon}_m$)

$\sigma_1\varphi = \ln\left(\frac{4|\dot{\varepsilon}_m|}{A_1}\right)$ and this is at the level of the flow stress:

$\sigma_1\varphi = \ln\left(\frac{2\dot{\varepsilon}_r}{A_1}\right)$ of element I (see for instance eq.(5.2.16)).

Thus flow of the elements limits the maximal possible mechano-sorptive stress.

An other aspect of eq.(7.44) is that: A_1/a is proportional to: $\exp\left(-E_1/kT + E_d/kT\right)$ and the activation energy of the process is the difference of the activation energy for creep and for diffusion, explaining a low retardation time or an high rate of the process.

7.3 Influence of ultimate flow stresses and moisture changes

In order to avoid complex calculations for creep at high moisture cycling and at higher stresses it is sufficient to use the property of the non-linear Maxwell elements of an approximate elastic-full plastic behavior (see e.g. fig. 5.4). This model can be compared with the model of [3] that consists of two parallel strings each consisting of a Maxwell element and a Voigt element in series. This is totally equivalent to a model with four parallel Maxwell elements and these four parallel linear Maxwell elements can be replaced by two parallel Maxwell elements with non-linear dashpots, because those dashpots contain one more parameter than the linear dashpots. Thus it follows that each of the two strings of [3] can be replaced by a spring attached to a non-linear dashpot which behaves identical to the de-

rived sorption equations. The loading of the two parallel strings in a creep test in the model of [3] was done by a running block that moved the total load between the strings by means of a hygroscopic element. This block may however be removed because this sorption effect is given by eq.(7.20) or eq.(7.39) and the behavior of the hygroscopic material is exactly the same as can be seen in eq.(7.19) where the part:
$(k\omega_s / a)\cdot(1 - \exp(-at))$ is identical to the time function of that element. The swelling and shrinkage is proportional to the adsorbed amount of water and has also this form:
$\omega = \omega_s \cdot (1-\exp(-at))$. In the model of [3] it is also assumed that the viscoelastic constants change according to this function, however eq.(7.19) and eq.(7.31) show immediate creep at the equilibrium moisture content of the end state and also this changing constants function may be removed. In [3] it is also assumed that there are two diffusion processes, one slow process of sorption, eliminating the differential shrinking with a = $23D/d^2 = 0.06$, and one quick process with a = 0.5, effecting the load bearing bonds. In most tests the change of moisture content is slow and the result has to be regarded as a succession of end states due to these two processes. The influence of the slow process can be eliminated by subtracting the strains of the dummy from the strains of the loaded specimen at moisture cycling.

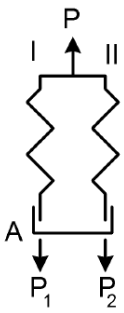

Fig. 7.2 Maxwell elements

In § 7.3.1 and § 7.3.2 are, for respectively compression and tension, the schemes given of the influence of moisture cycling, where the two elastic-plastic elements consist of: II, the layers with a dominating slip at desorption and I, layers with a pronounced slip at adsorption, which show, (in point A) more shrinking and swelling than the layers of II.
The initial loading of element I and II is: $P = P_1 + P_2$

7.3.1. Explanation of the data of Fig. 7.3.1 and Fig. 7.3.2.

To compare models, the mechano-sorptive forces can be divided in a part that eliminates the differential shrinking and a part that interacts with the loading as done in [3]. In an unloaded dummy only the first part is working. For an initial wet unloaded specimen, the first drying cycle will give the following forces:

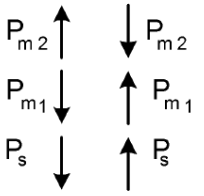

slip due to desorption in II

recovery of slip in I.

force due to differential shrinking of I.

I II The differential shrinking: δ_{sh} will cause the shrinking force: P_s.

The strain: δ of element I will be the same as of element II. Thus, with δ_α as free shrinking of the specimen, is:

I: $\delta = -\delta_{sh} + P_s / K_1 - \delta_\alpha$

II: $\delta = -P_s / K_2 - \delta_\alpha$ $\rightarrow$ From I - II follows: $P_s(1/K_1 + 1/K_2) = \delta_{sh}$

In II there will be a slip: δ_{m1} at drying in the direction of the compressive force P_s and the mechano-sorptive force P_{m2} will be against this force. In I there will be recovery of extensional slip: $-\delta_{m1}$ and a force P_{m1} in the direction of the tensile force P_s.

Thus: :

I: $\delta = -\delta_{sh} + P_s / K_1 - \delta_\alpha + P_{m1} / K_1 - P_{m2} / K_1 - \delta_{m1}$

II: $\delta = -P_s / K_2 - \delta_\alpha - P_{m1} / K_2 + P_{m2} / K_2 - \delta_{m2} \quad \rightarrow$ I – II: $\quad (P_{m2} - P_{m1}) / K = \delta_{m2} - \delta_{m1}$

where: $1/K = (1/K_1 + 1/K_2)$

It is possible that the mechano-sorptive forces eliminate the shrinking forces if drying is slow enough for interaction. Then: $P_s + P_{m1} - P_{m2} = 0$ and

I: $\delta = -\delta_{sh} - \delta_{m1} - \delta_\alpha$

II: $\delta = -\delta_{m2} - \delta_\alpha$ Thus I – II gives: $\delta_{m1} = \delta_{m2} - \delta_{sh}$

and δ_{m1} is limited by the amount: δ_{sh}.

For a loaded specimen the mechano-sorptive force can be divided in the part that occurs in the dummy and the part that interacts with the external forces. In the following the corrected strains, by subtraction of the dummy values, will be regarded. This will be compared with the measured values of [4] for compression that has the strongest mechano-sorptive mechanism with plastic deformations. For drying at compression is:

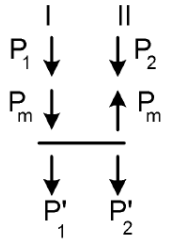

initial values of the external load

sorptive bond breaking causing slip: $-\delta_{m2}$ in II, and resultant flow δ_f in II

$P_m = P_{m1} + P_{m2}$

Total forces: $P'_1 = P_{u1}$, the flow stress of element I, and $P'_2 = P - P_{u1}$.

Thus: $P_m = P_{u1} - P_1$.

The initial deformation by the external load: $P = P_1 + P_2$ is:

$\delta_0 = P_1 / K_1 = P_2 / K_2 = P / (K_1 + K_2)$

As can be seen in fig. 7.3.1, P_m will cause a deformation of: $4\delta_0$. Thus:

I: $-4\delta_0 = -(P_{u1} - P_1) / K_1 - \delta_f$

II: $-4\delta_0 = (P_{u1} - P_1) / K_2 - \delta_{m2}$

The loading level is about 40 %. Thus by the ultimate load is the elastic deformation:
$P_{u1} / K_1 = P_{u2} / K_2 = P_u / (K_1 + K_2) = 2.5\delta_0$. Thus:

I: $-2.5 \cdot \delta_0 + \delta_0 - \delta_f = -4\delta_0 \quad \rightarrow \quad \delta_f = 2.5\delta_0$ (7.45)

II: $(K_1 / K_2) \cdot (2.5\delta_0 - \delta_0) - \delta_{m2} = -4\delta_0 \quad \rightarrow \quad \delta_{m2} = 4\delta_0 + 1.5\delta_0 (K_1 / K_2)$ (7.46)

On rewetting the specimen, after the first drying cycle, P_m changes of sign and the forces will be:

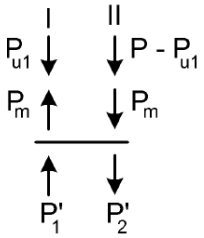

initial values

elastic forces by slip and flow

Total forces: $P'_1 = P_m - P_{u1}$ (= P_{u1} for low loading giving flow back of I)

$P'_2 = P - P_{u1} + P_m$ (= P_{u2} for high loading giving flow of II).

For low loading, element I may flow back and the strain at the end of the cycles show little or no change as mentioned in [4] for compression at the loading level of 24% and also can be seen in fig.7.3.8 during the second humidity cycle. For higher loadings P'_2 may reach

P_{u2}. Then there is an increase in flow and slip in each cycle and the maximum deformation will not tend to a limiting value but increases until fracture. This is discussed in § 7.3.2, and is verified by measurements, e.g.in [5] for bending.

Fig. 7.3 suggest that P'_2 may just have reached P_{u2} and the increase of deformation after each cycle is determined by the creep part for constant ω_e. It is probable that there is one limit for flow forwards and backwards and also P'_1 just reaches P_{u1}. Then:

$P'_1 = P_{u1}$ and: $P = P_{u2} - P_{u1}$ and because: $P \approx 0.4P_u = 0.4\left(P_{u1} + P_{u2}\right)$, is:

$1.4P_{u1} = 0.6P_{u2}$, or: $P_{u1} = 0.3P_u$, and $P_{u2} = 0.7P_u$,

and because the stiffness is proportional to the potential energy of the bonds it is to be expected that:

$$K_1 = 0.3K_t \quad \text{and} \quad K_2 = 0.7K_t \tag{7.47}$$

where $K_t = K_1 + K_2$

According to eq.(7.46) is: $\delta_{m2} = 4\delta_0 + 1.5\delta_0\left(K_1 / K_2\right) = \delta_0\left(4 + 1.5 \cdot 0.3 / 0.7\right) \approx 4.7\delta_0$.

The recovery of slip at rewetting is about $2.5\,\delta_0$. drifting to $2.7\,\delta_0$ (see fig. 7.2). Taking $2.6\,\delta_0$, the strains are, with $P_m = 2P_{u1}$, or with $P_m / K_1 = 2P_{u1} / K_1 = 5\delta_0$:

$$\text{I: } P_m / K_1 - \delta_{m1} \approx 2.6\delta_0 = 5\delta_0 - \delta_{m1} \quad \rightarrow \quad \delta_{m1} \approx 2.4\delta_0. \tag{7.48}$$

$$\text{II: } -P_m / K_1 + \delta_{m2} \approx 2.6\delta_0 = -\left(K_1 / K_2\right) \cdot 5\delta_0 + \delta_{m2} =$$

$$= -(0.3 / 0.7)5\delta_0 + \delta_{m2} \quad \rightarrow \quad \delta_{m2} \approx 4.7\delta_0 \tag{7.49}$$

It is seen that δ_{m2} is the same for drying as for rewetting. The difference $\delta_{m2} - \delta_{m1} \approx 2.3 \cdot \delta_0$ is equal to the part δ_{m2} for the dummy which is used with opposed sign to eliminate the differential shrinking. Thus δ_{sh} is smaller than or equal to $2.3 \cdot \delta_0$.

An analogous scheme for an initial dry specimen on first wetting is:

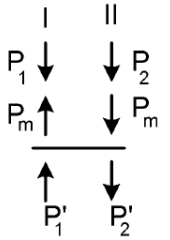

initial values

elastic forces by internal slip and flow

Total forces: $P'_2 = P_{u2}$ causing flow of element II; $P'_1 = P_{u2} - P$

The change of the force is: $P_m = P_{u2} - P_2$

The measured change of strain is $1.5 \cdot \delta_0$ and if δ_m is the resultant slip and flow, this strain is:

$$\text{II: } 1.5 \cdot \delta_0 = -\left(P_{u2} - P_2\right) / K_2 + \delta_{m2}$$

$$\text{I: } 1.5 \cdot \delta_0 = -\left(P_{u2} - P_2\right) / K_1 + \delta_{m1}$$

This leads to:

$$\text{II: } (-2.5 + 1)\delta_0 + \delta_{m2} = 1.5 \cdot \delta_0 \quad \rightarrow \quad \delta_{m2} = 3 \cdot \delta_0 \tag{7.50}$$

$$\text{I: } \left(K_2 / K_1\right) \cdot \left(2.5 - 1\right) \cdot \delta_0 - \delta_{m1} = 1.5 \cdot \delta_0 \quad \rightarrow \quad \delta_{m1} = 2 \cdot \delta_0 \tag{7.51}$$

These values of δ_m show that there is flow in both elements as also can be expected from the foregoing for this case of loading to the flow limit. Thus also P'_1 reaches P_{u1}. As a control, the equations are then:

$$\text{II: } 1.5 \cdot \delta_0 = -\left(P_{u1} + P_1\right) / K_2 + \delta_{m2}$$

$$\text{I: } 1.5 \cdot \delta_0 = -\left(P_{u1} + P_1\right) / K_1 + \delta_{m1}$$

or: $1.5\cdot\delta_0 = \delta_0\left(2.5+1\right)\left(0.3/0.7\right)+\delta_{m2} \quad \rightarrow \quad \delta_{m2} = 3\cdot\delta_0$ (7.52)

$1.5\cdot\delta_0 = 3.5\cdot\delta_0 - \delta_{m1}. \quad \rightarrow \quad \delta_{m1} = 2\cdot\delta_0$ (7.53)

as to be expected.

For re-drying the specimen, after the first wetting cycle, the forces are:

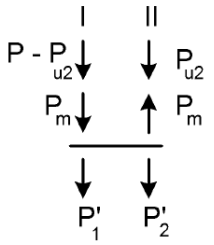

initial values

elastic forces by internal slip and flow

Total forces $P'_1 = P_{u1}$ and because $P'_1 = P - P_{u2} = -P_{u1}$, is

$P_m = 2P_{u1} = 1.5P$

The measured change of strain is $2{,}7\,\delta_0$, Thus, with $K_1 = 0.3K_t$ and $K_2 = 0.7K_t$ the strains are:

I: $-P_m / K_1 + \delta_{m1} = -\left(1.5/0.3\right)\delta_0 + \delta_{m1} = -2.7\delta_0 \quad \rightarrow \quad \delta_{m1} = 2.3\cdot\delta_0$ (7.54)

II: $P_m / K_2 - \delta_{m2} = -\left(1.5/0.7\right)\delta_0 - \delta_{m2} = -2.7\delta_0 \quad \rightarrow \quad \delta_{m2} = 4.8\cdot\delta_0.$ (7.55)

The difference $\delta_{m2} - \delta_{m1} \approx 2.5\cdot\delta_0$ is equal to δ_{m2} of the dummy. Because the change of the strain of the dummy is also about $2.5\cdot\delta_0$, is P_{m1} of the dummy about zero and also δ_{m1} and δ_α will be zero. Thus the free swelling and shrinking δ_α can be neglected and the differential shrinking or swelling will be about: $\delta_{sh} \approx 2.5\cdot\delta_0$ in this case.

The, for an explanation necessary, opposite behavior of adjacent layers follows from expansion movements. When the S_2 layers shrinks, the microfibrils become steeper, causing extension in grain direction, while at the same time the adjacent layers shrink in grain direction and expand perpendicular to grain in their microfibrils direction (see fig. 2.1.3 and § 2.2.2). In § 7.3.2. the schemes are given of the influence of moisture cycling at tensional loading. for the conditions of contained flow. The schemes however also may apply for compression and deliver an extension of the mechano-sorptive model. For bending the situation is complex because every layer has another plastic and elastic deformation and the tests, and a first analysis, show that the lever arm between compression and tension will be strongly reduced by the different behavior of the compression zone and the tension zone on moisture cycling.

It can be concluded that the theory makes it possible to understand and to describe the mechano-sorptive effect. The model predicts that for large dimensions of the test specimens, when $a = 23D/d^2$ is sufficient small, there will be only a small force exchange between the layers and the mechano-sorptive effect is not important. This does not apply for toothed plate and ring dowel joints, as discussed in § 7.3.3, where the diameter of the loaded core d is small and diffusion is easy in grain direction. It thus is necessary to block the accessibility for water by glue and paint.

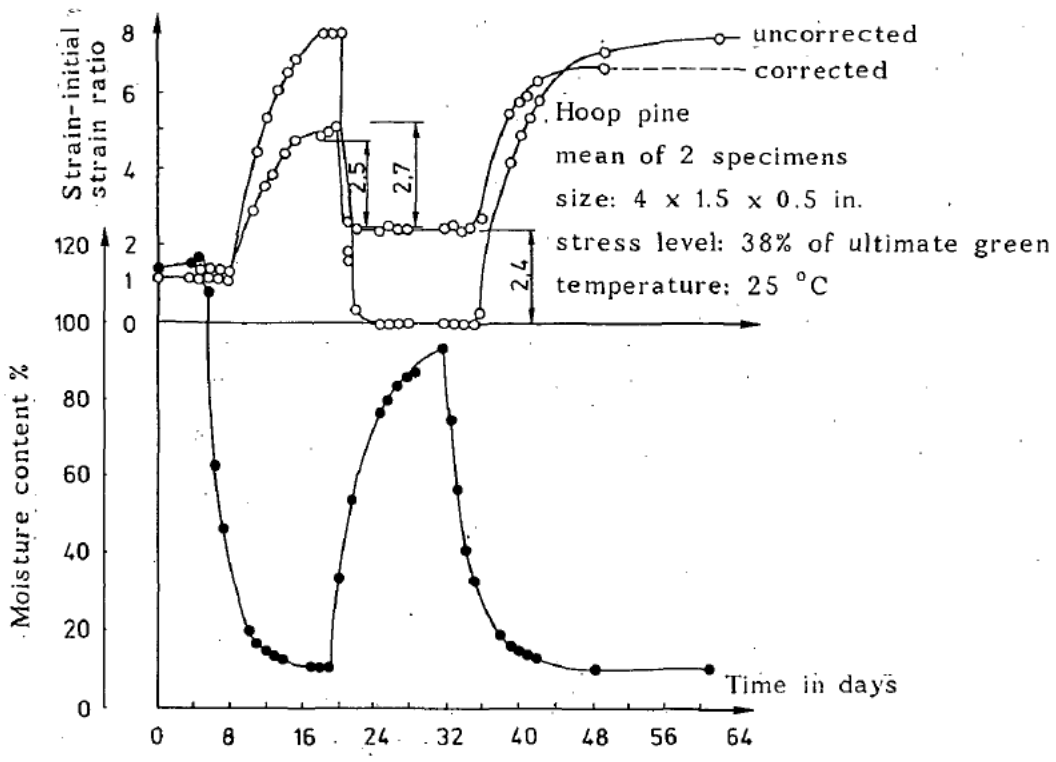

fig. 7.3.1 Strain ratio-time and moisture content-time curves for initially green compression specimens at moisture cycling [4].

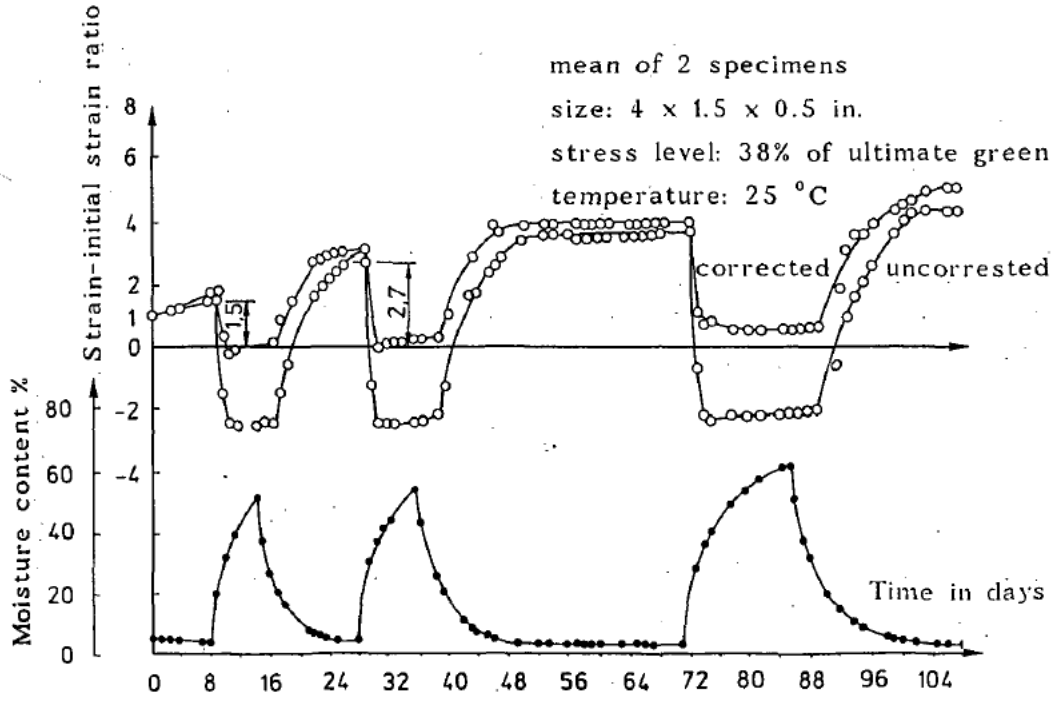

fig. 7.3.2. Strain ratio-time and moisture content-time curves at moisture cycling for compression, initially at 4% moisture content [4].

7.3.2. Explanation of contained flow as measured in [5].

In the following scheme of B(1989b), the elastic-plastic elements consist of II, layers with a dominating slip at desorption and I, layers with pronounced slip at adsorption, which show (in point A) more shrinking and swelling than the layers of II.

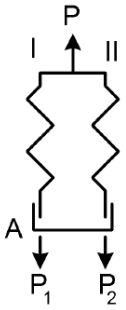

external stress P

spring

possibility of slip in both directions

initial loading of elements I and II $P = P_1 + P_2$

Fig. 7.2.

For an initial wet specimen, the first drying cycle will give:

I	II	
$P_1 \downarrow$	$\downarrow P_2$	initial values
$P_m \downarrow$	$\uparrow P_m$	sorptive bond breaking and reformation in a shifted position of II
$(P_s \downarrow$	$\uparrow P_s)$	(force due to shrinking of element I)
$P_1 \downarrow$	$\downarrow P'_2$	

Total forces: P_m may reach the order of P_2 in II. However, in I: $P_1 + P_2 \approx P > P_{u1}$ where P_{u1} is the force of flow of I. Thus $P'_1 = P_{u1}$ and $P'_2 = P - P_{u1}$. And there will be a large flow of I and a large slip of II. The shrinking force P_s cannot occur because of flow of element I.

For small values of P, e.g. P = 0, P_m will not develop because the bonds are not stressed and will after breaking by a moisture content change, reform in the same position. Because the bond breaking process is eight times faster than the development of the shrinking stresses, the process will be finished before the shrinking stresses occur, and it can be expected that an unloaded specimen will get only the internal shrinking stresses on drying and wetting (swelling stresses).

For rewetting of the specimen, after the first drying cycle, the forces will be:

I	II	
$P_{u1} \downarrow$	$\downarrow P - P_{u1}$	initial values due to the first drying cycle
$P_m \uparrow$	$\downarrow P_m$	due to sorptive bond and slip restoring II and slip of I
$(P_s \uparrow$	$\downarrow P_s)$	(force due to swelling of element I)
$P'_1 \downarrow$	$\downarrow P'_2$	

Total forces in general: $P'_1 = P_m - P_{u1} < P_{u1}$, except for unloading, and $P'_2 = P - P_{u1} + P_m < P_{u1}$ and the recovery of the deformation will be approximately: P_m / K_1.

Also in the next drying and rewetting cycles, the increase and decrease of the deformation will be about this amount and increase of the maximal deformation and decrease of the amplitude will depend on the slow creep process, giving an additional stress redistribution . Stresses due to differential shrinking and swelling will have an influence at a later stage.

For high loading P'_2 may reach P_{u2}. At this point there is an increase in flow and slip in

each cycle and the maximum deformation will not tend to a limiting value but increases until fracture. This also is known from measurements e.g. in [5] where, for P of about one eighth to one quarter of the ultimate load, this boundary of flow of element II is reached for bending. A analogous scheme for an initially dry specimen on first wetting is given below.

I	II	
$P_1 \downarrow$	$\downarrow P_2$	initial values
$P_m \uparrow$	$\downarrow P_m$	sorptive bond restoring of II and slip of I
$(P_s \uparrow$	$\downarrow P_s)$	(force due to swelling of element I)
$P_1 \downarrow$	$\downarrow P'_2$	Total forces: $P'_2 = P_{u2}$, causing flow of element II. $P'_1 = P - P_{u2}$.

Element I slips and will get the swelling movement, and is hardly noticeable as external movement.
For re-drying the specimen, after the first wetting cycle, the forces will be:

I	II	
$P - P_{u2} \downarrow$	$\downarrow P_{u2}$	initial values
$P_m \downarrow$	$\uparrow P_m$	sorptive bond breaking and reformation causing slip in II
$(P_s \downarrow$	$\uparrow P_s)$	(force due to shrining of element I)
$P'_1 \downarrow$	$\downarrow P'_2$	Total forces: $P'_1 < P_{u1}$ in general, and the increase of deformation wil be of the order of P_m / K_1. Also in the next drying and rewetting cycles, the increase and decrease of deformation will be approximately this amount, and the increase of the maximal deformation at each cycle will depend on the slow creep process giving an additional stress redistribution. For greater loadings P'_1 may reach P_{u1} and the stress situation of the first drying occurs. However, in that case, there will always be an increasing slip at each cycle loading to fracture when the ultimate strain condition [] is reached.

7.3.3. Influence of the mechano-sorptive effect on connections.

All figures 7.3 are from [13]. In the context of the war of CIB-W18 against theory, it is stated in [13] that a linear approach is sufficient accurate and is justified, contrarily to reports of the Stevin-laboratory (Ploos van Amstel - van der Put) where it is shown that any

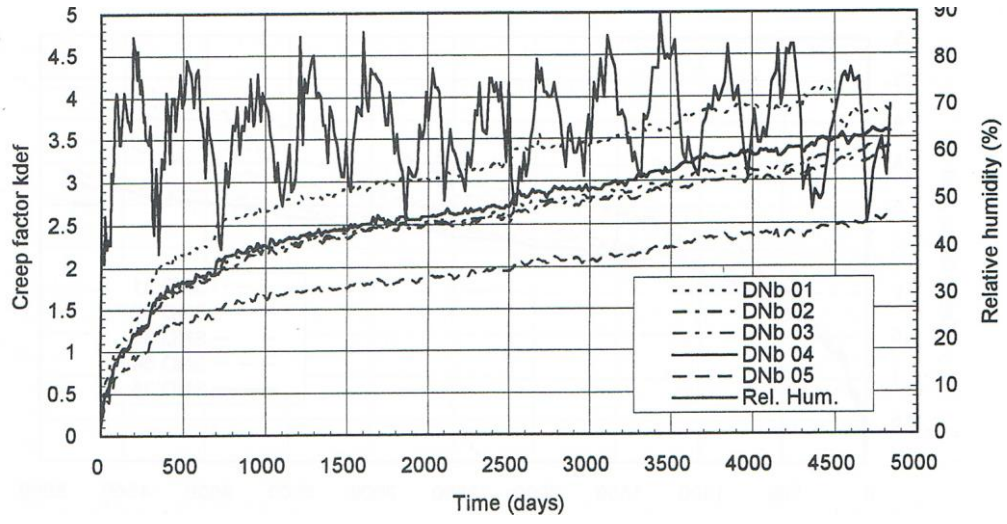

Fig. 7.3.3. |Creep lines of nailed joints at 30% load level []

extrapolation from linear fitted data, over any time range, provided a total wrong prediction of the later measured behavior. The fact that a faint part of a logarithmic curve, or exponential integral curve can be approximated by the linear exponential time curve, is not a proof of linear behavior. Any faint curve also can be approximated by a parabola, what is not a proof that Boltzmann statistics does not apply. Further, the high data variability shows that the mean fitted curve to any theoretical equation, will cause an "exclusion of fit" (with a very high probability) for all 5 separated measured data curves. This means that the data of every curve should be separately fitted to the theory equations, which fit will show a correlation close to one, because of the molecular high number statistics. Every specimen thus is significantly (at the highest confidence level) an unique giant molecule. Linear viscoelasticity does not exist. The linear parameters only approximately may apply for liquids of round molecules and may only then approximately describe behavior at different loading histories. An example is given by § 7.1, where water molecule bridges between hydrogen bonds of adjacent layers may act as such a liquid at near zero stresses.
For nailed joints, fig. 7.3.3 to fig7.3.6, the influence of the mechano-sorptive process is not strong, as follows from the small wavy curves at the start. The variation of the mean moisture content at the bearing part of the nail thus is small. The lines of fig. 7.3.6. therefore still show the dominating time stress equivalence of wood at near constant mean moisture content. Regarding the processes in the layers, it is mentioned in § 5.1 that 2 processes are possible: One with B = 0 in eq.5.1.1 and one with A = 0 in eq.5.1.1. The first process delivers the sites of the second process. Therefore, this second process is not noticeable at the start of a creep test, and is, after long times, suddenly noticeable by a strong deformation increase as e.g. given by the sudden rises of the curves as also applies for the start of local failure (shear plug failure of the middle lamellae) in fig. 7.3.13 (following the exponential integral function, what should not be confused with the exponential function). Only for high loading this process is directly measurable at the start due to the shift of the loading curve to shorter times by the time-stress equivalence (see e.g. shifts of fig. 7.3.6)
The process with A = 0, is a structural change process. It applies for damage increase but also e.g. for annealing and the most general solution of this differential equation is given in B(2010) or in Section B.3. applied to annealing. Fig. 7.3.6. shows this process by a long delay time before the steep rising branch at later times. An approximate solution (for parameter fitting) of this eq.(5.4.8) is given by eq.(5.4.16) which is a shifted equation with respect to eq.(5.4.5) and is then the same when A is replaced by $B\varepsilon_v$. The slope of the lines of fig. 7.3.6. at higher times t follows from an analogous eq.(5.4.16) of the creep factor: $\frac{\varepsilon}{\varepsilon_0}-1=\frac{1}{\varphi K_2\varepsilon_0}\ln\left(1+c\cdot\left(t-t'\right)\right)$,
is $1/\varphi K_2\varepsilon_0$, which is independent of stress, temperature at a constant, mean, moisture content. Due to the time stress equivalence this curves shift to shorter times for higher stresses (see fig.7.3.6). This is opposed by the mechano-sorptive process, which acts on the changing moisture content conditions, and wherefore φ is constant (as known since B(1989a)).
The mechano-sorptive process acts during the first, or first two, m.c. cycles, until the adjacent layers are shifted to the position of the mean moisture content (m.c.) condition.
For toothed plate joints, the mechano-sorptive process (with constant φ) dominates and creep lines $\varepsilon-\varepsilon_0$ (and not the creep factor-lines $\varepsilon/\varepsilon_0-1$) at different stresses, then are comparable with the same slope. The creep factor lines therefore show, after the first complete cycle, which ends after about 300 days, the reduction of the creep factors by $1/\varepsilon_0$ or relatively by $1/\sigma_0$ of respectively: 1/0.30 ; 1/0.40 ; 1/050, for the 30%, 40% and 50% load level. Thus where, after 300 days, the mean creep factor ≈ 2, of the five, 30 % curves of

fig. 7.3.7, this creep factor is (30/40)·2 = 1.5 for the 40 % curves of fig. 7.3.8 and (30/50)·2=1.2 for the 50 % level curves of fig.7.3.9. This is in accordance with the measurements of the figures, due to constant φ. The slope of the logarithmic lines of fig. 7.3.10 also show the slope difference according to a constant value of φ.This tendency is less clear for split ring joints at the 50% level because of the start of dominating damage processes at this load level (which fits should be subtracted). For less high m.c. changes of the tests in more controlled environment, the logarithmic lines show no longer the dominating mechano-sorptive process with constant φ, but a constant C ($\varepsilon_0\varphi$) of a dominating time – stress equivalence. (see fig. 5.3.4 of [13]) as always dominates for nailed joints. Conclusions are only possible after the data fit to the right theoretical equations. As mentioned this should be based on the given solution of the annealing equation in B(2010) or Section B.3. Of interest is the highly non-linear damage function of the steep rises of the curves of fig 7.3.13, which show the form of the exponential integral function and represent shear plug failure of the middle lamellae. At constant climate conditions fig. 5.3.3. of [13] shows the necessary one creep factor line, independent on the load level, temperature and m.c. as follows from eq.(4.5.4).

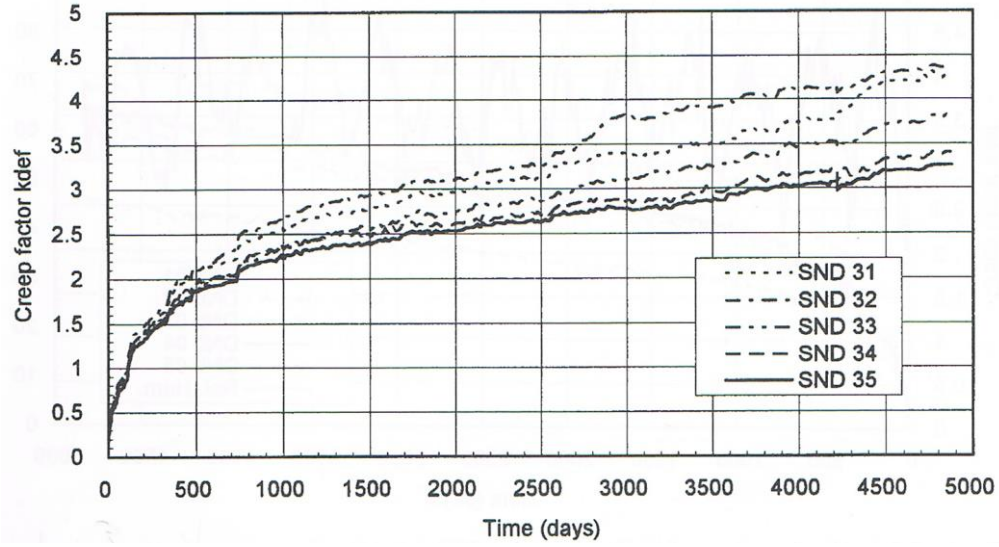

Fig. 7.3.4. Creep lines of nailed joints at 40% load level []

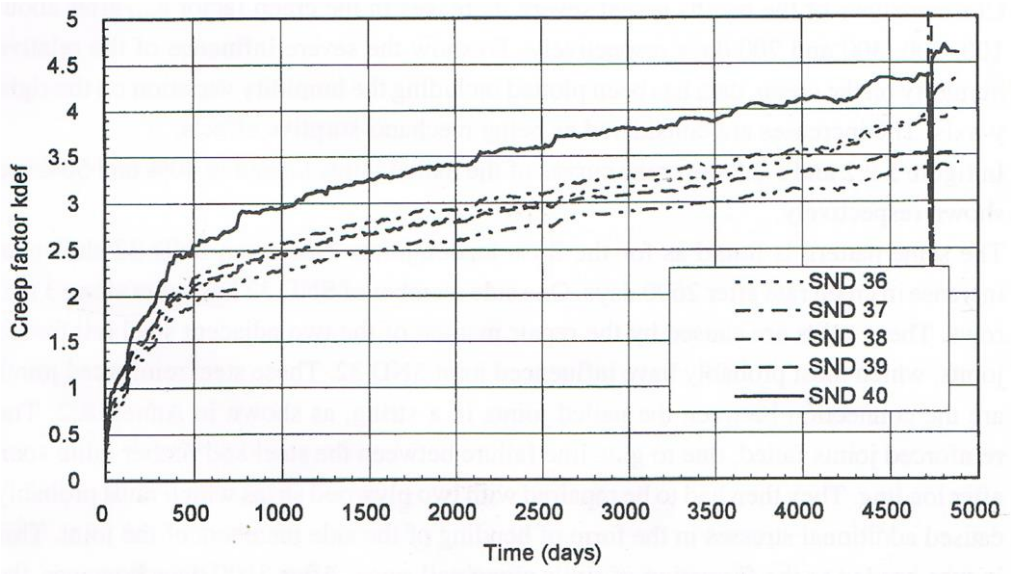

Fig. 7.3.5. Creep lines of nailed joints at 50% load level []

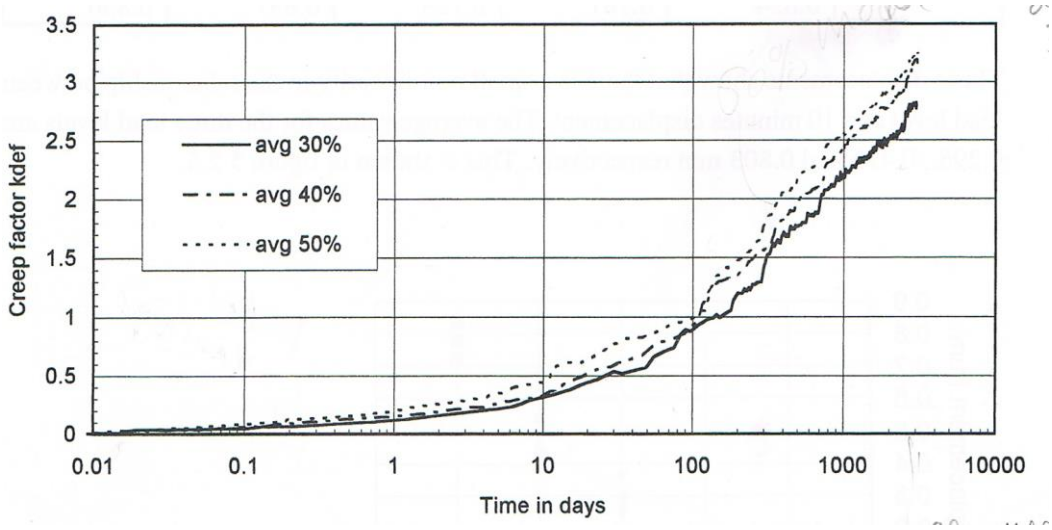

Fig. 7.3.6. Average creep curves of 30%, 40%, and 50% nailed joints

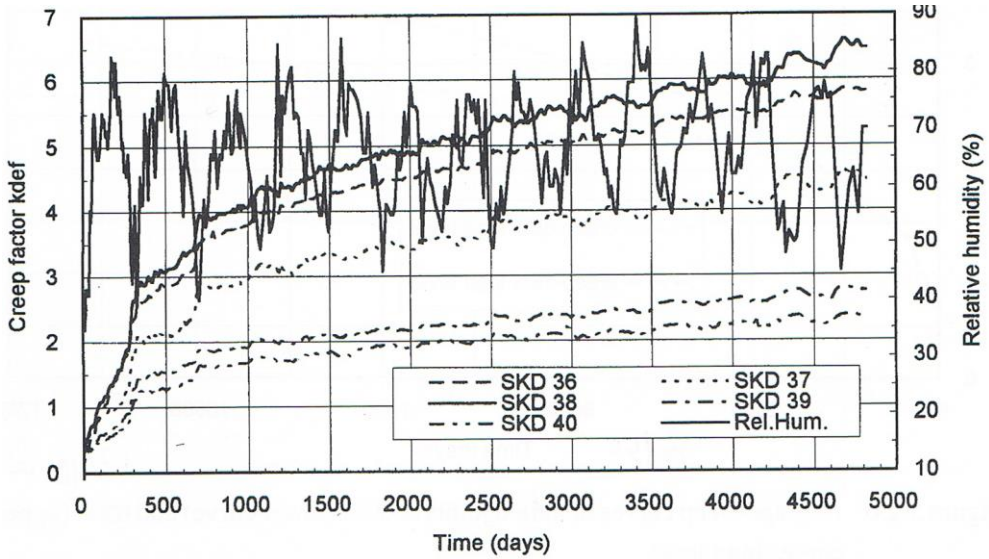

Fig. 7.3.7. Creep results of five toothed plat joint at 30% load level.

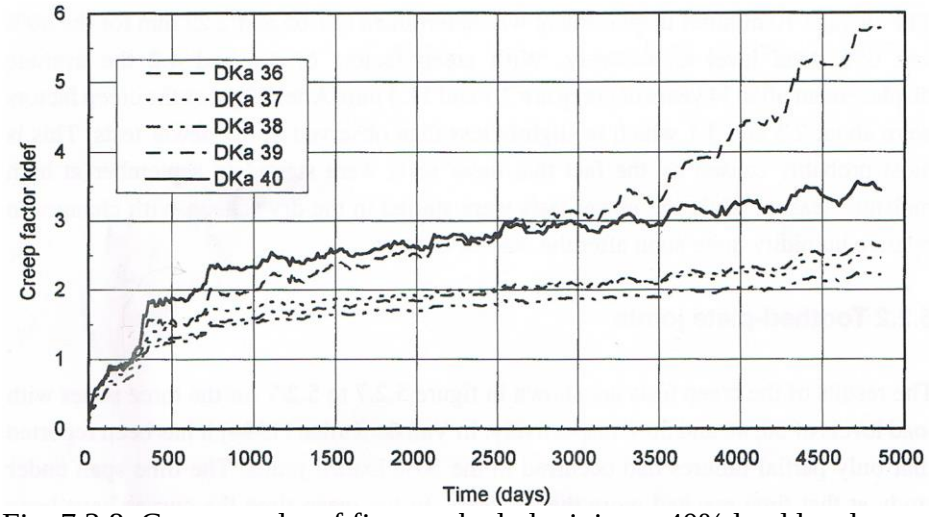

Fig. 7.3.8. Creep results of five toothed plat joint at 40% load level.

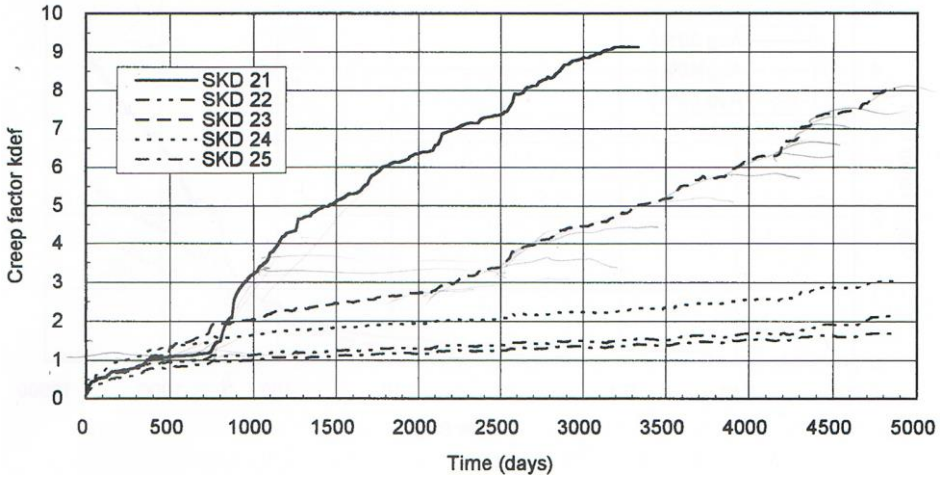

Fig. 7.3.9. Creep results of five toothed plat joint at 50% load level.

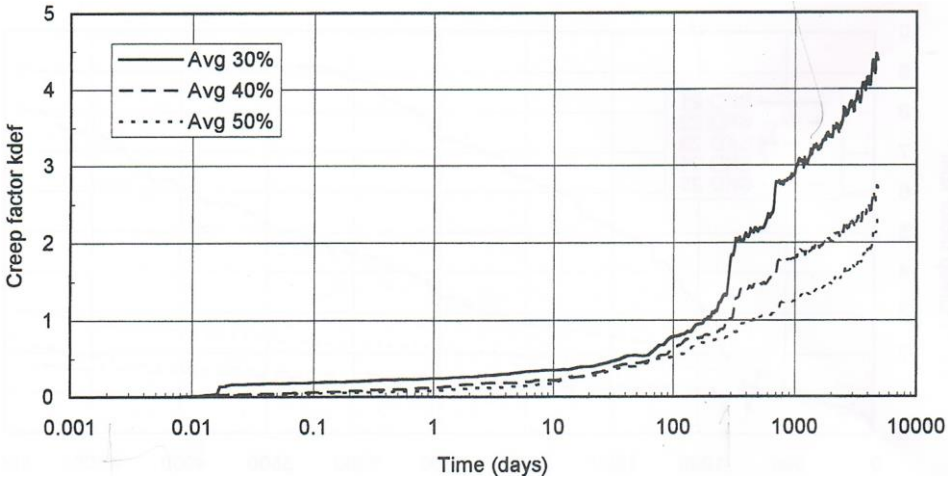

Fig. 7.3.10. Average creep curves of toothed plate joint at 30%, 40%, 50% load level.

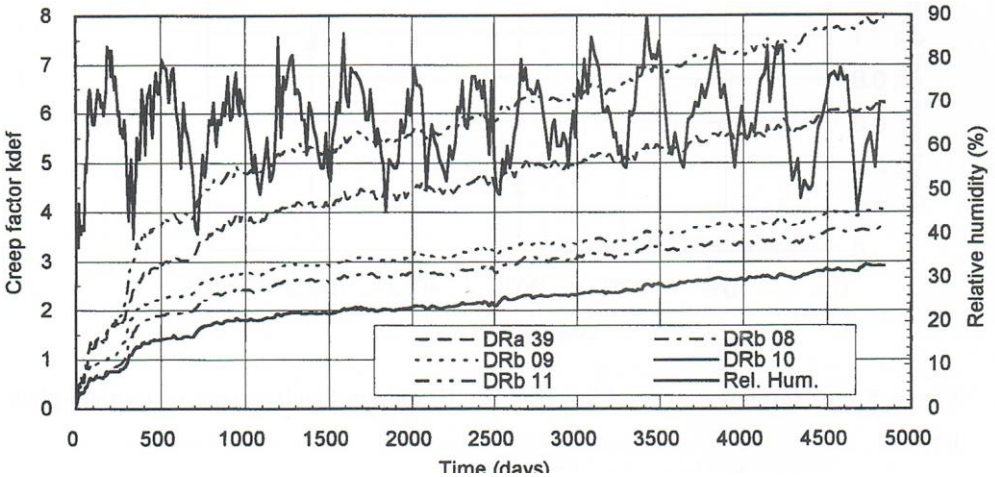

Fig. 7.3.11. Creep results of five split ring joints at 30% load level.

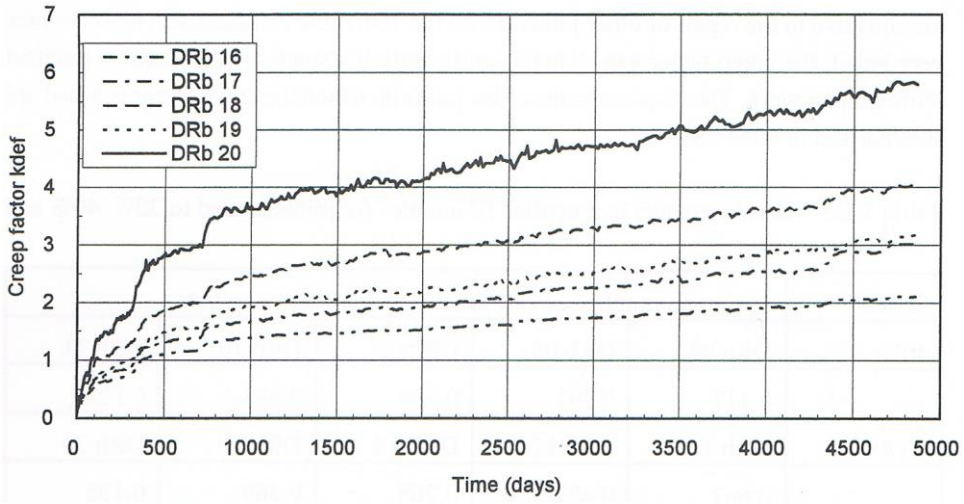

Fig. 7.3.12. Creep results of five split ring joints at 40% load level.

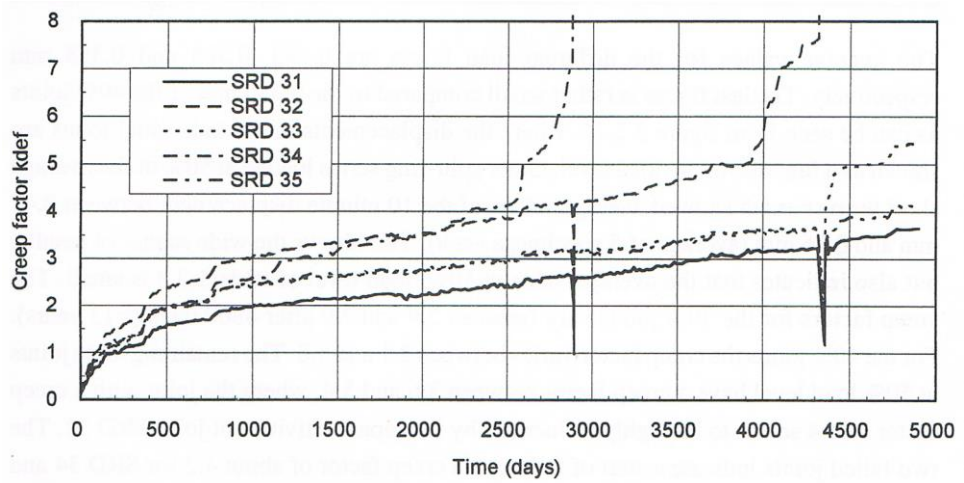

Fig. 7.3.13. Creep results of five split ring joints at 50% load level.

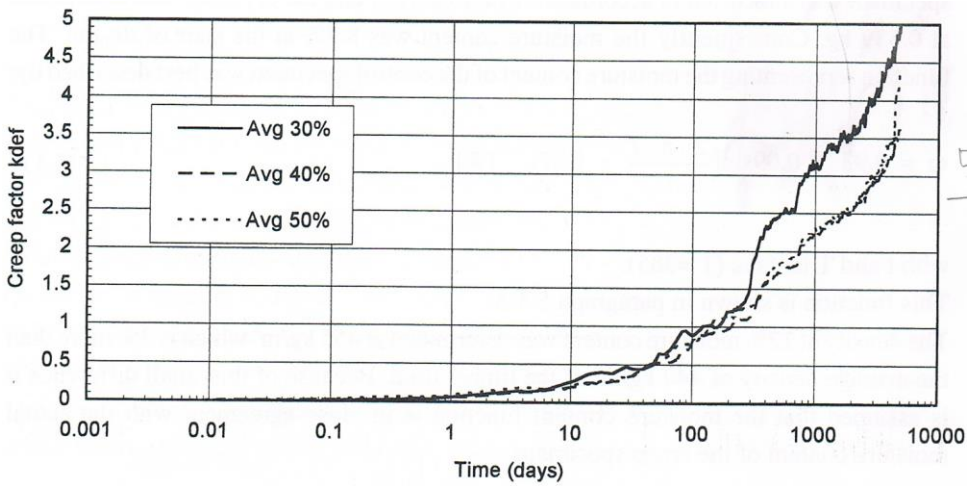

Fig. 7.3.14. Average creep curves of split ring joints at 30%, 40%, 50% load level.

7.4 References

[1] Deformation kinetics, A.S. Krausz, H. Eyring 1975 John Wiley & Sns.
[2] Plastic properties of wood in relation to the non-equilibrium states of moisture content, T. Takemura, Mem. Coll. Agric.,Kyoto Univ., No 88, 31 (1966).
[3] Modeling and simulation of viscoelastic behaviour of wood under moisture change, J. Mukudai, S.Yata, Wood Science and Techn. Vol. 20 (1986) p.335-348.
[4] The effect of moisture content changes on the deformation of wood under stress, L.D. Armstrong, R.S.T. Kingston, Wood Science 1979, p. 301-306.
[5] Moisture content changes and creep of wood, R.F.S. Hearmon, J.M. Paton, For. Prod. Journ. Aug. 1984. p. 357-358.
Other publications on the subjects of § 6 and § 7 can be found in [6] to [11].
[6] Derivation of the mechano-sorptive effect by the kinetic approach, T.A.C.M. van der Put, Comportement Mechanique du bois, coll. scientific rheologie du bois, Bordeaux juin 1988.
[7] Explanation of the mechano-sorptive effect, T.A.C.M. van der Put, Proc. IUFRO, S 5.02 conf. 1988.
[8] Basis of the Clouser-type power equations for creep,
[9] Derivation of the WLF-equation for glass transition,
[10] Retardation spectra,
[11] Explanation of phenomenological laws by the theory of deformation kinetics,
[12] Deformatin and damage processes in wood.
[8] to [12] by: T.A.C.M. van der Put, Proc. IUFRO, Turku, Finland.
[13] Duration of load effects in timber Joints, dissertation, J.W.G. van de Kuilen, Delft University Press, 1990.

8. Experimental research

8.1 Scope of the experimental program

Testing is always necessary to show the predictions of the theory and the values of the parameters, dependent on temperature and moisture content. Because of the very small viscoelastic deformations, at constant rate tests, a precise determination has to wait until very accurate testing machines are available. The loading machine showed an oscillating behavior, probably due to disturbances of the electricity network, that has an influence on the scatter of the data, especially at low loading. There was, however no noticeable drift of the machine. Because of the goal to measure the mean overall behavior, this was accepted and for that reason, also no corrections of the data were made for temperature differences around the mean temperature and dummy movements due to oscillating moisture differences. Because data are available for perfect constant humidity conditions, it was decided to use periodical relative air humidity conditions, as may occur in practice. The theoretical derivation leads to similar behavior as a parallel system of Maxwell elements with the general strain rate equation (of element i) in accordance with thermodynamics:

$$\dot{\varepsilon} = \frac{\dot{\sigma}_i}{K_i} + \left(A_i + B_i\varepsilon_i\right)\sinh\left(\sigma_i\varphi_i\left(1 - C_i\varepsilon_i\right)\right) \qquad (5.1.1)$$

where σ_i is the stress on the Maxwell element i, ε_i is the strain of the nonlinear dashpot and K_i is the spring stiffness. A_i, B_i, C_i and φ_i are constants.

The process, which is determining at the start of the creep test, shows no delay time and thus $B_i\varepsilon_i$ is negligible in comparison with A_i in eq.(5.1.1) and also $C_i\varepsilon_i$ shows a negligible influence in the first creep stage. Because the relaxation times of the different processes are far apart from each others, only one process can be regarded. Thus the first estimate of the parameters has to be based on:

$$0 = \frac{\dot{\sigma}_i}{K_i} + \left(A_i\right)\sinh\left(\sigma_i\varphi_i\right) \qquad (8.1)$$

for a relaxation test, and:

$$0 = \frac{\dot{\sigma}_i}{K} + \left(A_i\right)\sinh\left(\sigma_i\varphi_i\right), \qquad (8.2)$$

for the creep test, with $K = K_1 \cdot K_2 / (K_1 + K_2)$.

The solution of eq.(8.2) for the early part of the total creep process is:

$$\frac{\varepsilon}{\varepsilon_0} = 1 + \frac{1}{\varphi K_2 \varepsilon_0}\ln\left(1 + \frac{K_1 K_2 A\varphi t}{2\left(K_1 + K_2\right)}\exp\left(\sigma_{v0}\varphi\right)\right) \qquad (8.3)$$

This equation has the form:

$Y = 1 + C\cdot\ln(1 + t/T)$ (8.4)

Where t = time in seconds and T is a "delay" time in seconds.

The estimation of the parameters C and T can easily be done by a simple regression procedure.

8.2 Test program

It was planned to do creep and relaxation tests. However the parameters of both types of tests appeared to differ not much. Thus relaxation tests in tension were done, in combination with creep tests, to show this conformity with creep tests.

For comparison creep tests were done in compression, tension and shear, along the grain and perpendicular to the grain. According to table 8.1, 5x2x3 specimens are tested in creep mostly at 2 temperatures depending on the moisture content. Two series of test specimens were used, cut close behind each other from one board. One series was conditioned at about 45% relative air humidity, and the other at 85%. The tests were done on Spruce and the dimensions of the specimens are given below.

Table 8.1 Overview of test-numbers

Test-type	humidity	Load -type	temperatture	Specimen nr.
1 compr. // 2 compr. ⊥ 3 tension // 4 tension ⊥ 5.shear	1 45 % 2 85 %	1 relaxation 2 creep	1 – 25 deg. 2 + 5 3 + 25 4 + 50 5 + 70	1 to 3

example: test-code 32241 is: tension 2; wet; creep test; 50 ^{0}C; specimen nr. 1.

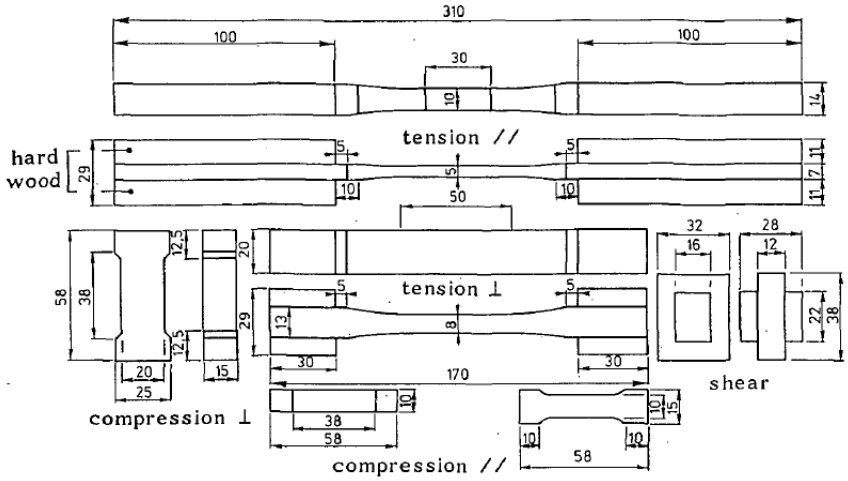

Fig. 8.1 Dimensions of the test-specimens

The loading sequence of the tests (see fig. 8.2) was:
The specimen is loaded at a constant strain rate to a stress level of about 70% of the short term strength, followed by a creep test during about 1 to 3 hours, depending on the deformation. Then the load is decreased to the level of zero creep, what is found by a searching procedure, and maintained at this level during approximately 1 hour. At this level the "dashpot" of the 3-element model is unloaded and creep will not occur. Then, after unloading, the recovery is measured. The times of each sequence depends on the amount of creep. With this loading cycle it is in principle possible to determine the constants of a three element model. To maintain the different temperatures and moisture contents, climate boxes were used around the test-specimens. Before the loading, the three specimens of each test-type, were conditioned in the climate boxes until the movement of the specimen due to the moisture exchange was small. Then the test was done on one specimen, while the other two served as dummy to detect weight differences due to change of moisture content. If the temperature was raised, higher relative humidity was sometimes necessary to stop the movement of the dummy due to water exchange. The weight and the dimensions of the test-specimen was controlled, just before and after the test. To study the influence of moisture content, mainly tests were done above 0 ^{0}C

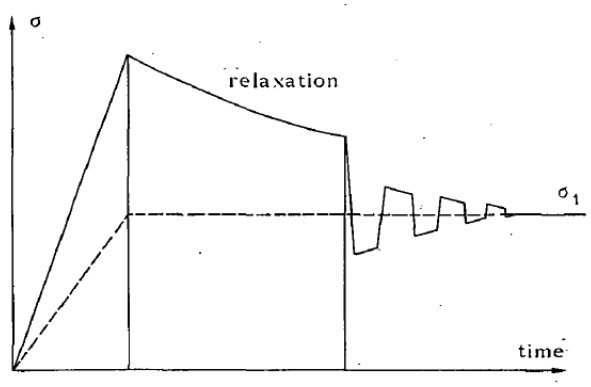

fig. 8.2 Scheme of the searching procedure for zero relaxation

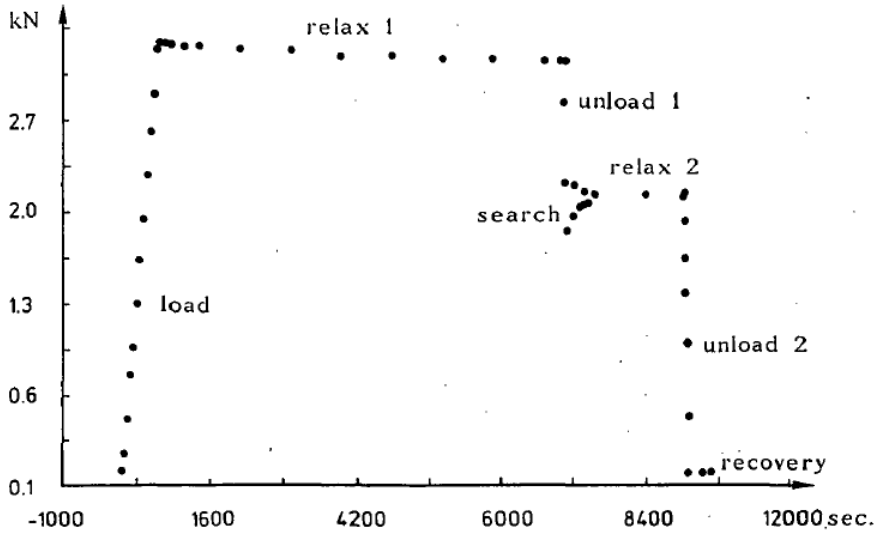

8.3 Loading sequences of the relaxation test

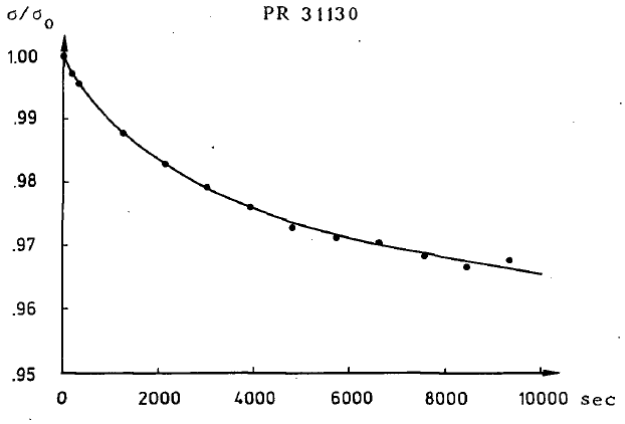

Relaxation

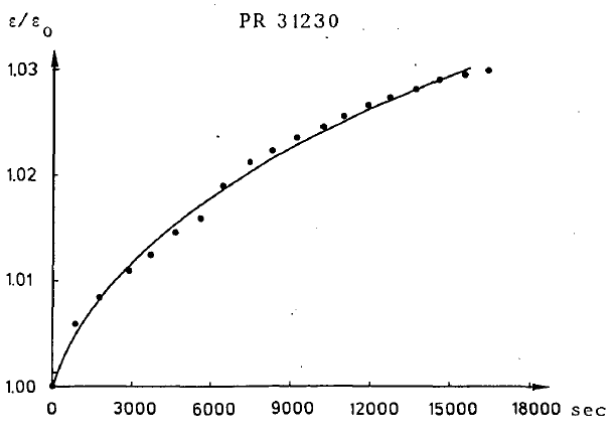

fig. 8.4 Regression of relaxation and creep on one specimen

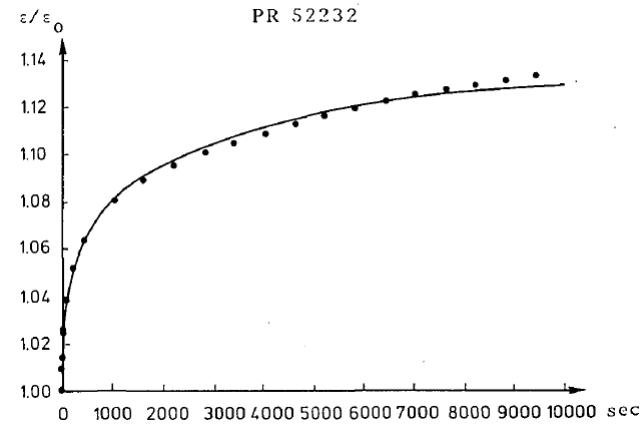

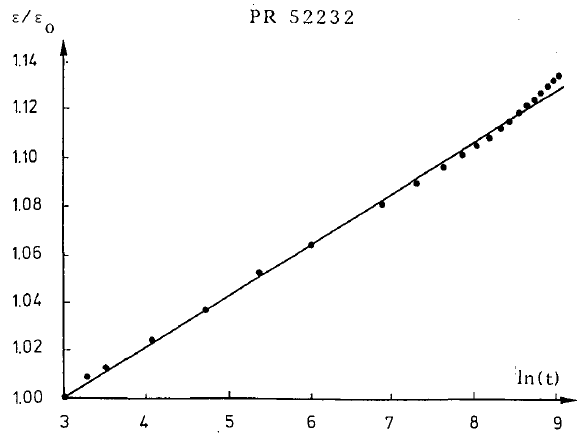

fig. 8.5 Creep test in shear

The measurements were taken with a data logger and stored on files. An example of loading sequences of a relaxation test is given in fig. 8.3.
An example of the regression for relaxation and for creep in tension along the grain, done on the same specimen, is given in fig. 8.4
An example of creep in shear is given in fig. 8.5, together with a plot on logarithmic time scale. Probably there is a start of a second process at the end.

8.3 Results of the parameter estimation

In general, the stress-strain loading line was only faintly curved and nearly straight, indicating a constant value of C for loading and a gradual increase of stiffness. The first unloading to the level of zero creep, showed a perfectly straight line, thus no recovery of stiffness and viscoelastic strain. The second unloading line was curved, showing recovery. Because of the small viscoelastic effects and the scatter, curve fitting of the loading and unloading tests is inaccurate. When these lines are approximated by linear lines, the general tendency is that the mean stiffness of the first unloading line is the highest, and the mean stiffness of the loading line is mostly the lowest. In fig. 8.6 and 8.7, the loading and unloading lines are given of a compression test, which show the most pronounced stiffness differences.

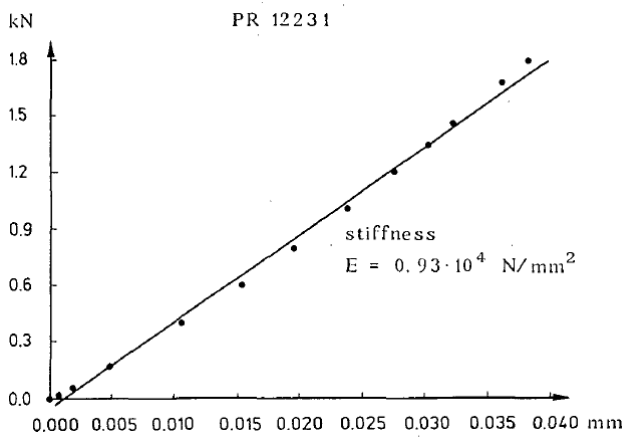

fig. 8.6 First loading of a compression test

The estimation of the compound parameters of the relaxation tests and creep tests, according to eq.(8.4), are given in technical reports [1] to [5] of the Stevin-laboratory.
For some tests the level of zero creep or relaxation was maintained for long times in order to verify the three element model by control the constancy of the parallel "spring constant". In one test in tension (series 3), for instance, this level remained perfectly constant during the available test time of 20 hours, despite the changing relative humidity (+and - 15% around equilibrium level). This delivers the empirical proof of possible zero relaxation.

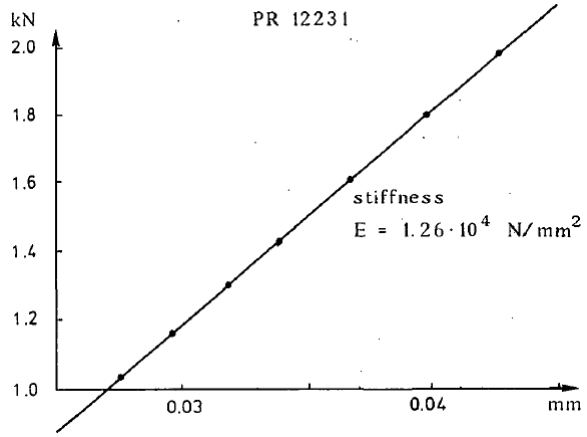

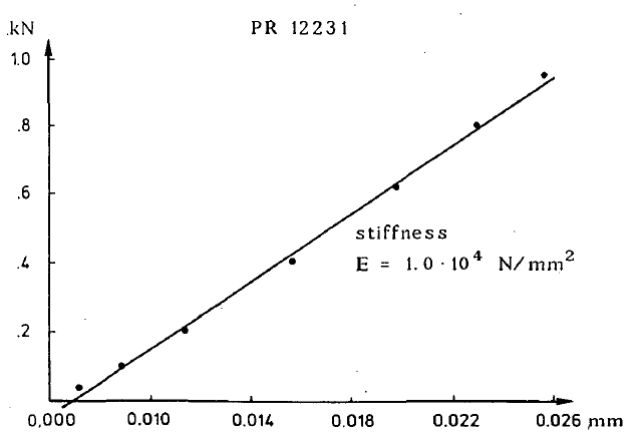

fig. 8.7 First and second unloading sequences of a compression test

8.3.1 Model-parameters, discussed for shear

An overview of the parameters C and T of eq.(8.4) for shear is given in table 8.2 of B(1989a). The parameter T of the creep equation, which is a measure of the delay time, is the result of a multiplication of a very large value by a very small value and determination of these parameters, containing the relaxation time, will be inaccurate. A better determination of the relaxation time, by increasing the creep time, appeared to be not possible in this

Table 8.2 Results of the shear tests along the grain

Test nr.	Force kN	R.H.	Temp. deg.C	C		T	
				mean	95%confid.	mean	95%confid.
52231	1.6	.64	29	.015	.014/.017	20	12/27
2	1.6	.74	31	.021	.020/.023	22	16/29
3	1.6	.87	30	.027	.025/.030	19	9/28
52251	.8	.88	51	.050	.047/.054	125	97/153
2	.8	.85	50	.028	.024/.032	79	41/117
3	.8	.88	49	.039	.036/.042	47	32/61
51231	2.0	.58	27	.013	.011/.014	12	5/19
2	2.0	.63	28	.016	.015/.017	13	10/15
3	2.0	.45	27	.021	.020/.023	21	13/28
51251	1.0	.27	74	.14	.13/.15	249	204/293
2	1.0	.29	74	.10	.10/.11	292	228/355
3	1.0	.28	75	.064	.06/.07	131	102/160

way because of the start of a second mechanism after longer times. The value of T is highly dependent on the initial flow unit density or initial plastic strain and the variation shows that this is a random property for wood. A long delay time indicates a low initial flow unit density and the process reflects a structural change with an increase of flow unit density. The automatic control of the air humidity could show rather great oscillation around the

mean value, depending on the temperature and the humidity. To maintain a sufficient low humidity cycle, hand steering appeared to be necessary.
The value T/C is:

$$\frac{T}{C} = \frac{2}{KA} K_2 \exp\left(-\sigma_{v0}\varphi\right) = \frac{K_2}{K\alpha\dot{\varepsilon}} = \frac{1}{c\alpha} \qquad (8.5)$$

where α is given below eq.(5.2.7) of B(1989a) and c is a constant for loading to the creep level at constant strain rate ($3\cdot10^{-5}\,\mathrm{sec}^{-1}$). It appears that the mean value of T/C is about $1.0\cdot10^{-3}$ for series 52231/3 and 51231/3 and about $2.2\cdot10^{-3}$ for series 52251/3 and 51251/3, in accordance with the two times slower rate that was chosen for these series. Thus α is not dependent on the moisture content and temperature and the main influence on the variability of T is due to the variability of C. The parameter C is the slope of the strain-log(time) plot. Every specimen has another value of C as can be seen in the series, where the stress and the climatic conditions are the same in the tests but the values are outer each confidence intervals. This indicates different structures and loading histories of the fibres during lifetime in the tree and in the drying process.
The value of C ranges from 0.013 to 0.04 for resp. high and low stresses for not too high oscillations of air humidity. For higher R.H.-oscillations and high temperatures there appeared to occur a transition of φ giving a much higher value of C. This was controlled in series 51251/3 where the specimens were conditioned at 50% R.H. and tested at 28% R.H. causing a decrease in moisture content during the test. Thus moisture movement is the major influence on the value of φ and the model has to be adapted for this phenomenon.
For the series with small cycling humidity conditions the product of the force with C appeared to be constant. This shows that C is stress dependent or that φ is constant, independent on temperature and moisture content.

8.3.2 Constancy of model-parameter φ

It appears that at cycling moisture content conditions, $C = 1/\sigma_0\varphi$ is no longer constant, but that φ is constant as follows from the following tables of the shear tests and of the tests of compression and tension along the grain.

φ is constant, when $C\sigma_0$ is constant. Or, in the table, when P·C is constant. It is seen in Table 8.2, that below the transition temperature of 74 ^{0}C, there is a very small, (negligible) influence of temperature and m.c. on φ.

Table 8.2. Shear tests along the grain, mean values.

Test nr.	Force kN P	R.H.	Temp. deg. C	mean factor: C	Constant φ = Force times C = P·C
52231/3	1.6	0.75	30	0.021	1.6·0.021=0.0336
52251/3	0.8	0.87	50	0.039	0.8·0.039=0.0312
51231/3	2.0	0.55	27	0.0166	2·0.0166=0.0332
51251/3	1.0	0.28	74	--	transition values

This small influence has to be regarded as the delay time of the structural change process which will dominate at a later stage of at higher stress loading,
An overview of the parameters C and T of eq.(8.4) for compression along the grain is given in table 8.5 of B(1989a).
An overview of the parameters C and T of eq.(8.4) for tension along the grain is given in table 8.6 of B(1989a).

Because of the similarity of the constants so far and the independency of the parameters of the moisture content, only tests at one moisture content were done for tension in grain direction and to verify the independency on temperature at low temperatures, measurements were taken at lower values of the temperature. The tests were done in relaxation, and for comparison some tests in creep were done on the same specimens as well (specimen 31130 is the same as specimen 31230, and specimen 31133 is the same as 31233). For specimen 0, first the relaxation test was done and for specimen 3, first the creep test. After each type of test, there was a recovery period. The strain of the creep test of specimen 3, was waved by the following of the humidity and temperature cycles, and temperature correction of the data had a strong influence. The influence of this correction on the relaxation tests was negligible.

The ratio of the parameters C for creep and for relaxation of these tests:

$\varphi\sigma_0 / \varphi\varepsilon_0 K_2 \approx (K_1 + K_2)K_2 = 0.016 / 0.013$ to 0.020/0.016 = 1.23 to 1.25,

suggests a ratio of the spring stiffness in the model of $K_1 / K_2 = 0.24$, or:

$K_1 / (K_1 + K_2) \approx 0.2$, as found and applied before.

Table 8.5. Compression tests in grain direction, mean values.

Test nr.	Force kN P	R.H.	Temp. deg. C	mean factor: C	Constant φ = Force times C = P·C
11251/3	1.28	0.34	70	0.036	1.28·0.036=0.046
12231--	1.93	0.77	29	0.027	1.93·0.027=0.052
12231/3	1.00	0.55	48	0.050	1.00·0.050=0.050
				--	

The same applies for Table 8.5, showing constant φ below about the same transition temperature, thus showing hardly an influence of temperature and moisture content on φ.

Table 8.6. Tension tests in grain direction.

Test nr.	Force kN P	R.H.	Temp. deg. C	mean factor: C	Constant φ = Force times C = P·C
52231/3	1.6	0.75	30	0.021	1.6·0.021=0.0336
52251/3	0.8	0.87	50	0.039	0.8·0.039=0.0312
51231/3	2.0	0.55	27	0.0166	2·0.0166=0.0332
51251/3	1.0	0.28	74	--	transition values

This does not apply for tension in grain direction. The quick, small, humidity changes could not be followed by the tensile specimens due to the long grain lengths of the specimen. For these tests C is constant and is about:

C ≈ 0.15, or n = 1/C = 1/0.15 = 67 as also found by other investigations at constant climate conditions.

The tests, for compression and tension perpendicular to grain, were tests on small clear specimens, with a very short grain length, in the direction of a small dimension of the specimen, showing therefore a transition to a flexible state at m.c. cycling at high R.H. or at high temperature conditions. Only the series at standard climate conditions did show a common C value of about C ≈ 0.15 (n ≈ 67). All other specimens did show the transition to the flexible state.

An overview of the parameters C and T of eq.(8.4) for tension in tangential direction is given in table 8.3 of B(1989a). The parameters are comparable with those of the shear tests when relative humidity fluctuations are kept small (see 41231/3). Deviations occur near the

process transition temperatures i.e. about 50 ^{0}C for wet wood, and about 70 ^{0}C for dryer wood. The mean values of T/C of the series show no tendency and can probably regarded to be constant independent on temperature and moisture content. The great variability shows a major influence of the structure and previous history.
An overview of the parameters C and T of eq.(8.4) for compression perpendicular to the grain in radial direction is given in table 8.4 of B(1989a). Except near the transition temperature (22241/3), the mean value of T/C can likewise be regarded as a constant with respect to temperature, humidity and stress.

8.4 Conclusions

- Because data are available for perfectly constant moisture conditions and because changes in moisture content may have a great influence on the parameters of the overall process, the tests were done by cycling relative air humidity conditions, as will be encountered in practice, to see this influence on the different processes.
- The creep behavior is well described by the kinetic theory, showing one dominating process in the first hours. For this process $B_i\varepsilon_i$ and $C_i\varepsilon_i$ in eq.(5.1.1) were zero. Thus it follows that for relaxation processes eq.(8.2) applies and although A_1 and φ_1 in this equation act mathematically as constants, they can be expected to be random because of the random values of the initial plastic or viscoelastic strains ε_i, depending on the loading and temperature history during the lifetime and the drying process. Further it is possible that eq.(8.2) represents the mean behavior of all processes with comparable retardation times. In order to distinguish for instance, between the processes of diffusion and creep, it is necessary to have some orders difference in relaxation times of these processes. This is possible by using thin specimens. However, as shown before, the mechano-sorptive effect is quite different then.
- It appears that (per process) the three-element model holds and that the parallel spring is constant. The retardation time for creep of the Maxwell-element is very long with respect to the testing time of three hours, and the behavior can be described by the logarithmic law: $\varepsilon/\varepsilon_0 = 1+C\ln(1+t/T) \approx 1+C\ln(t/T)$ (8.6)
representing the theoretical equation for the early part of the total creep with the approximation for longer times after the start of the creep. The breakdown of this logarithmic law [6] is predicted by the theory. This law only applies in the first creep stage (and t >> T).
The same equation holds for relaxation:
$\sigma/\sigma_0 = 1-C'\ln(1+t/T) \approx 1+C'\ln(t/T)$ (8.7)
Because C ≈ C', and T ≈ T' and C.ln(t/T) << 1, the product of eq.(8.6) and eq.(8.7) is:
$\sigma\varepsilon/\sigma_0\varepsilon_0 \approx 1$ (8.8)
This is not a prove of linearity of the viscoelastic behavior, as generally assumed, and as is applied p.e. in [6], but is an indication that the spring constant: $K_1 << K_2$ in the three element model.
- The values of the parameters are comparable, independent of the type of loading and loading direction, showing that the same process is acting.
- The ratio of the parameters C for creep and for relaxation suggest a ratio of spring stiffness in the model of approximately 0.24. This means that the lowest spring constant is 1/5 of the total stiffness according to the model of fig. 2.3 of not fully bonded cellulose chains.
- Oscillating relative air humidity at a relative high frequency appeared to have influence on the parameter C for the short grains of the specimens for shear and compression and for

tension and compression perpendicular to the grain. The accessibility of moisture determines whether the mechano-sorptive process dominates and whether softening may occur.
- The parameter T of the creep equation, which is a measure of the delay time, is the result of a multiplication of a very large value by a very small value and determination of these values, containing the retardation time, will be very inaccurate. A better determination, (in this way), of the retardation time, by increasing the creep time, appeared to be not possible because of the start of a second mechanism after longer times. The value of T can be highly dependent on the initial dislocation density or initial plastic strain and the variation shows that this is a random property for wood. A long delay time indicates a low initial flow unit density and indicates a structural change with an increase of flow unit density.
- It appears that the mean value of T/C is about constant, but has a higher value near the transition temperatures. Thus α is not dependent on the moisture content of wood and can be dependent on temperature in the neighborhood of the transition regions and the main influence on the variability of T is due to the variability of C.
- The parameter C is the slope of the relative strain-log(time) plot. Every specimen has another value of C. This indicates differences in structure and loading history of the fibres during lifetime in the tree and at drying.
- At cycling humidity conditions, the value of C is not constant, as under fixed climate conditions, but the product of the force (stress) with C is constant. This shows that C is stress dependent or that φ is constant, independent of temperature, stress and moisture content. This constancy of φ is a property of the mechno-sorptive mechanism.
- If the mean moisture content cycling is low, as in the specimen of the tension along the grain test, a constant value of C dominates. This will be the case for structural dimensions.
- For higher R.H.-oscillations and high temperatures there appeared to occur a transition of φ giving a much higher value of $1/\varphi$ and of C (at constant T/C, containing not the value φ). Thus moisture movement is the major influence on φ and any model has to account for this phenomenon. The mean values of this high C (C = 0.16) suggest not much influence of moisture content and temperature. Near the transition temperatures, i.e. about 50 ^{0}C for wet wood, and about 70 ^{0}C for dryer wood, is C twice this value. The mean values of T/C of the series show no tendency and can probably regarded to be constant independent on temperature and moisture content. The great variability shows a major influence of the differences of the structure and the previous history.

8.5 References

[1] Shear test along the grain. Parameter determination of a non- linear rheological model based on deformation kinetics. Report 4-86-5 June 1986. Put, dr. T.A.C.M. van der
[2] Tension tests in tangential direction of Spruce. Parameter determination of a deformation kinetics model. Report 4-86-6 June 1986. Put, ir. T.A.C.M. van der
[3] Compression tests in radial direction in Spruce. Parameter estimation of a nonlinear rheological model based on reaction kinetics of bond breaking. Report 4-86-7 June 1986.
[4] Compression tests in grain direction in Spruce. Parameter estimation of a nonlinear rheological model based on reaction kinetics of bond breaking. Report 4-86-8 June 1986.
[5] Reaction kinetics of bond exchange of deformation and damage processes in wood. Proc. IUFRO-Conference Firenze Italy, Sept. 1986.
[3] to [5] Put, ir. T.A.C.M. van der
[6] Some aspects of the rheological behavior of wood III, Tests of linearity. Aust. J. Appl. Sci. 14, 305-317. October 1963. P.U.A Grossmann, R.S.T. Kingston

9 Conclusions

- An extension has been given to the theory of molecular deformation kinetics by the development of a general limit analysis (thus exact) theory, which is solely based on the reaction equations of the bond-breaking processes, and dimensions of the flow units accounting for the derived necessary thermodynamic relations of energy exchange.
By expressing the concentration of flow units of the reaction equation in the dimensions of the flow units, the expressions for the strain rate, fracture, hardening and delay time are directly derived. The reaction (in solids) is derived in section B.2 to be of first order.
- A (Fourier- type) series expansion of the potential energy curve, leads to parallel acting systems of symmetrical consecutive barriers. Each consecutive row acts as a single symmetrical barrier, what provides the derivation of the thus far empirical generalized flow theory, showing, the premises on which this theory thus far was based, are consequences of the series expansion. This delivers a parallel system of simple symmetrical processes, far apart from each other. This general theory is generally applicable for the description of time dependent behavior of materials including transformations and fracture processes.
- Therefore, as also, additionally, shown by Section B.2, the developed new equilibrium theory of deformation kinetics explains all aspects as creep, damage, aging, annealing, nucleation, transformations as glass transition, rubber behavior, diffusion, etc. by the same constitutive equation. By the solutions of the theory equations for transient processes, at different loading histories it is shown that the theory is able to explain the phenomenological laws of creep and fracture. It explains for instance the yield drop and the logarithmic strain rate law of the modulus of elasticity in the constant strain rate test; the logarithmic time law of the strength in the constant loading rate test; the logarithmic time law of the creep and the bend off of the creep line at long times (delay time of the structural change process) and the shift of this line along the time axis depending on the stress level and depending on the temperature (time – stress and time - temperature equivalence).
- For wood at creep, 2 processes can be noticed. The first process with the smallest slope in fig. 5.9 contains a high density of flow units (zero order reaction) and produces the flow units of the second process, which shows a long delay time (thus starts with a negligible slope) and a steep slope at later times. When the creep loading is high, this second steep curve may act directly at the start. This is due to the time stress equivalence, shifting curve of higher loadings to shorter times, as given by fig. 5.10 for cellulose, making prediction possible of long term behavior at the lowest applied stress level. Thus, depending on the load level, it is possible that in a test the damage increase of two processes are measured or only the delay time of one process.

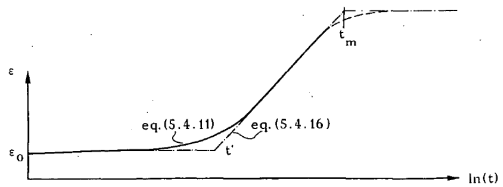

fig. 5.9 Creep eq.(5.4.4) and eq.(5.4.11)

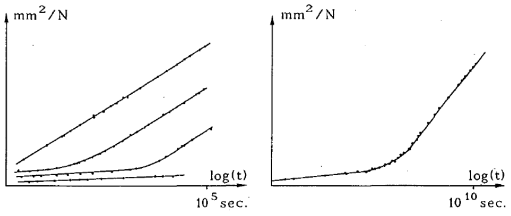

fig. 5.10 Creep compliance behavior

The power law description, then delivers meaningless powers, which are not able to predict other, general, behavior. For instance the power n = 64 represents mainly the waiting time of the fracture steps in a controlled crack propagation test. Thus finding at testing, the power 64 by the power law equation, this only means that stable crack propagation occurred, which response has to be described by the theory of deformation kinetics.
- Of the two processes, measured in § 4.7-[15], the quick one had a very high internal

peak stress, as occurs at a crack tip, indicating stable crack propagation (and showing forward activation only). The activation energy was approximately 50 kcal/mole, high enough for primary bond rupture. The slower process was approximately symmetrical and had an activation energy of about 21 kcal/mole. The activation energy of this process is comparable with values found in § 4.7-[17], where from creep tests at different temperatures for bending: H'= 22 kcal/mole to 24.4 kcal/mole, depending on the temperature range, have been found. From normal-to-grain relaxation tests 23 kcal/mole was reported for wet beech-wood in § 4.7-[18]. This energy can be regarded to be the energy of cooperative hydrogen bond breaking (as calculated below fig. 2.3). The activation energy of 50 kcal/mole is high enough for cooperative C-O--bond or C-C-bond rupture.
- Because at determination of the short term strength, both processes act combined, without delay time, the estimated value of the enthalpy and H' of about 36 kcal/mole in § 4.5, eq.(4.5.10) is the result of a mixture of primary and secondary bond breaking at the same apparent activation volume. Both processes are then regarded to be one coupled process.
- The theory made it possible to derive the different power models (Andrade, Clouser, Forintek, of the power of the stress or of the time), giving the physical meaning of the exponents and constants. It is e.g. shown that the Gerhard's model is an expression of forward activation only and this will be right for high loading in the end state. The Andrade-type equation is shown to be equivalent to the theoretical logarithmic creep behavior. The inverse of one of the parameters of the Andrade or Clouser equations is equal to the work parameter of the activation energy ($n = \sigma V/RT$) and has same meaning as the exponent n of the experimental power law equation for the creep rate and the exponent of the Forintek damage model. Further is 1/n the slope of the normalized logarithmic creep and relaxation lines and of the logarithmic time to failure law of the creep strength or long duration strength. The power value of n is p.e. in the Clouser equation $n \approx 33$. In the Forintek model is n = 34. As slope of the logarithmic creep-to-failure law n = 38 is found, if the line is scaled to the ~ 1 sec. short term strength, but this n = 34 when scaled to the 5 min. strength. The value of n following from the universal form of the WLF-equation as applied for the glass transition of lignin is: n = 2.3 x 17.44 = 40, equivalent to a scaling to a very short duration (instant loading) strength. Thus it appears that n (the activation volume parameter) is essentially a structure constant and is as such unaffected by (constant) moisture content and temperature.
- The values of n between 33 and 38, depending on scaling of the short term strength, apply for secondary hydrogen bond breaking processes.
- As will be discussed in Section B.3, a kinetics explanation of the WLF-equation (Williams-Landel_Ferry is WLF) for glass transition and temperature dependence of creep above glass- rubber transition is derived, showing that the change of the concentration of mobile segments and not necessarily the change of the free volume concentration is the cause of the transition. The theory is extended for cross-linked polymers at transient creep for the element that performs the transition. It follows from the theory that for the special case of constant concentration of flow units the temperature dependence is according to the Arrhenius equation. For higher values of the activation enthalpy, if not the entropy alone is dominating, the theory predicts a shift factor between the Arrhenius- and WLF-equation. The WLF- equation is further extended for the influence of the time scale of the process.
- The nonlinear viscoelastic deformation problem is often linearized by splitting up the contribution to the rigidity in numerous linear viscoelastic processes giving a relaxation spectrum. However, the zero relaxation test shows that a real spectrum does not exist.
- It further is shown that a single process may explain the measured, broad, nearly flat spectra of glasses and crystalline polymers and the total relaxation spectrum for wood can be explained by two processes in stead of the assumed infinite number of linear processes.

This also applies for the spectrum of energy loss at forced vibrations and the activation volume therefore shows a special relationship. Also fatigue behavior can be explained by one dominating mechanism in a wide frequency range, and the behavior at long term loading and at fatigue loading is coupled by the same mechanism. Thus it will be possible to use fatigue tests in order to predict long term strength.

- For clear wood in compression there in no indication of hardening and yield drop, showing the influence of a amorphous polymer (lignin). Thus the thermodynamic possible terms $B_i\varepsilon_i$ and $C_i\varepsilon_i$ in eq.(5.1.1) or B' an C in eq.(5.2.8) can be neglected in this case..
- For timber (with knots) in compression along the grain however there is a small yield drop, superposed on the behavior of the clear wood between the knots, indicating the acting of another Maxwell element (crack propagation by shear failure at the knots). Thus knots act as flow units with a low density. Hardening in compression by combined stresses is only possible as system hardening by confined dilatation as shown in D(2008a).
- For wood in tension there is a high yield drop, showing the influence of a crystalline material (cellulose) dominated by a low initial flow units density ρ_0. There is also no indication of hardening,
- For wood therefore, is follows that $C_i\varepsilon_i$ of the derived creep eq.(5.1.1), can be neglected. Thus hardening is not due to this term but is due to the influence of the parallel processes. When the parallel processes are still regarded as one coupled process, then σ_i has the form of $\sigma_i = \sigma - M\varepsilon$, where M is proportional to the spring constants of that parallel element and $M\varepsilon >> C_i\varepsilon_i$.
- For wood the logarithmic law of the relative creep-to-failure strength, eq.(4.5.4), is one line for different wood species (=different densities), moisture contents, stress states (bending, shear, compression etc.) and types of loading, showing $n = \sigma_s\lambda / NkT$ is constant and thus that the concentration of sites N is proportional to the dry short term strength σ_s. Therefore also the activation enthalpy and entropy are independent of the constant moisture content. The activation volume is however strongly dependent of the moisture content (and thus the inverse of the strength has the same dependency). Based on this form of the activation energy, the experimental creep- to-failure tests at different temperatures and moisture contents could be explained as well as the straight line of the strength on log-time scale for dry wood as the curved line for saturated wood (fig. 4.5.1). Saturated wood shows an enthalpy of about 36 kcal/mole above a transition temperature of - 8 ^{0}C (see fig. 4.5.2) and about 30 kcal/mole below this transition temperature. Dry wood doesn't show this transition. For creep processes N is proportional to the highest ever applied stress.
- The measured negative contraction of creep in bending tension is the indication of a stress redistribution mechanism, causing mainly shear with compression in the wood matrix and increasing the tensile stress in the fibres.
- The activation-parameters are different for every piece of wood, indicating an unique structure of every test-specimen. The average values are comparable for tension, compression and shear, along the grain and perpendicular to the grain.
- The 3-element model is shown to explain the necessary possibility of zero creep and zero relaxation. Thus after a period of creep, at constant loading, there exist a load level after unloading to that level, where there is no further creep deformation., because the internal stress on the creep sites is zero..
- This zero creep test shows that the ratio of the spring constants of the 3-element model is about 1:4. The weakest spring contains the non-linear dashpot.
- This first creep process can be destroyed by mechanical conditioning. The response of the then next process can not be measured in common testing times (due to the too long re-

laxation time)

- For dense species with a high lignin content, a flow unit multiplication mechanism dominates with a stress independent relaxation time. It can be deduced that for this mechanism $K_2\varphi\varepsilon_{v0}$ or $K_2\varphi\varepsilon_0^2$ is constant. Thus the density of the flow units is then proportional to the plastic strain. The constancy of $\varphi\varepsilon_v$ applies only for constant temperature and moisture content. Probably $1/K_2\varphi\varepsilon_v$ is linear dependent on ω and T. This process causes rotation of the relaxation lines at short times in proportion of the strain. When this process is finished ($t = t_m$), it can be seen from eq.(5.5.10), that the relaxation lines for longer times ($t > t_m$), are shifted vertically according to: $\sigma_1 / \sigma_2 = \varepsilon_{01} / \varepsilon_{02}$. Thus, besides horizontal shifts, also vertical shifts can be necessary at some stress levels for the construction of a master creep curve for long loading times.
- The in literature reported existence of a mechanism with constant φ applies for the mechano-sorptive mechanism at changing moisture content and a creep model has to contain all these processes as parallel acting mechanisms.
- The constancy of $\sigma\varphi$ can be explained as follows: For compression the number of developing slip planes N is about linear proportional to the stress level σ at lower stress levels. Thus $\sigma/N = c$, and $\sigma\varphi = \sigma\lambda / NkT = \sigma\lambda' T / NkT = \sigma\lambda' / Nk = c\lambda' / k$ is constant. At a level of about 50 to 65% creases are formed, leading to the second mechanism of gross buckling of the cell walls where a constant buckling stress f may be expected. Thus $\sigma\lambda / N = f\lambda_2\lambda_3\lambda$ is constant, or σ / N is constant. Analogous is for crack propagation in tension the real stress f at a sharp crack at any stress level equal to the "flow" stress and is $f\lambda_2\lambda_3\lambda$ constant or is σ / N constant.
- To know the shift of the compliance along the time axis due to temperature, the same stress level has to be used in all tests at different temperatures. Then the shift:

$$\ln(t_a) - \ln(t_b) = E'/kT_a - E'/kT_b$$

where E' is the activation energy. This is only true if $1/\sigma\varphi K_2$ is constant, independent of the temperature (e.g. for creep). If this is not perfectly constant, reduced strains are necessary to obtain the right activation energy.
- As mentioned, wood shows a dominating process with a high initial site concentration, which doesn't change much with respect to the initial value, (thus determines a zero order reaction), what leads to the condition: $N_f = 0.5N_0$ for fracture, as experimentally found (i.e. the small crack length is about the crack distance, or the intact area has reduced to 0.5 times the initial area when instable crack propagation starts). This leads to the small crack merging model of fracture mechanics of B(1989a), which explains the measured mode I and mode II final softening behavior and gives the fracture mechanics explanation of the "ultimate stress condition" of limit analysis.
- Detailed conclusions regarding the experimental investigation are given in § 8.4.
- These creep test showed one dominating process in the first hours, following eq.(5.1.1) with: $B_i = C_i = 0$, leading to eq.(5.4.1): $\dot{\sigma}_v + KA\sinh(\varphi\sigma_v) = 0$ for creep.
- As first explorative investigation, the independency of the parameters of moisture content, stress type and temperature was indicated when not too close to a transition to a second process.
- By the application of small clear specimens, all processes did show a dominatingprocess with a constant value of φ, due to moisture content cycling, in stead of a constant $\sigma_0\varphi$, as applies for constant climate conditions. Necessary for the mechano-sorptive mechanism is a change of the mean moisture content in a specimen. Humidity cycling around this mean

m.c. therefore are not noticed in common structural elements. Only the yearly m.c. changes

- The bearing parts of toothed plate and ring dowel connections are highly accessible to moisture, what also strongly depends on structure deviations as initial cracks, causing a high variability of the mean moisture content of those parts and by that of the deformation by the mechano-sorptive effect. Protection by glue or paint is necessary for reliability.
- Outer the common process which acts at constant climate conditions, thus by the mean temperature and mean moisture content, a mechano-sorptive process is acting, due to the cycling moisture content. The first process shows a constant slope of the logarithmic plot of the relative creep (constant 1/n), while the mechano-sorptive process shows a constant slope of the logarithmic plot of the creep (constant $1/\varphi$). This explains the for joints measured, increasing reduction of the creep factor by the increase of the load level.
- The general conclusion always made, that by a high data variability any curve will fit and thus a linear elastic one is good enough, is not right. Such fit is not able to predict behavior in other circumstances and other loading histories. A high variability indicates an "exclusion of fit" (with a very high probability) for all separated data curves to the mean theoretical equation. This means that the data of every specimen (every structure) should be separately fitted to the theory equations, which fits will show a correlation close to one, because of the molecular high number statistics. Every specimen thus is significantly (at the highest confidence level) an unique giant molecule.

Notations

A = reaction rate constant times the constant "concentration" of flow units ε_{v0}. A = $\varepsilon_{v0} \cdot C$
= $\varepsilon_{v0} \upsilon \exp(-E/kT) \approx$ (for cellulose: $\varepsilon_{v0} \approx 1$) $\approx \nu \cdot \exp(-E/kT)$.
a = $23D/d^2$; D is the diffusion coefficient; d is diameter of the specimen
Bε_v = the same as A, however with changing ε_v.
C_p = the heat capacity at constant pressure
C = reaction rate constant
$(\kappa kT/h)\exp(-E/kT) = (\kappa kT_m/h)\exp((-E/kT) - \ln(T_m/T) =$
$= \upsilon \cdot \exp((-E/kT) - \ln(1 + (T_m - T)/T)) \approx \upsilon \cdot \exp(-E/kT - kT_m/kT + 1) =$
$= \upsilon \cdot \exp((-E - kT_m)/kT) \approx \upsilon \cdot \exp(-E/kT)$ because: $kT_m - kT << E$.
E = the activation energy
f = local real stress on the flow unit in the direction of the movement
G = Gibb's free energy
H = enthalpy (H is also used as height of the relaxation spectre)
h = Planck's constant = $4.135*10^{-15}$ eVsec
k = Boltzmann's Constant = $8.616*10^{-5}$ eVK
K = local rigidity
N = the number of flow units per unit area.
n = exponent of the power law, or work term of the activation energy:
$n = f \cdot \lambda \cdot \lambda_2 \cdot \lambda_3 / kT = \sigma_v \lambda / (NkT) = \sigma_v \varphi$
P = pressure
Q = heat of the system
R = gas constant = $N_m k$ = 1.987 cal K^{-1} mol^{-1}, where $N_m = 6.02.10^{23}$ is Avogadro's number.
S = entropy
T = the absolute temperature
t = time; t_r = (apparent) relaxation time

U = internal energy
V = volume
W = work done by the system
α see β (α a and β b are also locally used as constants)
$\beta = \dot{\varepsilon} / A$ or $\dot{\varepsilon} / B$; $\beta\alpha \approx (\dot{\varepsilon} / A) \cdot (1 - \exp(-\varphi \varepsilon_v K_1))$ or $\approx \dot{\varepsilon} / (B\varepsilon_v)$.
ε = strain; ε_v = viscoelastic, or viscous strain; ε_{v0} is the initial value.
$\varphi = \lambda / (NkT)$ (see n)
γ = deformation
η = viscosity = $\sigma_v / \dot{\varepsilon}$
κ = transmission coefficient or the ratio of activated complexes going into the product state and don't return to the reactant state. $\kappa \approx 1$
λ = jump of the flow segment at activation; $\lambda_2 \cdot \lambda_3 =$ area of the flow unit; $\lambda \cdot \lambda_2 \cdot \lambda_3 =$ activation volume; λ_1 = length of the flow segment or distance of points of flow
υ = frequency or also: $\upsilon = kT_m/h$ is the Debye frequency (about 10^{-12})
ρ = concentration of flow units = $= N \cdot \lambda \cdot \lambda_2 \cdot \lambda_3 / \lambda_1$
σ = mean stress; σ_v = part of the mean stress on the flow units: $\sigma_v = N \cdot f \cdot \lambda_2 \lambda_3$
ω = moisture content
μ = the chemical potential